9-11-2013 12:00 AM

Ignition Method Development and First Field Demonstration of In Situ Smouldering Remediation

Grant C. Scholes
The University of Western Ontario

Supervisor
Dr. Jason Gerhard
The University of Western Ontario

Graduate Program in Civil and Environmental Engineering
A thesis submitted in partial fulfillment of the requirements for the degree in Master of Engineering Science

IGNITION METHOD DEVELOPMENT AND FIRST FIELD DEMONSTRATION OF *In Situ* SMOULDERING REMEDIATION

(Thesis format: Monograph)

By

Grant C. Scholes

Graduate Program in Engineering Science

Department of Civil and Environmental Engineering

A thesis submitted in partial fulfillment of the requirements for the degree of

Master of Engineering Science

The School of Graduate and Postdoctoral Studies

Western University

London, Ontario, Canada

October 2013

Abstract

Self-sustaining Treatment for Active Remediation (STAR), a smouldering combustion-based technology for remediating sites contaminated by industrial liquids, has been extensively studied in the laboratory. The technology had not been demonstrated at a real site. Moreover, the ignition method (based on heat conduction) for the process used in the laboratory was not appropriate for field deployment and an alternative was required. This work first presents the development of a new ignition method for smouldering combustion. This ignition technique (based on heat convection) was proven effective via laboratory tests, and then applied and improved through two field tests. These field tests, conducted on coal tar-contaminated soils below the water table at a former industrial facility, represent the first *in situ* demonstrations of the STAR technology. Self-sustained smoldering was demonstrated within two soil layers at the site: a fill located 3 m below ground surface (bgs) (shallow test) and a sand located 8 m bgs (deep test). The shallow test destroyed 3,728 kg of coal tar over 10 days while the deep test destroyed 864 kg of coal tar over 10 days. Concentration reductions of 99.3% and 97.3% were achieved in soils within the treated areas (i.e. zones where combustion was observed) of the shallow and deep tests, respectively. The performance of the technology in the field (rate the reaction travelled, peak temperatures, extent of cleanup, spread of drying zone) was found to be consistent with the previous laboratory studies. Overall, this work successfully transitions the smouldering remediation concept shown in the laboratory to a field-proven technology with a robust ignition technique that allows rapid, effective deployment at contaminated sites.

Keywords: site remediation, smouldering, STAR, NAPLs, subsurface, ignition

Co-Authorship

This thesis was written by the candidate in accordance with the guidelines and regulations for monograph format as stipulated by the Faculty of Graduate Studies at the University of Western Ontario. The candidate developed, performed and analyzed the laboratory experimental program under the close guidance and supervision of Dr. Jason Gerhard and with assistance from Paolo Pironi. Experiment 8 was performed by Paolo Pironi. The field trials were completed as an industrial project through Geosyntec Consultants Inc., and a confidential industrial client. The candidate was an integral team member in the design and implementation of field trials. Specifically, the candidate was responsible for generation of the design packages for Phases II and III. The candidate designed and sourced equipment, procured subcontractors, communicated and collaborated with heater manufacturers, travelled manufacturers facilities to participate and direct the heater testing program, managed field teams in the installation of the field trial test cells, participated in shakedown/troubleshooting activities and initial operations of the field trials and managed field teams throughout the remaining operation of field trials. Additionally, the candidate performed all data analysis and write up of laboratory and field results presented herein.

Chapter 4 was written by the candidate in a manuscript format for submission to a peer reviewed journal, as: “Smouldering Remediation of Coal Tar Contaminated Soil: Pilot Field Tests of the STAR Technology”

By Grant C. Scholes, David Major, Gavin Grant, Jason I. Gerhard, Jose Torero, Christine Switzer, Paolo Pironi

G.C. Scholes:	design and implementation of field trials (including on site activities and data collection) and heater testing. Performed all data interpretations and wrote draft of chapter.
J.I. Gerhard:	initiated research topic, supervised experimental program, assisted in field trial design, assisted in data interpretation and reviewed/revised draft chapter.
D. Major	provided access to field site, collaborated in design and implementation of field trials. Assisted with data interpretation and reviewed/revised draft chapter.
G. Grant	collaborated in design and implementation of field trials. Provided input on laboratory testing program, and assisted with data interpretation, reviewed/revised draft chapter and reviewed/revised draft chapter.
J.Torero	provided design input for field trials and assisted with data interpretation.
C. Switzer	provided design input for field trials, provided on site start up assistance during Phase II, and assisted with data interpretation.
P. Pironi	provided design input for field trials and assisted with data interpretation.

Intellectual Property

The Intellectual Property for *in situ* STAR is owned by the University of Edinburgh (United Kingdom). It is collaboratively developed under research license at Western University (Ontario, Canada), the University of Strathclyde (Glasgow, Scotland), and University of Queensland (Australia). Commercial application of STAR is exclusively available through SiREM, a wholly-owned subsidiary of Geosyntec Consultants Ltd based in Guelph, Canada. STAR is the subject of several patents (International PCT Filings PCT/GB2006/004591 and PCT/US12/35248, Granted Patents US 8,132,987 B2, AU 2006323431 B9, JP4934832, and ZL 2006 8 0052554.X).

Acknowledgements

I would like to extend my sincere gratitude to my supervisor Dr. Jason Gerhard for his support, technical guidance, and patience over the last few years.

Thank you to the entire STAR team of Jason Gerhard, Jose Torero, David Major, Gavin Grant, Christine Switzer, and Paolo Pironi for welcoming me into the team to help develop this exciting technology. Specifically thanks to Christine for teaching me the ropes of STAR during long overnight shifts at the field trials and thanks to Paolo for navigating me through laboratory studies at Western.

This work has been supported by Geosyntec Consultants, and I would like to specifically thank David Major and Gavin Grant for their on-going encouragement, technical assistance, and friendship. I also extend my sincere thanks to Mark Watling, Bill Bingham, Scott Douglas, Russ Hyatt, Dave Liefl, Luana Jo and Kitty Chow for all of their hard work on site during the often trying field trials.

Finally, I am most thankful to all of my family and friends for their support; most importantly to S'rana for everything.

Dedication

For S’rana, Caroline, and Samantha

Table of Contents

List of Tables

List of Figures

List of Appendices

List of Abbreviations

amp	ampere
bgs	below ground surface
BTEX	benzene, toluene, ethyl benzene, xylene
CEMs	continuous emissions monitoring system
cm	centimeter
cm/s	centimeter per second
CO	carbon monoxide
CO_2	carbon dioxide
cP	centipoise
EPA	United States Environmental Protection Agency
EPH	extractable petroleum hydrocarbons
ERH	electrical resistance heating
GAC	granular activated carbon
ISTD	in situ thermal desorption
kg/m^3	kilograms per cubic meter
kJ	kilojoules
kW	kilowatt
kW/m^2	kilowatts per square meter
m	meter
m^3/hr	cubic meter per hour
mg/kg	milligrams per kilogram
MGP	manufactured gas plant
mm	millimeter
mm/hr	millimeters per hour
NAPL	non aqueous phase liquid
^oC	degrees Celsius
PCB	polychlorinated biphenyl
SEE	steam enhanced extraction
S-ISCO	surfactant enhances in situ chemical oxidation
STAR	self-sustaining treatment for active remediation
SVE	soil vapor extraction
TPH	total petroleum hydrocarbons
V	volts
W	watts

1 Introduction

1.1 Problem Overview

Non-aqueous phase liquids (NAPL), including coal tars and creosote, heavy hydrocarbons, chlorinated solvents, and polychlorinated biphenyls (PCBs), comprise a class of organic contaminant that persist in the subsurface at tens of thousands of sites worldwide.

Coal tar and creosote (composed of various coal tar fractions), produced as a byproduct of historical manufactured gas plant (MGP) operations and blast furnace coke production [1], comprise a class of NAPLs whose physical and chemical properties create a particular challenge for remediation [2] [3]. Technologies including excavation, encapsulation, in situ thermal desorption (ISTD) and surfactant enhanced in situ chemical oxidation (S-ISCO) have been used on coal tar and creosote impacted sites; however, each of these technologies have significant technical and/or economical limitations and the majority of these sites remain without solution.

Self-sustaining treatment for active remediation (STAR) is a novel remedial technology based on the principles of smouldering combustion. STAR has recently shown significant potential for the treatment of coal tar NAPLs at the laboratory scale [4] [5] [3]. Smouldering combustion is a slow moving, flameless form of combustion which occurs on the surface of a condensed phase fuel within a porous medium [6], and can produce a self-sustaining reaction following an initial heat input [7]. In the STAR process, NAPLs (acting as the condensed phase fuel) are smouldered within a soil matrix (acting as the porous medium). Laboratory scale testing has demonstrated remedial effectiveness of NAPL smouldering and evaluated the sensitivity of the process to key operating parameters [5].

In STAR laboratory experiments, ignition of the smouldering reaction has been achieved using a conductive heating method in which an electric heating element is buried at the base of the contaminated soil pack [3] [5]. An initial proof of concept field trial (Phase I) of the STAR technology transferred the conductive ignition process to the field scale (Design A), however; this method was found to be unreliable and impractical due to costs for installation and inability to access, maintain, or reuse the directly buried heater element. As such, a new ignition method suitable for field scale application was required in advance of a robust, reproducible field demonstration of STAR.

1.2 Research Objectives

The overall objective of this work was to demonstrate the *in situ* application of the STAR at a real field site. To accomplish this objective, a new ignition approach using convective heating was developed, representing the first ignition of a smoldering reaction in this manner. Proof of concept of the convective ignition method was demonstrated through a series of laboratory experiments. Two field trials (Phases II and III) were then performed, using field versions of this new ignition method, to demonstrate STAR *in situ* and below the water table at a former industrial facility. The Phase II field trial using the convective ignition approach (Design B) demonstrated STAR in shallow fill materials at the site. A revised heater system was designed and tested (Design C) in advance of being used in the Phase III field trial in a deeper sand unit at the site.

1.3 Thesis Outline

This thesis is written in as an integrated article format in accordance with the guidelines and regulations stipulated by the Faculty of Graduate Studies at the University of Western Ontario. Each of the chapters in the thesis is described below.

Chapter 2 is a review of relevant literature and presents a review of contaminated sites, existing remedial technologies and challenges associated with remediation. An introduction to smouldering combustion is presented as well as a review of laboratory studies on NAPL smouldering, and a summary of the Phase I proof of concept STAR field trial.

Chapter 3 presents the development of the convective ignition procedure. A series of eight laboratory column experiments are presented to demonstrate proof of concept of convective ignition. Two convective ignition designs, Design B and Design C are evaluated in the Phases II and III *in situ* STAR field trials respectively, and a quantitative comparison of heater design performance based on above ground testing of the heaters is presented.

Chapter 4 presents the full results of the Phases II and III field trials. This chapter is written in a manuscript format for submission to a peer-reviewed journal.

2 Literature Review

2.1 Coal Tar Contaminated Sites

2.1.1 Introduction

Non aqueous phase liquids (NAPLs), including coal tars and creosote, heavy hydrocarbons, chlorinated solvents, and PCBs, comprise a class of organic contaminant that persist in the subsurface at tens of thousands of sites worldwide. NAPL contamination is the result of historical and continued releases, both accidental and intentional, related to industrial activities such as chemical manufacturing, petroleum exploration and refining, and industrial liquid storage and transport [8]. These NAPL-contaminated sites present significant risks to human and ecosystem health as well as challenges for remediation and redevelopment. Coal tar and creosote (composed of various coal tar fractions) NAPLs, the primary contaminants addressed in this work, contain a complex mixture of aliphatic and aromatic compounds produced as a byproduct of historical manufactured gas plant (MGP) operations, and blast furnace coke production [1]. While coal tar typically can contain several hundred organic compounds its dominant chemical constituents of environmental and/or toxicological concern include benzene, toluene, ethylbenzene, xylene (BTEX), naphthalene, benzo[a]pyrene and phenanthrene [9].

MGP operations began in the mid-1800s with a significant increase in operations through the late 1800's supplying gas for lighting, heating and cooking. By the mid 1950's the majority of MGP operations had ceased as natural gas replaced coal gas [10]. The New York State Department of Environmental Conservation reports more than 300 former MGP sites may exist within the State,

with 200 already identified and designated for remedial work [10]. The United States Environmental Protection Agency (US EPA) reports over 1,500 coal tar contaminated sites within the United States. The international Agency for Research on Cancer classifies coal tar as a human carcinogen driven by the effects of benzo[a]pyrene [11].

2.1.2 Remediation of Coal Tar and Creosote Sites

Existing remediation technologies have had limited effectiveness on coal tar and creosote sites. To the author's knowledge, at present, no full scale *in situ* remediation of a coal tar-contaminated site exists in the peer reviewed literature. The physical and chemical properties of coal tar and creosote NAPLs make their remediation especially challenging. Their low density (1,010 to 1,100 kilograms per cubic meter [kg/m^3]) and high viscosity (20 to 100 centipoise [cP]) results in long migration periods and extended lateral migration distances from release areas and also limits their ability to be removed via pumping based technologies, such as multiphase extraction [2] [9] [1]. Their chemical complexity is associated with high boiling points which renders ineffective volatility-based extraction methods such as soil vapour extraction (SVE) and air sparging. Furthermore, the long-chain hydrocarbons which make up coal tar and creosote NAPLs cannot be metabolized by microorganisms and are therefore resistant to biodegradation [12]. The most common mitigation measures for coal tar-contaminated sites are (a) excavation, which can be very expensive, still requires treatment or disposal of the soils, and is prohibitive for contamination at depth [3] [13], or encapsulation, which leaves the contaminated material in place and attempts to minimize interactions with the surrounding environment, thereby limiting options for future use of the site.

Innovative technologies have shown some promise for the treatment of coal tar and creosote though none have yet to be proven to be consistently economically or technically feasible. Thermal remedies such as in situ thermal desorption (ISTD), electrical resistance heating (ERH) and steam enhanced extraction (SEE) have shown some ability to treat coal tar and creosote NAPLs. Thermal remedies actively heat the entire target aquifer to change the thermodynamic properties of NAPLs to enhance their phase change and extraction. Heat can be applied to the subsurface conductively via vertically installed heater wells in ISTD [14], via electrical current passed between heater wells in ERH, and/or through injection of steam (applicable in high permeability materials) in SEE [15]. Successful implementation of these remedies depends on achieving target temperatures within the entire treatment area and the processes targeted are all endothermic; thus, high rates of energy are often applied continuously for months to achieve and maintain subsurface temperatures [15].

Thermal remedies can be applied in two modes: low and high temperature. Low temperature thermal remedies elevate subsurface temperature up to 100 degrees Celsius (^{o}C), the boiling point of water, at which point NAPL viscosities decrease, NAPL mobility increases (enhancing liquid extraction) and lighter fraction compounds are volatilized and extracted as vapours to be treated above ground [15]. These lower temperatures can be achieved through any of ISTD, ERH or SEE. While effective in removing the lighter components of a NAPL (e.g. highly effective on chlorinated solvent NAPLS) [15] [14], significant fractions of heavier NAPLS such as those found in coal tar and creosote are left behind. In order to volatilize the heavier compounds in a coal tar NAPL, high temperatures are required. High temperature ISTD can be used to increase the temperature of the entire subsurface treatment area to temperatures above

400^{o}C for a considerable period (e.g., months) [14] [16] [13]. While high temperature ISTD has been reported to be effective [16], the energy requirements to heat the subsurface above 100^{o}C (requiring hydraulic control or boiling off of all water) over a large area and sustained time can be cost prohibitive [13].

Surfactant-enhanced in situ chemical oxidation (S-ISCO) has recently been reported to show some promise for reducing coal tar concentrations in soil and groundwater [17]. S-ISCO involves introduction of an amendment containing a mixture of surfactant(s) and oxidant(s) directly to the subsurface (via injection wells, trenches, excavation, or horizontal wells, etc.). The surfactant enhances the solubility of non-aqueous phase contaminants so that they can be chemically oxidized in the dissolved phase to non-toxic end products. The technology is dependent on the ability to deliver the amendment directly to the contaminant in the subsurface, which can be impracticable in very fine grained materials due to limited radius of influence and high pressures required of injected fluids, and can also be limited by heterogeneity in subsurface materials controlling the flow of amendments.

2.2 Self-Sustaining Treatment for Active Remediation

STAR is an emerging technology based on the principles of smouldering combustion and has been identified as a potential alternative for treatment of contaminated soils containing NAPLs such as coal tar, creosote and heavy hydrocarbons [18] [5] [3] [4]. STAR utilizes the combustible nature and energy content of NAPLs to fuel a self-sustaining smouldering reaction which propagates through a contaminated soil volume, consuming the NAPL and leaving behind

clean, inert materials. The following sections present a general review of the smouldering combustion process, laboratory scale development of the STAR technology, ignition methods utilized in smouldering processes, and a description of the first proof of concept STAR field trial.

2.2.1 Smouldering Combustion

Simply defined, combustion is the exothermic oxidation of a fuel. For organic (i.e., carbon-based) fuels, the end products of a complete combustion reaction are carbon dioxide (CO_2), water, and heat energy. Combustion can occur as both flaming and smouldering reactions. Flaming combustion occurs when a gasified fuel is oxidized in the open air space above the fuel, whereas, smouldering combustion is a flameless oxidation reaction that occurs on the surface of a condensed (i.e., solid or liquid phase) fuel [6] [19]. Smouldering requires the presence of a porous matrix, either a porous fuel (e.g., coal) or porous medium, because it relies on air diffusion from pores to the fuel surface, and thus is typically an oxygen-limited kinetic reaction [6] [19]. Smouldering combustion typically produces lower peak temperatures and propagation rates than flaming combustion reactions with peak temperatures of the former in the range of 500-700^{o}C and the latter in the range of 1500-1800^{o}C [4].

In the context of NAPL destruction and/or soil remediation, flaming combustion has been demonstrated to effectively exploit the combustible properties of NAPLs through incineration processes [20] [13]. Because oxidation through flaming combustion occurs in open air space, heat losses in a NAPL flaming combustion reaction are high and sustaining the reaction requires the input of supplemental fuel and energy, resulting in high costs for incineration-based soil/liquid treatment [13].

In contrast, because smouldering combustion occurs within a porous medium, heat evolved from the exothermic oxidation reaction is retained and utilized to sustain and propagate the reaction, making smouldering combustion an energy efficient process [3]. Charcoal briquettes in a barbeque (Figure 2.1) are a common example of smouldering combustion, and many porous organic solids can undergo smouldering reactions including polyurethane foam, tobacco, dust, paper, peat, coal and cotton [4].

Figure 2.1: Glowing red charcoal is a typical example of smouldering combustion.

Smouldering reactions involve complex and heterogeneous processes of heat transfer, fluid flow and chemical reactions occurring within the porous media [21] and can occur under natural (i.e., ambient) air flow and through forced (i.e., air actively supplied to the reaction) flow [4]. Propagation rates and peak temperatures in a forced smoulder reaction are typically significantly higher than under natural conditions [4]. Smouldering front propagation velocities in polyurethane foam experiments performed under natural flow conditions have been reported on the range of 10 to 30 millimeters per hour (mm/hr) [6], while similar materials smouldering

under forced air conditions have reported front propagation velocities in excess of 90 mm/hr [21]. Propagation of a smouldering reaction occurs in two distinctive modes: forward, where the reaction moves in the direction of the oxygen supply; and opposed, where the reaction travels against the direction of oxygen flow, and generally exhibits a lower smouldering front velocity [22], [21], [4] [23]. A typical smouldering reaction can be categorized into three distinct regions consisting of a central 'char' zone where reaction temperatures peak and glowing is observed, sandwiched between a leading 'pyrolysis zone' where materials are undergoing rapid temperature increases and a preceding 'residual char' zone in which is undergoing cooling [19]. Development of a solid/ self-supporting residual char is critical for self-sustaining smouldering reactions in solids as the char insulates the smouldering reactions, and materials that would melt or shrink away from the reaction front would not retain the reaction heat sufficiently, or allow the flux of oxygen to the reaction [19] [7].

The first widely available published work into smouldering phenomena was presented by Palmer et al in 1957 and examined temperature and smouldering front propagation velocities of smouldering reactions within dust piles and fibrous materials [22]. Palmer's study examined forced flow versus natural flow smouldering and identified preliminary direct relationships between air flow rate in a forced forward smoulder and reaction propagation velocity. Much of the more recent literature on smouldering is in the context of fire safety and involves studies on the smouldering properties of polyurethane foam, a common material used in furniture construction. Studies of forced flow forward smoulder experiments on polyurethane foam have further supported the direct relationship of air flow to smoulder propagation rate reported by Palmer [21].

Examples of smouldering in polyurethane foam or charcoal briquettes are cases in which the condensed fuel and the porous media are one and the same; however, a smouldering reaction can also occur on a distinct liquid fuel within an inert porous media [4]. An example of a liquid smouldering reaction is lagging fires, in which leaked combustible fluids from process piping or equipment soak into porous insulation (lagging) and can produce a smouldering reaction in the presence of heat and oxygen [4] [19]. The process of 'fire flooding' used in the petrochemical industry involves subsurface combustion (assumed to be smouldering) in oil reservoirs to decrease viscosity and drive oil to production wells [24] [4]. Smouldering of liquid contaminants in soil in the context of remediation (STAR) has been characterized in detail in the laboratory, and is described in the following sections.

2.2.2 Laboratory Scale STAR Testing

Proof of concept experiments demonstrating the ability to smoulder liquid contaminants in soils and mineral sands are first presented in 2009 by Switzer et al [3] and Pironi et al [18]. Figure 2.2 presents a schematic of the apparatus for a typical STAR laboratory experiment.

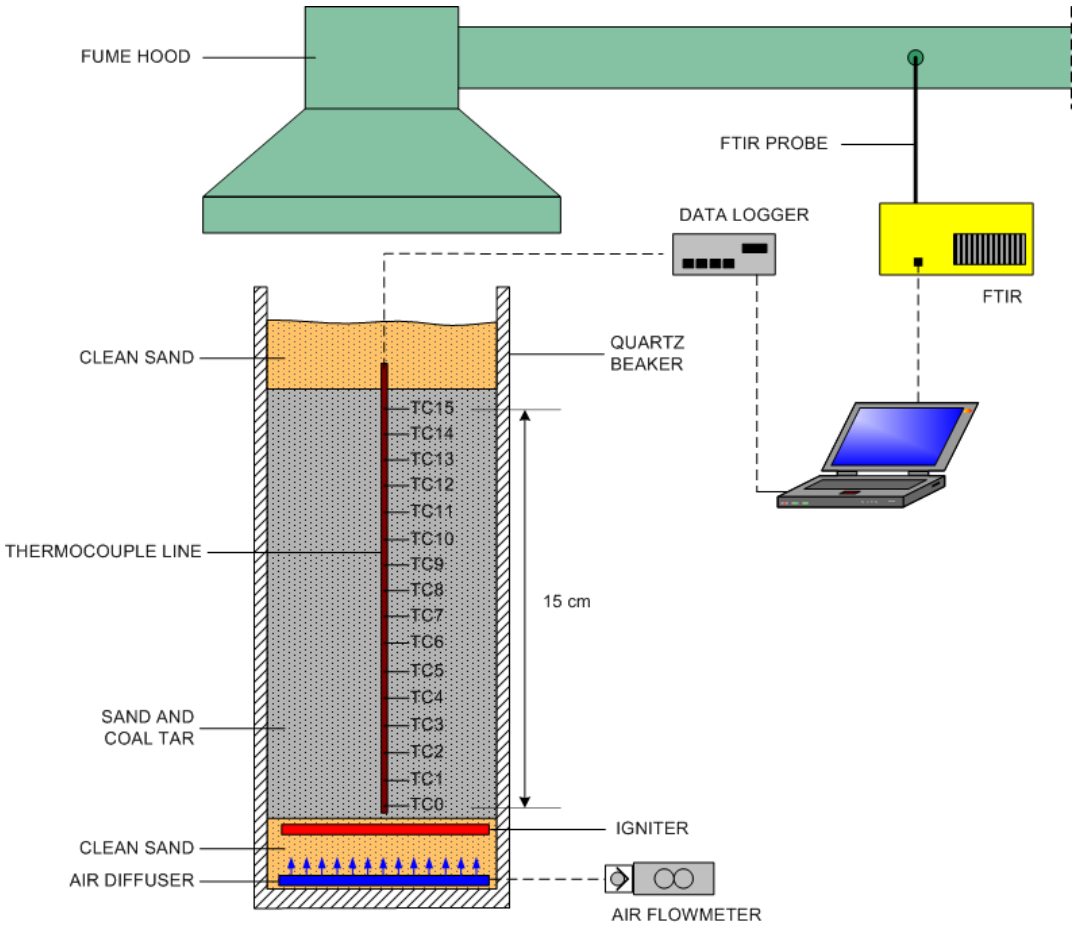

Figure 2.2: Schematic of apparatus for a typical STAR laboratory column test; (from [3]).

The standard apparatus for STAR column experiments is similar to that for forced forward smoulder experiments performed on polyurethane foam [21]. The configuration consists of a quartz or stainless steel column fitted with an air diffuser at the base embedded in a layer of clean sand. An igniter (typically an electrical cable heater coiled into the diameter of the column) is place above the air diffuser upon which a volume of contaminated media is emplaced, followed by a thin layer of clean sand. A series of thermocouples is inserted along the central axis, and the vapours emitted are collected under vacuum for analysis. The position, peak temperatures and progress (i.e., propagation velocity) of the smouldering front is inferred through the temperature data collected by the thermocouples. Collected vapours may be

analyzed to assess combustion gases as a secondary indicator of smouldering status and/or volatile emissions.

Figure 2.3 presents a temperature versus time plot of thermocouple data collected in a typical STAR column experiment. Self-sustaining smouldering is demonstrated by the series of overlapping temperature peaks following termination of heater operation [3].

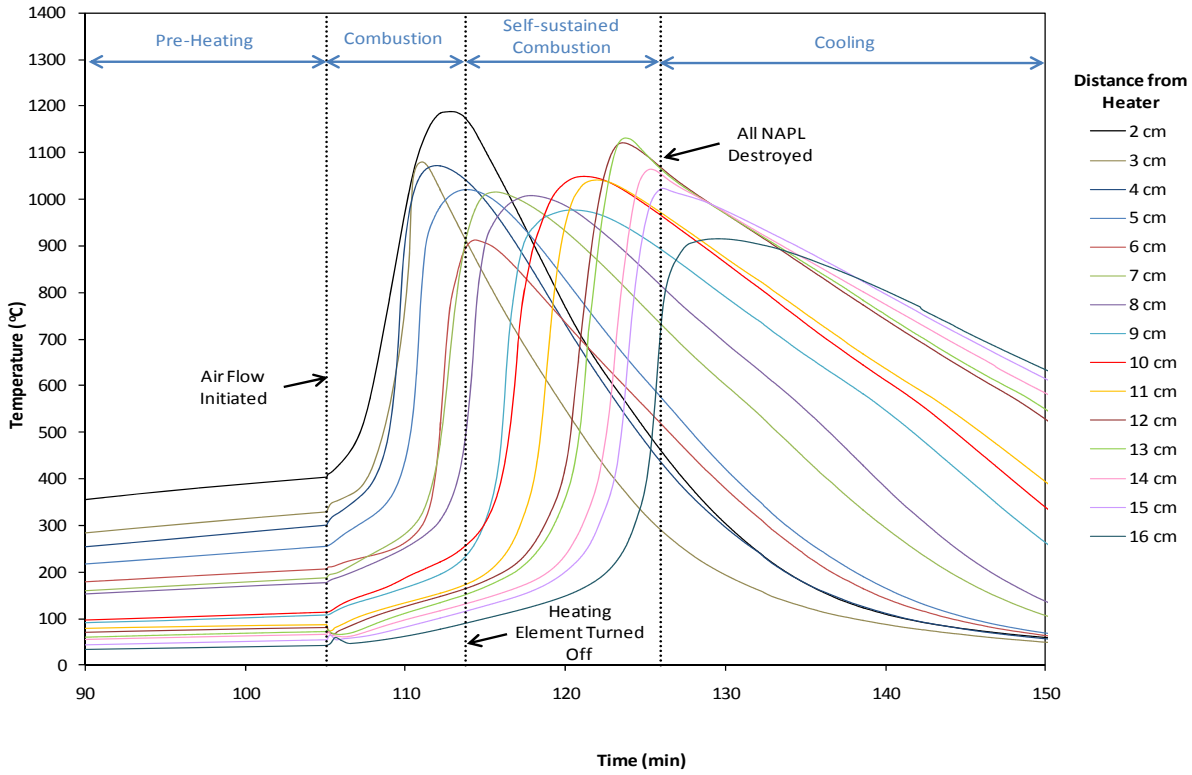

Figure 2.3: Typical temperature versus time data for a STAR column experiment. Conductive ignition test showing the stages of preheating, ignition, self-sustaining combustion and cooling. Modified from [18].

Successful self-sustaining smouldering behavior has been demonstrated at the laboratory scale for a range of soil types from silts to coarse sands as well as for simple layered systems [3] [5]. NAPL types including coal tar, mineral oil, vegetable oil, crude oil and mixed NAPLs have all been successfully smouldered at the laboratory scale [3] [5].

Concentration of total petroleum hydrocarbons (TPH) in laboratory smouldering experiments on coal tar contaminated sands have demonstrated complete NAPL destruction following STAR treatment (i.e., non-detect in post-treatment samples) from initial concentrations in the tens of thousands of milligrams per kilogram (mg/kg) TPH [3]. Self-sustaining smouldering of coal tar contaminated sands has been demonstrated for concentrations equivalent to 10% to 100% saturation of pore space [5]. Experiments performed on beaker, column, and drum scales have demonstrated an increase in reaction efficiency with scale as heat losses related to boundary effects are reduced [25]; this implies that the lower pore space saturation limit in the field may be well below 10%. Experiments on coal tar-contaminated sands have demonstrated that the energy produced by the smouldering process is sufficient to maintain self-sustaining behavior even when the remaining soil porosity is water saturated, though at decreased peak reaction temperatures and propagation velocities [5]. The NAPL smouldering process has been demonstrated to be self-terminating (i.e., extinguished once all NAPL in the column was consumed) or can be extinguished manually through termination of the air supply [3], and the smouldering front propagation of STAR is the subject of a reported two dimensional numerical model [26].

Commercial treatability testing performed by SiREM (unpublished) has demonstrated successful self-sustaining behavior, typically resulting in complete (i.e., 100%) concentration reductions following STAR treatment, for 15 samples of contaminated soils from field sites worldwide (Table 2.1).

Table 2.1 Summary of Commercial Treatability Studies (SiREM)

No.	Origin	Media Type	Contaminant	TPH before (mg/kg)	TPH after (mg/kg)	Self-sustaining?
1	Canada	Sandy clay loam	Petrochemical hydrocarbons	31,000	ND	✓
2	Canada	Fill	Coal tar	10,500	ND	✓
3	USA	Sandy clay	Coal tar	34,650	ND	✓
4	USA	Silty sand	Petrochemical hydrocarbons	74,000	ND	✓
5	Belgium	Fill	Coal tar	10,500	ND	✓
6	Belgium	Fill	Coal tar	23,317	ND	✓
7	Belgium	Fill	Coal tar	35,948	ND	✓
8	USA	Fill	Coal tar	23,400	140	✓
9	USA	Silty sand	Coal tar	25,000	ND	✓
10	USA	Silty sand	Creosote	29,300	ND	✓
11	USA	Sand	Coal Tar	37000	ND	✓
12	USA	Sand	Coal Tar	15000	ND	✓
13	Australia	Gravel	Coal tar	14400	120	✓
14	USA	Fill	Petrochemical hydrocarbons	24300	ND	✓
15	USA	Alluvial Sand	Petrochemical hydrocarbons	5980	ND	✓

2.2.3 Ignition Methods

Ignition of a smouldering reaction requires an initial heat flux to initiate the oxidation process. Heat transfer can occur in three modes: conduction, convection, and radiation. Conductive heat transfer refers to a transfer of heat through a stationary medium as a result of a temperature gradient [27]. Convection refers to heat transferred between a surface and a moving fluid of differing temperatures [27]. Radiation heat transfer is the net heat transfer between two surfaces, in the absence of an intervening media, through electromagnetic waves [27].

Reported studies on smouldering combustion have typically used conduction heat ignition via direct contact heaters embedded in the porous medium [5] [3] or radiant heat ignition via cone

heaters located above the porous medium [21]. Palmer initiated smouldering reaction in dust piles using a small flame as the initial heat source [22].

Three distinct stages occur within the porous medium in advance of ignition of a self-sustained smouldering reaction: (i) a warm up stage, (ii) the unsteady smoulder and (iii) the self-sustained smoulder stage [7]. Stages (i) and (ii) are both controlled by the external heat flux to the medium, while stage (iii) is controlled by energy generated by the exothermic smoulder reaction [7].

Anderson et al (2000) demonstrated the temperature and mass loss signatures for the three ignition stages and determined the minimum temperature (target ignition temperature) requirement of 575 Kelvin for polyurethane foam [7]. The study presents temperature profiles of experimental smouldering data versus predicted heating profiles for a semi-infinite inert solid. Ignition of the smouldering reaction is evidenced by an inflexion in temperature at the onset of oxidation, where temperatures in the experimental data first begin to exceed predicted temperatures of the inert solid due to the contribution of exothermic smouldering [7]. Energy requirements for ignition vary depending on experimental conditions. Ignition of smouldering in polyurethane foam has been reported by applying a heat flux of 2 kilowatts per square meter (kW/m^2) [4] and at heat fluxes of 6.1 to 6.8 kW/m^2 [7].

All STAR experimental work to date has utilized a conductive ignition method by which the base of the contaminated soil pack is preheated to an ‘ignition temperature’ before air flow is initiated. Switzer reported the target ignition temperature for coal tar to be 400^oC measured 1 cm

into the porous medium [3]. This temperature was achieved after approximately 105-115 minutes of heating using an electric cable heater with a maximum heat flux of 26 kW/m^2 [3].

2.2.4 Initial Proof of Concept Field Study

An *in situ* proof of concept field study (Phase I) was undertaken in 2009 by Geosyntec (unpublished) in a coal tar contaminated former lagoon at a former industrial facility in New Jersey (treatability study soil no.8, Table 2.1) to demonstrate the STAR technology below ground and below the water table. The field study employed a conductive ignition method utilizing an electrical resistive heater (Design A) formed into a 20 centimeter (cm) diameter coil around a 5 cm diameter air injection well and buried directly within a 30 cm diameter borehole (Figure 2.4) designed to mimic the ignition method performed in laboratory experiments.

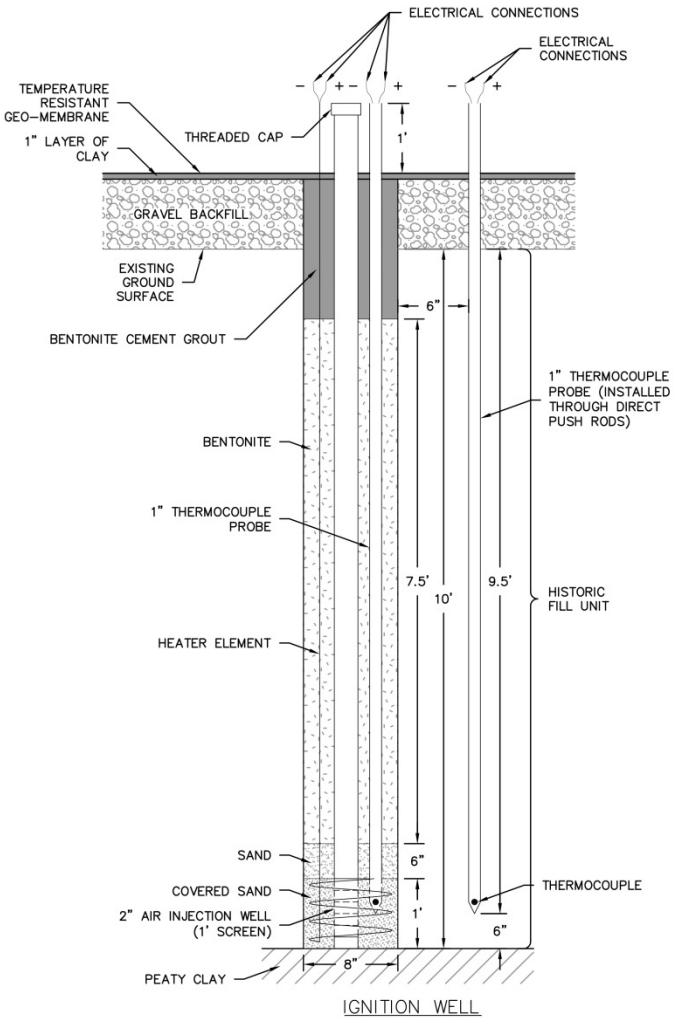

Figure 2.4: Schematic of *in situ* ignition well construction from Phase I proof of concept field trial with Design A conductive heater installed around well screen (from Geosyntec). Note drawing in imperial units.

A target temperature of 900 ºC as measured by the thermocouple located inside the heater coil (Figure 2.4) was selected as a conservative target ignition temperature to ensure an adequate volume of soil outside of the borehole reached the 'true' anticipated ignition temperature (assumed to be approximately 400 ºC 1 cm outside the heater element). Figure 2.5 presents the temperature profiles during preheating and ignition for the thermocouple located inside the heating coil and the next nearest monitoring thermocouple located approximately 25 cm outside of the ignition well boring.

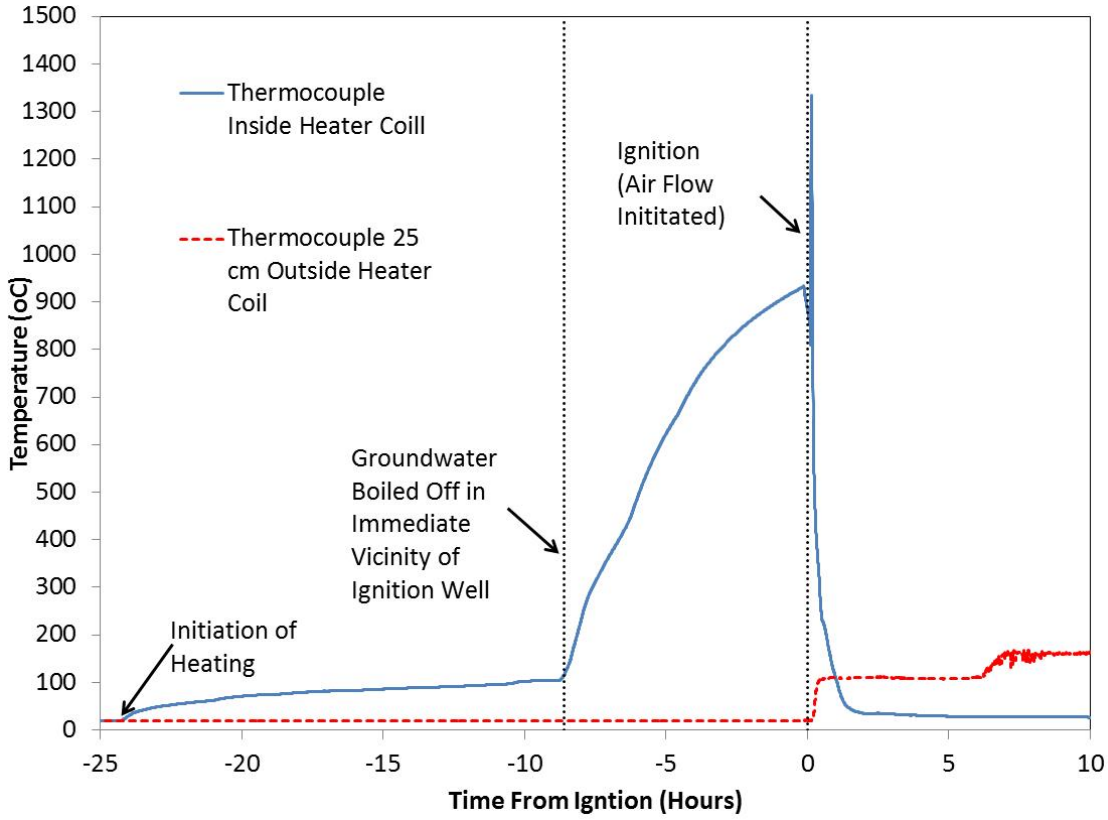

Figure 2.5: Temperature versus elapsed time during the Phase I ignition event.

Following approximately 17 hours of preheating, the TC-34 was observed to increase in temperature above 100^{o}C indicating that all water in the immediate vicinity of the heater had been boiled off. A sharp rise in temperature to 900^{o}C was observed over the next 8 hours of heating. Air flow was initiated to the well following approximately 25 hours of preheating at which point a rapid spike in temperature indicative of ignition of the smouldering reaction was observed in both the ignition and monitoring thermocouples. Combustion was further confirmed through the detection of combustion gases measured in vapours collected from the test cell. The proof of concept test maintained a self-sustaining smouldering reaction in the subsurface, below the water table, for a period of nine days (confirmed through the continuing presence of

combustion gases in vapours). Propagation of the combustion front however, was not observed beyond the immediate vicinity of the ignition well. During the ignition process, the electrical coil used for ignition was destroyed, likely due to exposure to high temperatures and corrosive environment as a result of being directly buried. Moreover its installation method meant that it could not easily be fixed or replaced and therefore a second ignition attempt was not possible. Recommendations from the Phase I trial were for a more detailed field study of the STAR technology and the need for development of a more robust ignition system.

2.3 Conclusions

Coal tar and creosote contaminated sites present a significant human health risk and a challenge to remediation. To date, no conventional *in situ* technologies exist that are both economically viable and technically effective for remediating coal tar and creosote contamination. The STAR technology, utilizing self-sustained smouldering combustion, has been identified as a potentially low cost, highly effective method for treating NAPLs including coal tar and creosote *in situ*. Laboratory scale work has defined the conditions for STAR applicability and demonstrated the effectiveness of STAR treatment and process sensitivity to a range of operating conditions. An initial proof of concept field trial demonstrated that smouldering of coal tar NAPL could be achieved *in situ* and below the water table; however, a more sustainable and robust *in situ* ignition method is required as well as a more detailed field demonstration. This work presents the development of a revised ignition method for the *in situ* implementation of the STAR technology (Chapter 3) and presents the detailed results of two STAR field trials (Chapter 4).

3 Convective Ignition of a Smouldering Reaction

3.1 Introduction

The conductive ignition method, traditionally used for laboratory scale STAR experiments and the initial proof of concept *in situ* STAR field trial, is not a robust or practical method for full scale *in situ* field applications for several reasons:

1) The electrical element is directly buried in the ground, exposing it to extreme temperatures and a potentially corrosive environment which accelerate heater failure;
2) Direct burial of the ignition element requires large diameter boreholes for ignition well installations which significantly increase implementation costs;
3) Direct burial of the ignition element precludes reuse of the ignition system beyond a single ignition location; and
4) The conductive ignition approach required significant preheating time to achieve ignition.

Full scale application of STAR at a site may require tens to hundreds of ignition points; therefore, minimizing the required borehole diameter, increasing heater robustness, increasing heater reusability and decreasing time to ignition are all critical factors in developing STAR into an economically viable *in situ* remedial technology.

In this work, an innovative smouldering reaction ignition method was developed whereby the heat energy is applied to the porous media convectively through the injection of hot air. For the *in situ* application, this is achieved using a removable in-well heater operated in conjunction with

pressurized air injection at the well head which injects heated air into the subsurface via a well screen installed at the base of the target treatment area (Figure 3.1). To the best of the author's knowledge, and in the experience of a leading expert on combustion science (Professor Jose Torero, University of Queensland), ignition of a smouldering reaction via convective air injection has not been previously reported.

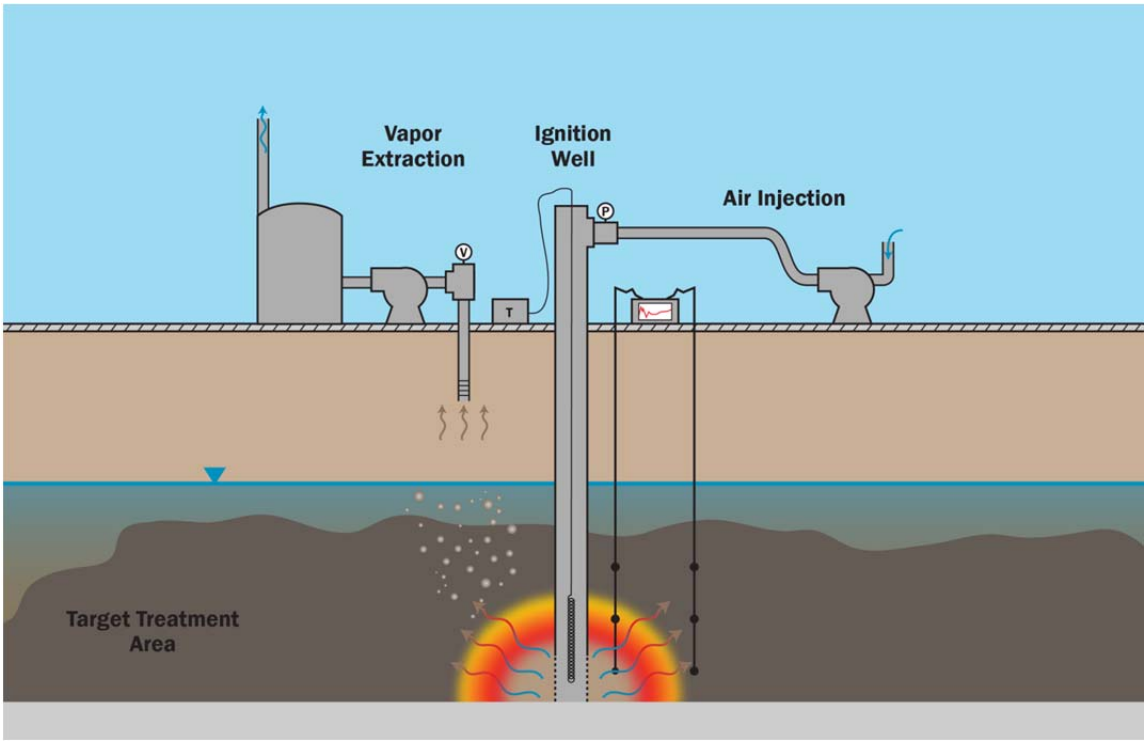

Figure 3.1: Conceptual diagram of the *in situ* STAR application with convective ignition method.

The convective ignition method was proven, developed and tested through a series of laboratory column tests and *in situ* field trials described below.

3.2 Laboratory Proof of Concept Experiments

Eight laboratory scale 'proof of concept' experiments were performed to demonstrate the convective ignition approach for initiating a smouldering combustion reaction. The laboratory experiments conducted are summarized in Table 3.1. The experimental program was not intended to provide a rigorous characterization of the convective process, but was designed to demonstrate proof of concept of achieving an ignition in the absence of a direct contact heating element (i.e., conductive method) and to roughly quantify the power requirements and pre-heating durations for convective ignition at the laboratory scale.

Table 3.1: Convective Ignition Laboratory Experiments

Exp. Number	Heater Type	Heating Duration (min)	Contaminated Sand Pack Height (cm)	Coal Tar Saturation (% pore space)	Air Flow Rate (LPM)	Successful Ignition?	Additional notes
1	Single cable heater	59	12	25	62	yes	
2	Double cable heater	17	12	25	41	yes	
3	Double cable heater	not available	12	25	20-62	yes	100% Water saturation
4	Double cable heater	57	7	25	40-60	yes	through clean sand layer
5	External heater	63	15	25	80	yes	
6	External heater	76	15	25	60-80	yes	
7	External heater	71	30	25	60-80	yes	
8	External heater	60	30	25	60-80	yes	

3.2.1 Materials and Methods

All laboratory experiments were performed using a mixture of commercially available coarse quartz sand (Number 12, Bell & MacKenzie Co.) and laboratory grade coal tar (Alfa Aesar, density 1200 kg/m^3 at 20^{o}C) at a target saturation of 25% of pore space (approximately 71,000 mg/kg) consistent with the 'base case' material used in published studies [3] [5] [18]. The mixture was prepared by manually mixing pre-weighed amounts of sand and coal tar. The sand had a calculated average bulk density of 1623 kg/m^3 and porosity of 40%, and the coal tar had a density of 1,200 kg/m3. The mixture was then manually emplaced into the columns at packing heights ranging from 7 to 30 cm (Table 3.1 [individual experiment configurations available in Appendix A]).

Experiments 1 through 4 were carried out in a 13.8 cm diameter; 30 cm tall quartz beaker fitted with a stainless steel mesh screen supported approximately 10 cm up from the base of the column by a stainless steel ring insert. An air diffuser and heater element(s) were installed beneath the screen leaving an 'air plenum' of approximately 4-5 cm between the heater element and the screen (i.e., contaminated sand pack interface). The heater element(s) were 450 watt (W) electrical cable heaters (Watlow ltd.) coiled into a spiral shape fitting the diameter of the column. A single cable heater coil was used for Experiment 1, while Experiments 2 through 4 utilized two cable heater coils placed on top of one another in the air space below the screen. Power to the heater cables was controlled by manually adjusting a variable auto transformer (variac) power source (STACO Energy Products). Figure 3.2 presents a schematic layout of the column configurations for Experiments 1 through 4 (Figure 3.2a) and 5 through 8 (Figure 3.2b). While

at first glance this appears to mimic the experimental setup described for typical conductive ignition of smouldering experiments, the fact that the heaters are not in contact with the contaminant or soil means that heat energy transfer by conduction is eliminated as a means of preheating the base of the contaminated material.

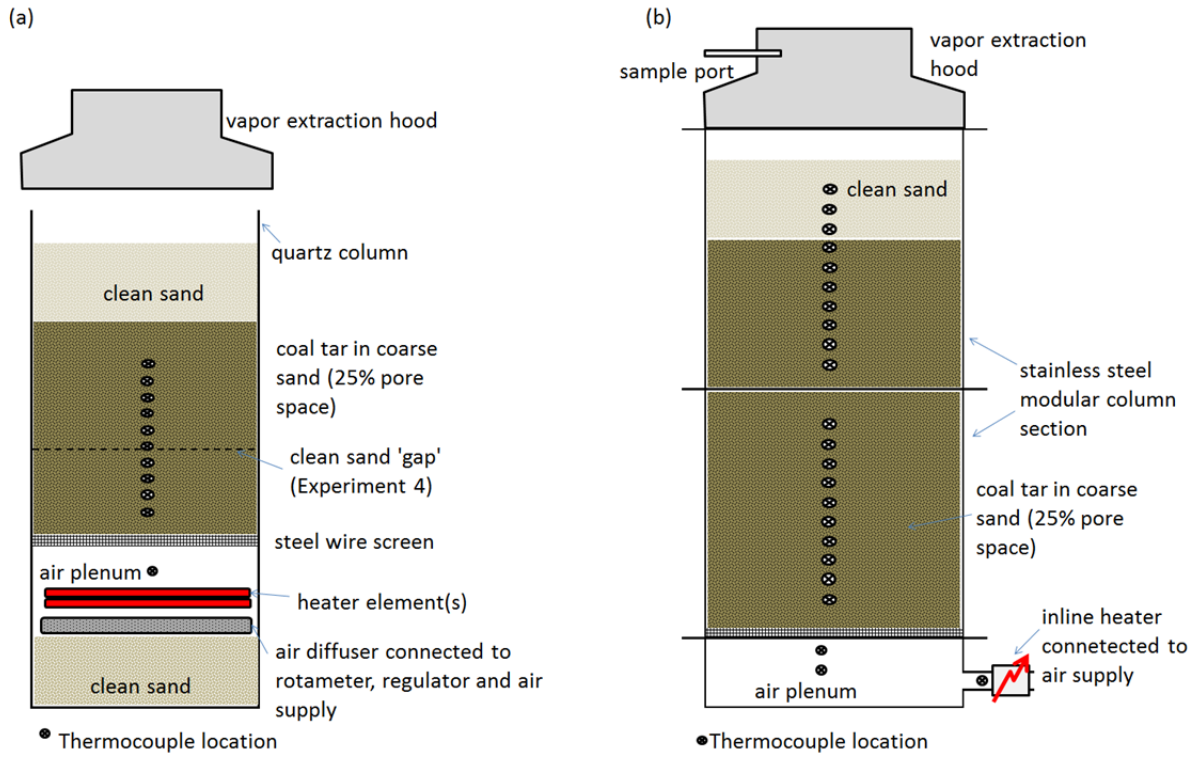

Figure 3.2: Schematic column configurations; Experiments 1 to 4 (a); and Experiments 5 to 8 (b).

Experiment 3 was conducted under fully water saturated conditions, to roughly simulate the ignition process below the water table. Following packing of the column, water was added to the coal tar/sand mixture until free water pooled at the top of the column (coal tar saturation of 25%, water saturation of 75% and air saturation of approximately 0% of pore space). Experiment 4 was conducted with a 4 cm layer of clean sand emplaced between the screen and the contaminated sand pack in order to absorb the radiation component of the heating apparatus

(which may have been a significant component of the heat transfer in Experiments 1-3) for a more representative convective ignition.

Experiments 5 through 8 were conducted in a custom designed 16 cm diameter modular (20 cm tall sections) stainless steel column with an integrated air plenum at the base and conical vapour 'hood' for collection of vapour samples at the top. Experiments 5 through 8 were repeat experiments (varying only packing height) to evaluate consistency and quantify energy of ignition. The column was designed to produce a more rigorous convective ignition set up where the heat input for the ignition process was supplied by an external inline heater connected to the outside of the column. Modular sections of the column enabled varying the height of media packing between experiments. The external heater was a 1.8 kilowatt (kW) inline air heater (Slyvania, Threaded in-line air heater 6kW model operated as 1.8kW by utilizing a 120V/15 ampere [amp] power supply) installed immediately outside the column. Power to the heater was controlled by manually adjusting a variac power source. For all experiments reaction air was supplied to the air plenums from laboratory air lines, controlled by an inline regulator and throttling valve and measured using an inline rotameter and pressure gauge.

Ignition status and reaction front propagation was monitored using 1.5 millimetre (mm) diameter Type K Inconel thermocouples (Omega) connected to a data acquisition system (Multifunction Switch/Measure Unit 34980A, Agilent Technologies) recording temperatures at five second intervals throughout the tests. In the quartz column (Experiments 1 through 4) thermocouples were inserted into the column packing, clean sand layers, and air plenum space vertically through the top of the column (see Figure 3.2a). In the stainless steel column (Experiments 5 through 8)

thermocouples were installed horizontally through bored-through compression fittings installed at discreet depths along the column wall (see Figure 3.2b). In each column configuration, temperature in the air plenums were measured using thermocouple(s) placed immediately beneath the screens.

CO_2 and volatile organic compound concentrations were monitored in Experiment 8 using a portable analyser (MultiRAE IR). The analyser was connected to a sample line connected to the exhaust port of the column, and was equipped with internal data loggers.

Figure 3.3 presents a photo of the convective test apparatus with external inline heater. Experiment specific layouts of the screen, heater, diffuser and thermocouple locations as well as packing arrangements, heater power and air flow details are provided in Appendix A. All experiments were conducted within laboratory fume hoods at the University of Western Ontario.

Figure 3.3: Convective ignition apparatus with external inline heater (Experiments 5 through 8).

3.2.2 Results and Discussion

Ignition of a smouldering combustion reaction was achieved in all experiments. Selected data is presented herein and detailed experimental summaries including plots of full datasets for all experiments are provided in Appendix A.

In Experiment 1, preheating for ignition was performed by manually manipulating the air flow rate (between 25 and 62 lpm) to maximize temperature observed in the air plenum thermocouples. Temperatures in excess of 400^{o}C in the thermocouple located 1 cm above the air plenum (ignition condition for similar materials characterized through conductive ignition

experiments to be 400^{o}C measured 1 cm above the heater [3]) were observed following approximately 30 minutes of preheating. After 51.5 minutes of preheating, temperatures at the 1 cm thermocouple of the column began to exceed the temperatures observed within the air plenum, providing evidence of exothermic processes (i.e., smouldering reaction, Figure 3.4). This crossover point was observed at a temperature of 535 ^{o}C; however an upwards inflexion in curvature of the heating profile in thermocouples located at 1, 2 and 3 cm above the air plenum, also indicative of initiation of smouldering [7], occurred at temperatures around 450-475 ^{o}C. This inflexion in temperature occurs as a very smooth, 'automatic' transition in contrast to the sharp increase in temperatures reported at the onset of air flow during conductive ignitions of similar materials (Figure 2.3, [3] [5]).

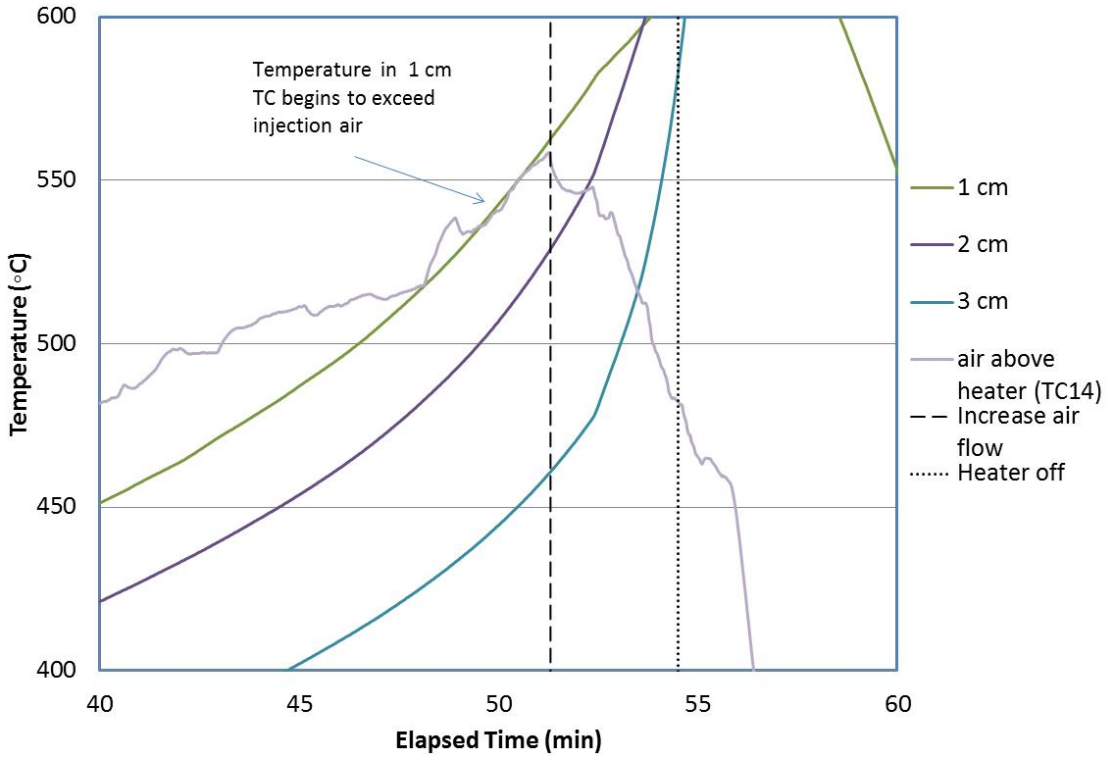

Figure 3.4: Zoomed in portion of thermocouple data versus elapsed time for Experiment 1. Cross over of 1 cm thermocouple data with 'air above heater' (air plenum) temperature confirms ignition of an exothermic smouldering reaction. Full test thermocouple data in Figure 3.5.

At 51 minutes, the injection air flow rate was increased from the preheating rate of approximately 25 lpm (3 centimetres per second [cm/s], as Darcy flux) to approximately 62 lpm (7 cm/s) and temperature spikes in excess of 800^{o} C were observed, consistent with previously reported smouldering profiles for these materials (Figure 2.3; [3] [5]). The heater was powered off following 54.5 minutes and the reaction was observed to progress upwards through the column to the top of the contaminated sand pack, travelling approximately 12 cm over the course of a 15 minute period (Figure 3.5).

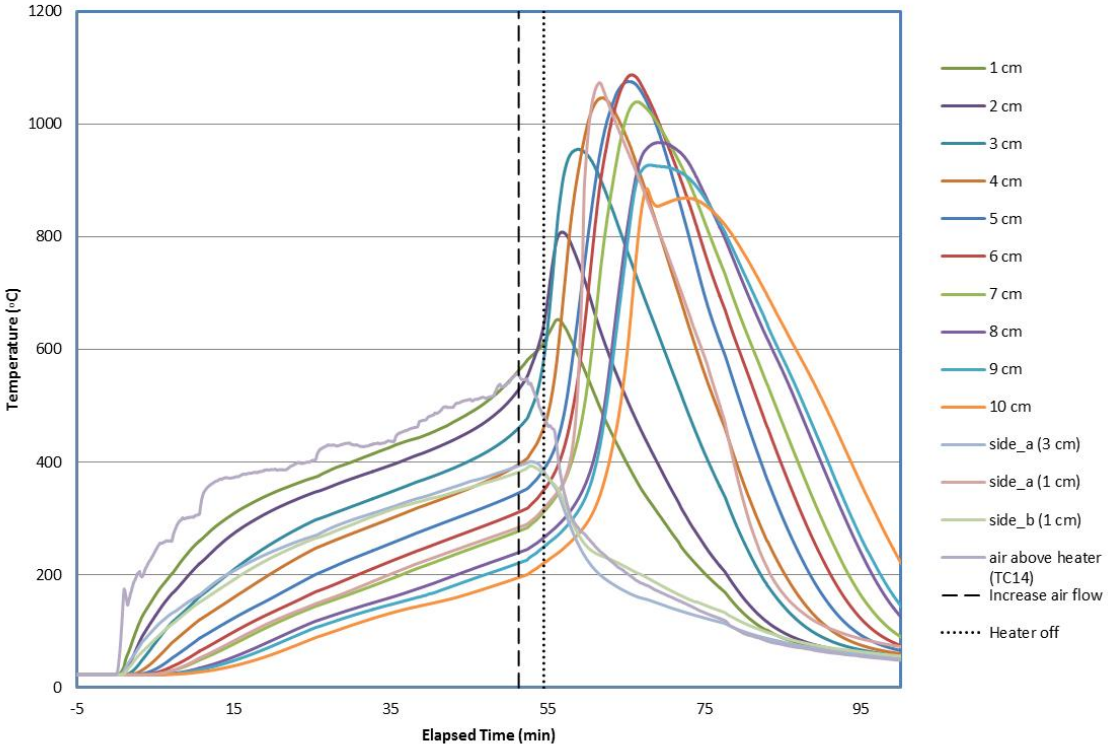

Figure 3.5: Temperature versus elapsed time profiles for Experiment 1. "x cm" indicates thermocouple location x cm from the screen (along the central axis of the column unless otherwise indicated).

Experiment 2 was performed using two identical cable heaters coiled into the air plenum space, and the air injection rate was held at a constant rate of 41 litres per minute (Darcy flux of 4.6 cm/s) throughout preheating and propagation of the smouldering reaction. Three thermocouples were located along a plane 1 cm above the screen (one on the central axis and one each on either side located approximately one half of the radial distance between the central axis and outer column wall). An inflexion in the temperature trends, indicative of combustion, was observed in the 1 cm thermocouples following about 15 minutes of preheating at a temperature ranging from approximately 400-445 ^{o}C (Figure 3.6). At t=16 minutes, temperatures at one of the off-centre, 1

cm thermocouples began to exceed that of the injected air at temperatures near 600 ^{o}C. At t=17 minutes, the heater was turned off and the reaction propagates through the column (Figure 3.6).

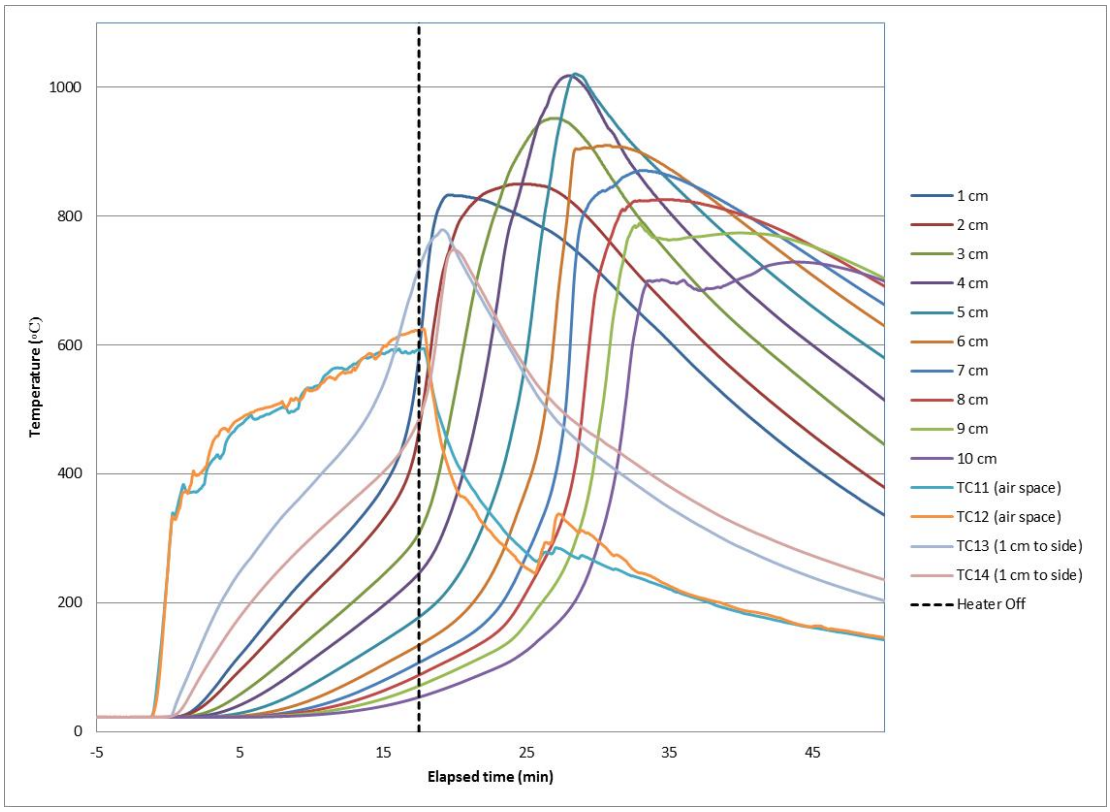

Figure 3.6: Temperature versus elapsed time for Experiment 2.

Experiment 3 was performed under fully water saturated conditions. Air flow rates were manipulated manually between 20 and 60 lpm to maximize air plenum temperatures. Ignition of smouldering was achieved following approximately 120 minutes, though failure (and subsequent repair) of the heater elements during preheating contributed to this extended heating duration.Self-sustained smouldering was observed at lower peak temperatures (approximately 700^{o}C) following approximately 150 minutes (Figure 3.7).

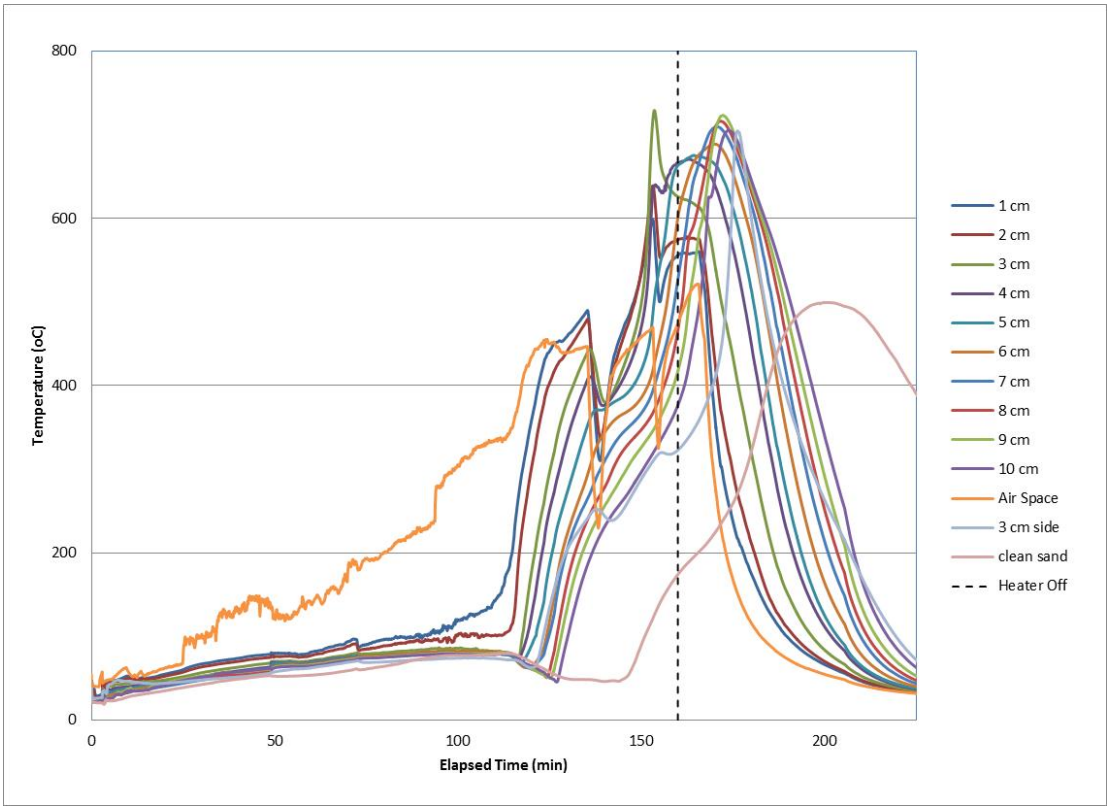

Figure 3.7: Temperature versus elapsed time for Experiment 3

A potential contributing factor for the very rapid ignition observed in Experiment 2 is that heat transfer to the media occurred not only convectively via the movement of the injected hot air, but also via direct radiation from the heaters due to their proximity to the media, and the minimal shadow provided by the screen. Experiment 4 was performed with a 7 cm thick clean sand layer placed between the screen and the contaminated media to minimize heat transfer via radiation and to demonstrate proof of concept of ignition though convective heating alone. In Experiment 4; ignition was observed following 55 minutes of preheating (heater turned off after 57 minutes) at air flow rates from 40 to 60 lpm (Figure 3.8).

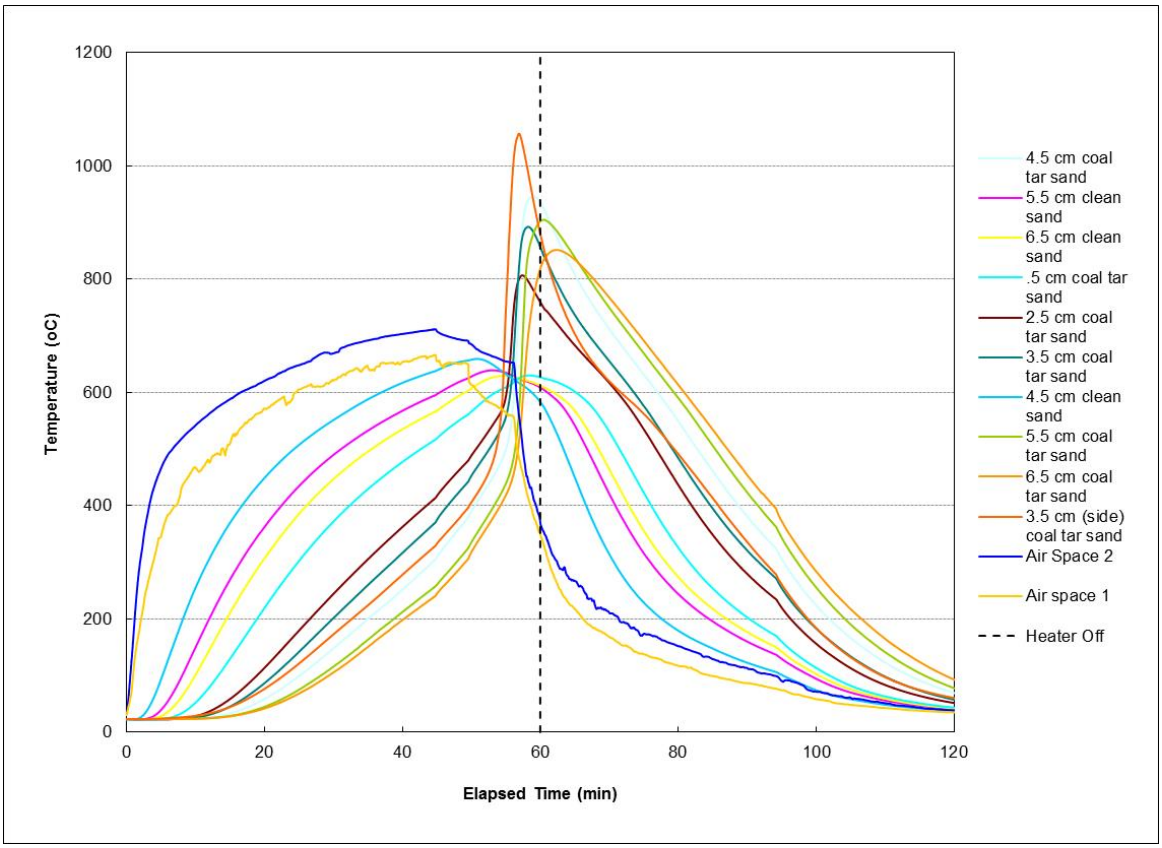

Figure 3.8: Temperature versus elapsed time for Experiment 4.

Experiments 5 through 8, repeat experiments (slight variations in air flow rate between 60 and 80 lpm, and otherwise varying only packing height), used the stainless steel column with external inline heater designed specifically for convective ignition testing. In each experiment, ignition of smouldering was achieved by injecting externally preheated air. Convective ignition, defined as the first observation of media temperatures exceeding air plenum temperature occurred in Experiments 5, 6, 7 and 8 following approximately 58, 62, 55 and 60 minutes respectively. Figure 3.9 shows the thermocouple profiles for Experiment 8, which also included collection of CO_2 as a further indicator of the smouldering reaction.

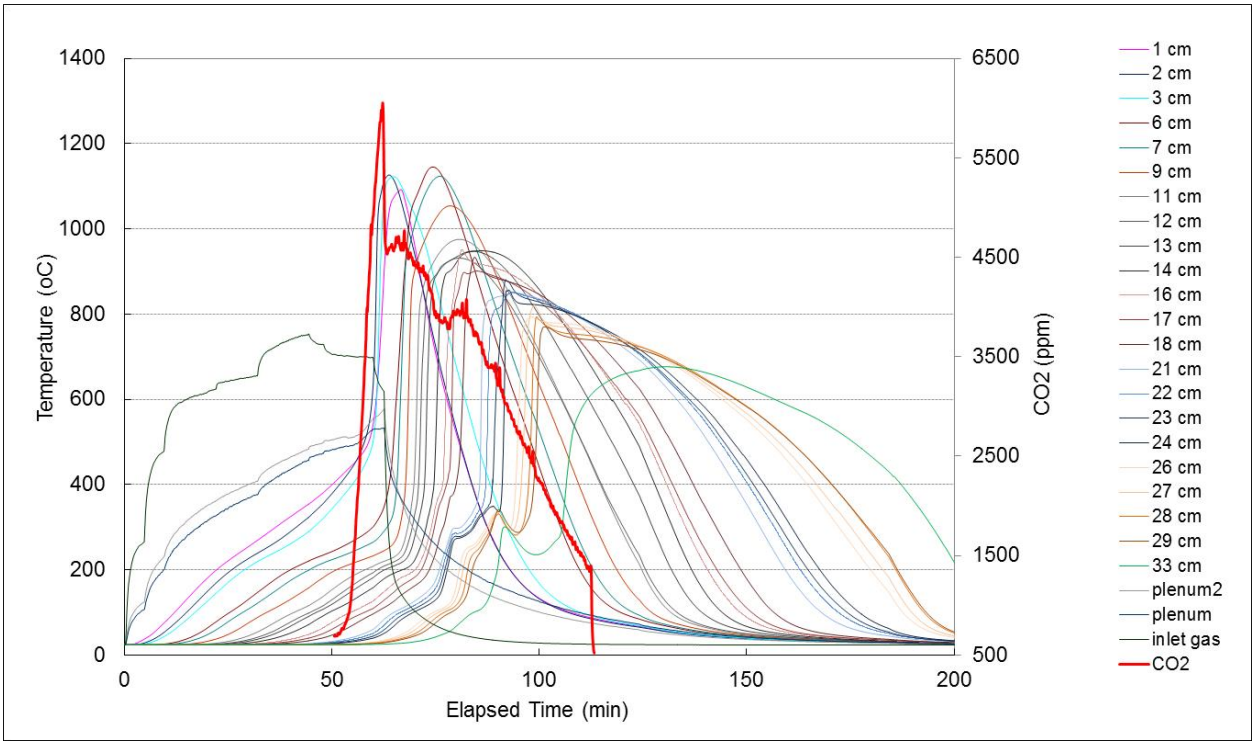

Figure 3.9: Temperature versus elapsed time, and carbon dioxide data for Experiment 8.

The gaskets sealing the modular sections of the column were continually compromised during Experiments 5 through 8, evidenced by visible leakage of vapours and liquid product on the outside of the column at the flange locations. This leakage may have affected the peak temperatures of the reaction in the upper section of the column due to reduced air flow.

During the ignition process, the voltage output of the variac transformer was adjusted manually to slowly increase the injected air temperature. The maximum heater output of the inline heater was 1152 W or a heat flux of approximately 57 Watts per square meter (W/m^2). The total energy supplied for ignition was estimated for Experiments 5 through 7:

$$E_{igntion} \approx 3.6 \times \sum_{i=0}^{n} etime_i \times \%_{variac_i} \times V_{supply} \times A_i \quad \textbf{[3.1]}$$

Where:

$E_{igntion}$ is the total energy supplied for ignition in kilojoules (kJ);
$etime_i$ is the elapsed time for time step *i* in hours*;*
$\%_{variac}$ is the variac transformer voltage output for time step *i* in percent;
V_{supply} is the maximum supply voltage connected to the variac in volts (V, 120 V);
A_i is the amperage for time step *i* given by I = V/R (R = 8 ohms); and
3.6 is a conversion factor from watt hours to kilojoules (kJ).

The estimated energy for ignition for Experiments 5, 6 and 7 was 4028, 4124, and 4240 kJ respectively, for an average energy supplied for ignition of 4131 kJ (calculations in Appendix B). A conductive ignition test performed in the same column on similar materials (Appendix A) achieved ignition following approximately 40 minutes of preheating, and supplied a total of 813 kJ of energy to the ignition process (Appendix B). It should be noted that in each case, the energy calculated is the total energy supplied for ignition, and not the energy required for ignition (i.e., neither process is optimized, nor are heat losses considered). Figure 3.10 compares the rate of heating at 2 cm into the contaminated media in convective Experiment 8 and a conductive ignition experiment performed in the same column on similar materials (data in Appendix A).

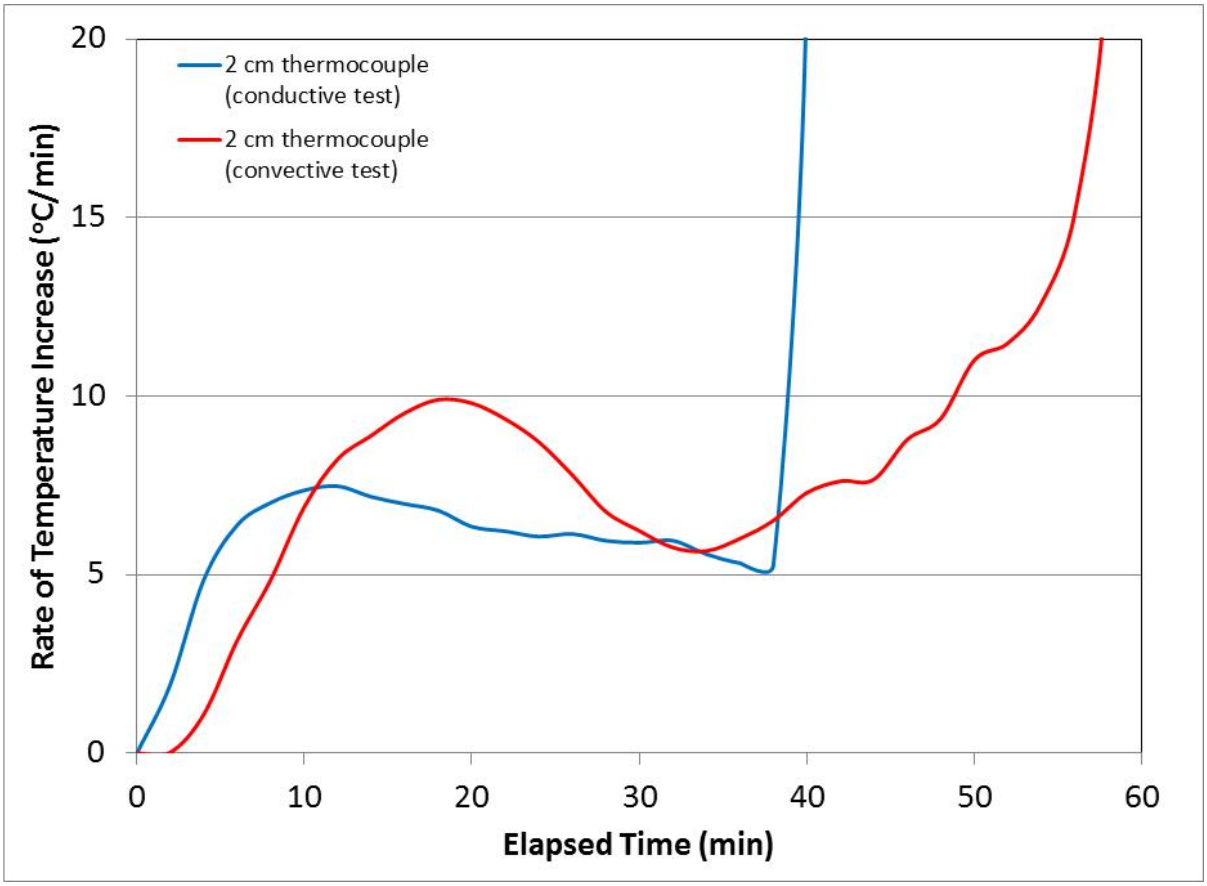

Figure 3.10: Comparison of the rate of heating (2 cm into column) for a conductive and convective column test. Convective test data from Experiment 8, conductive test data from an experiment run on similar materials within the same column. All data available in Appendix A.

The two heating methods show a similar profile at the 2 cm thermocouple, with initial heating rates increasing rapidly in the first ten minutes of heating to between 6 and 10 ^{o}C/min where they plateau until ignition. The ignition point in the conductive experiment is characterized by a very sharp increase in heating rate at approximately 40 minutes when air flow is initiated, while the conductive case transitions into ignition heating rates more gradually between 50 and 60 minutes into the test. Figure 3.11 presents the temperature profile with depth in the column at the point of ignition for the same conductive and convective ignition tests.

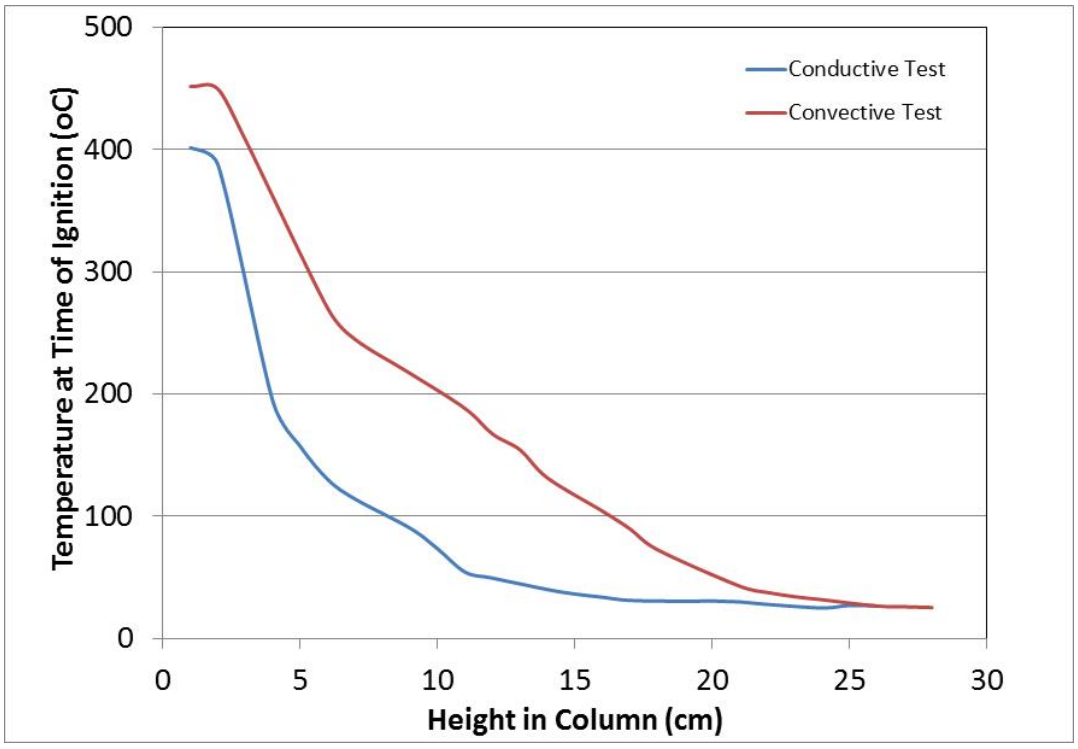

Figure 3.11: Temperature profiles as a function of height in column at the time of ignition for the conductive (40 min into heating) and convective (60 minutes into heating) column tests from Figure 3.10. Full data provided in Appendix A.

Comparison of the temperature profiles at the time of ignition demonstrates that the convective method heats a much greater portion of column in advance of ignition. This increased heating zone is likely the primary factor associated with the observed difference in ignition energy supplied between the conductive and convective tests. Although this may result in a higher energy supply at the column scale, a larger preheated zone may be beneficial to a field scale application where a greater volume of material at ignition temperatures will result in a more robust smouldering reaction.

3.3 In Situ Field Trial Ignitions and Heater Development

Laboratory experiments successfully demonstrated convective ignition of coal tar contaminated sands, and that the relative power requirements of a convective ignition were acceptable (Section 3.2). Convective ignition was thus the selected ignition approach for *in situ* field trials of the STAR technology. Two field scale trials, referred to as Phase II (Shallow Test) and Phase III (Deep Test) were conducted at a former industrial facility in Newark, New Jersey. The Phase I trial was the initial proof of concept test performed at the same site [Section 2.2.4], which utilized the Design A heaters in a conductive ignition configuration. The following sections in this chapter detail the ignition field equipment and protocol development, and results of ignition events during the field trials, while Chapter 4 provides a detailed description of the site, test cell layouts and instrumentation, methods and results of the tests, Appendix C presents photographs from the field trials. Pertinent details on the Site and test configurations are summarized below.

Local geology at the site consists of five unconsolidated geological units which sit above an underlying shale bedrock. The geologic units, in descending order from ground surface are: (1) shallow fill unit, generally less than 6 meters (m) thick and consisting of heterogeneous fill materials and debris; (2) 'meadow mat', a semi-confining peat and clay unit ranging from 0 to 8m thick; (3) alluvium, or 'deep sand' layer, consisting of relatively uniform medium to coarse grain sands up to 10m thick; (4) lake bottom deposits, consisting primarily of sands and silts approximately 15m thick; and (5) glacial till unit, approximately 6m thick terminating at the shale bedrock. Groundwater is encountered at a depth of about 1m below ground surface (bgs) at the site. Historical industrial activities resulted in wide spread coal tar distribution, with mobile coal tar NAPL present in several areas across the 16 hectare site, primarily within the fill

and meadow mat units and extending into the deep sand unit in areas where the meadow mat may be discontinuous/ absent.

All field trials were performed in a former chemical storage lagoon area at the site. The Phase II trial developed the convective ignition protocol using an electrical resistance heater referred to as Design B (Section 3.3.1). The Phase II trials (performed in the same test cell as the Phase I trial) were performed in the shallow fill unit within a 6 m by 18 m cell contained by a sheet pile barrier keyed into the underlying meadow mat, and covered by a gravel vapour collection layer and lean concrete cap at ground surface. A series of nine ignition wells (IP-1S thought IP-9S) were installed along the centre line of the test cell with 30 cm screen intervals terminating at the top of the meadow mat (approximately 2.9 m bgs). The two ignition wells on the ends of the cell (IP-1S and IP-9S) were originally installed with the Design A heaters for Phase I and were reused (Design A heaters abandoned in place) as standard ignition wells in the Phase II testing.

Following the Phase II test, a custom designed cartridge heater, referred to as Design C, was developed and tested to provide a more robust and efficient ignition process (Section 3.3.2), that was then used in Phase III testing (Section 3.3.3) on the deep sand unit at the site. The deep test was performed in an adjacent test cell to the Phase II cell within the same former lagoon. The deep test was performed under natural groundwater flow conditions (i.e., cell not contained by sheet piling) through a centrally located ignition well (IP-5D) within a 15 m by 15 m vapour collection/cap.

Table 3.2 summarizes the field trial phases and corresponding ignition systems. In all field trials, ignition and propagation of the smouldering combustion reaction was inferred through temperature data collected from a series of subsurface thermocouples, and from combustion gases (CO_2 and carbon monoxide [CO]) detected in vapours collected under vacuum from the gravel vapour collection layers beneath the cell caps. Photographs from each of the field trials are provided in Appendix C.

Table 3.2: Summary of Field Trial Phases, Ignition Methods and Heater Designs

Phase	Test Name	Geologic Unit	Ignition Method	Heater Design	Heater Description	Details
I	Proof of concept test	Fill	Conductive	Design A	direct buried ~5kW electric resistance coil (around ignition well)	Section 2.2
II	Shallow test	Fill	Convective	Design B	down well heaters consisting of 1.95 - 4.1 kW electrical resistance elements	Section 3.3.1 (ignition process), Chapter 4 (overall test results)
III	Deep test	Alluvium	Convective	Design C	down well heaters consisting of 9kW cartridge heater with custom heat sinks	Section 3.3.2-3 (ignition process), Chapter 4 (overall test results)

3.3.1 Phase II Field Trial – Shallow Test

For the Phase II field trial, a convective ignition apparatus was developed utilizing a down well heating source designed to:

1. Heat injected air to temperatures in excess of 400^{o}C for delivery to the subsurface;
2. Be deployable within a standard 5 cm diameter steel well; and
3. Be removable and reusable for multiple ignition events.

The first generation convective heater, Design B, consisted of a 1.95 kW electrical resistance down-well heater (Figure 3.12). The heated section consisted of three 60 cm long U-shaped Inconel 800 elements, 0.8 cm in diameter, connected to a riser pipe to convey the electrical cables to ground surface. The total power output of the heater was limited by the heater watt density (maximum of ~23 kW/m^2 of element surface area, determined by the manufacturer) and the element lengths.

Figure 3.12: Photograph of two Design B convective heating elements. The 1.95 kW versions shown were replaced by longer 4.1kW models for the final Phase II ignition.

The heater was inserted into the ignition well which was fitted at ground surface with a standard cross fitting and blow out preventer valve through which the heater riser pipe passed. The gasket of the blow out preventer valve sealed around the riser pipe of the heater allowing the well to be pressurized by air injected through one of the horizontal ports of the wellhead cross (the final port was equipped with a pressure gauge). The heater element was equipped with two thermocouples; one clamped directly to the element surface to read ‘skin temperature’ and one

spaced between elements to measure temperature of air being injected into the subsurface. Figure 3.13 presents a photograph of the Phase II test cell layout in which the heater can be seen exiting the well head apparatus in the foreground.

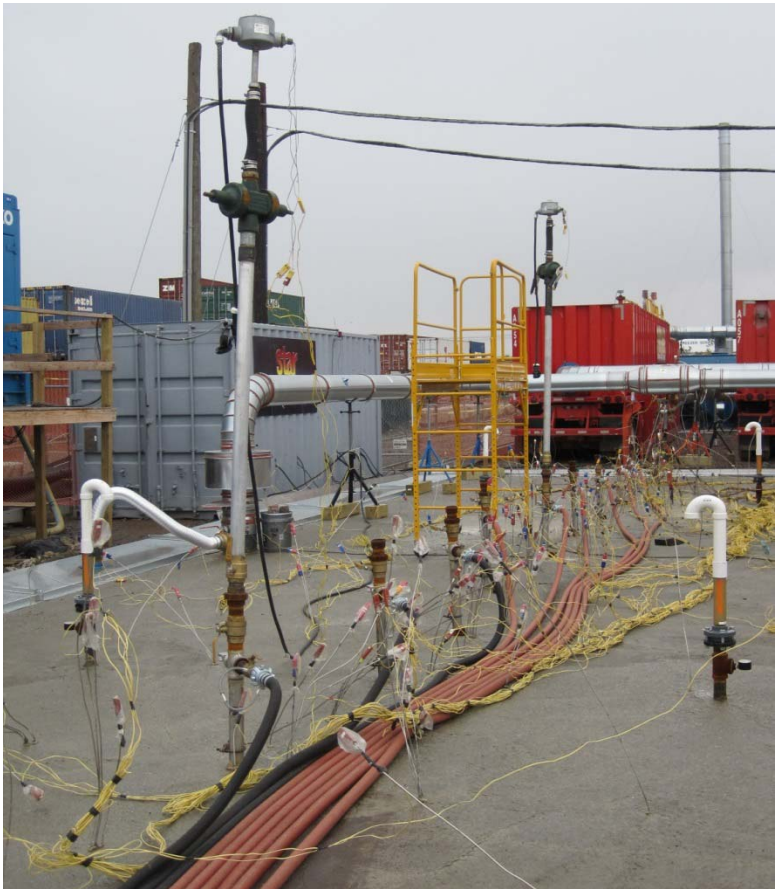

Figure 3.13: Photograph of Phase II field trial layout. Ignition well in foreground shows heater installed in well with air injection line connected to well head. Yellow cables connect subsurface thermocouples to data logging system.

Complexities associated with air injection geometry, buoyancy effects, and heat transfer and losses to infrastructure, and subsurface materials (including dynamics of the influx of groundwater) limit the ability to scale laboratory heat fluxes required for ignition to the field application. However, it can be generalized that the heat transferred to the subsurface is a function of the volume and temperature of injected air, which in turn is a function of the heater

power, maximum operating skin temperature of the element(s), and efficiency of the heater elements to transfer their heat to the injected air.

During the initial Phase II initial field mobilization, ignition protocols were tested by attempting ignitions with a variety of air injection rates, air injection pressures, heater placement depths, heater skin temperature set points and pre-heating durations. The maximum operating skin temperature of the resistive heating elements was approximately 650^{o}C (based on manufacturer recommendations), beyond which internal components of the heater became unreliable and heater life was severely limited.

Ideally, heater output would be sufficient to heat injected air beyond the targeted ignition temperature (400^{o}C) at a volumetric flow rate that could support combustion, such that materials would 'self–ignite' when a critical mass of material was at the ignition temperature (as observed in the convective column experiments). The alternate approach, is a 'timed ignition', in which the air injection rate during preheating is kept low in order to increase the temperature of injected air until a critical volume of material reaches (or is assumed to have reached) the target ignition temperature, and then increasing the air flow rate to provide sufficient oxygen to initiate and support combustion. The first approach (self-ignition) is limited by heater power and efficiency, while the second approach is limited in the field by the ability to instrument the subsurface sufficiently (i.e., install enough thermocouples) to accurately determine when to increase air flow rates.

Detection of combustion gases in extracted vapours was frequently used during *in situ* testing to detect ignition and quantify contaminant mass destruction rates (preferentially to subsurface temperature data as thermocouples were not always located where ignition occurred). The coal tar destruction rate can be estimated based on stoichiometric calculations using the combustion gas concentrations and volumetric flow rate of extracted vapours (described in detail in Section 4.3).

A total of 9 preheating/ ignition attempts were made during the initial mobilization of the Phase II trial. Of these 9 attempts, four resulted in successfully ignited smouldering reactions which lasted on the order of several hours, while the other five attempts were abandoned due to inadequate preheating, heater failure, or auxiliary (e.g., compressor) failure. Figure 3.14 presents the coal tar destruction rate versus time for the four ignition events attempted during the initial ignition protocol testing period of Phase II. With the exception of abandoned conductive heaters in IP-1S and IP-9S, all ignition wells had identical construction and depth, though significant heterogeneity in fill exists at the site.

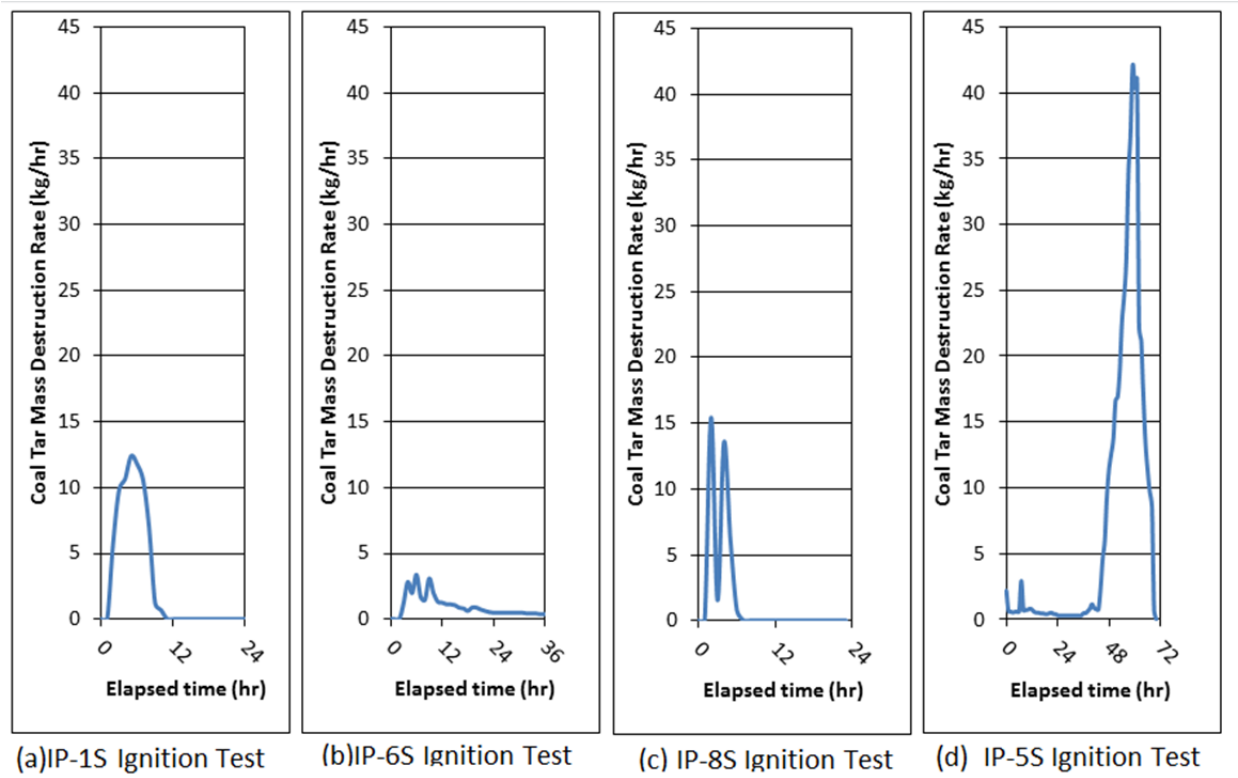

Figure 3.14: Ignition events during Phase II ignition protocol testing. Coal tar mass destruction rate is calculated using combustion gas and extraction flow rate data (described in detail in Chapter 4).

The ignition event at IP-1S (Figure 3.14, a) was achieved after increasing the injected air flow rate following 39 hours of preheating at a low air flow rate. The ignitions at IP-6S (Figure 3.14, b) and IP-8S (Figure 3.14, c) were achieved by increasing air injection rates following 51.5 and 43 hours of preheating respectively. Each of these ignitions were characterized by initial rapid rates of mass destruction followed by diminishing combustion gas levels likely as a result of insufficient critical mass of heated material to achieve a strong and self-sustaining ignition. During the IP-5S ignition event, a heater was operated at IP-5S and self-ignition was observed after approximately 19 hours of preheating (Figure 3.14,d). The initial reaction was relatively weak and progressed (likely through a preferential pathway) for a period of approximately 36 hours before increasing in strength and demonstrating very high rates of mass destruction

indicating a robust smouldering reaction; however, a leak in a seal between sheet pile walls resulted in incomplete capture of vapours and the reaction had to be terminated prematurely.

Following the ignition protocol testing period, the vapour collection system was repaired and a second field deployment undertaken. The second deployment utilized a similar heater design; however, the heater power was increased to 4.1 kW in an attempt to increase the volume of preheating air to promote self-ignition. This power increase was achieved by extending the heated section to a length of 120 cm in order to keep the watt density of the heaters at 21 kW/m^2. During the second deployment of Phase II field trial, self-ignition was observed following approximately 12 hours of preheating at IP-5S. The ignition at IP-5S resulted in a robust smouldering reaction which propagated in a self-sustaining manner throughout the southern portion of the test cell over a period of 10 days. Chapter 4 presents the results of this phase of the pilot testing program in detail.

3.3.2 Heater Bench Testing – Design C

The results of the Phase II *in situ* pilot testing demonstrated that self-ignition was the most reliable method for ensuring a robust ignition. In order to reduce preheating times, and further increase pre-heated injection air volumes, a revised heater design was developed and tested in advance of further field trials. As noted, heat transferred to the subsurface is a function of the volume and temperature of injected air, which in turn are functions of the heater power, maximum operating temperature, and the ability of the heater elements to transfer their heat to the injected air. Maximum skin temperature is a limitation of the materials used for construction, and use of high grade stainless steels alloys (selected for both temperature resistance and

corrosion resistance) was maintained through the development process. Ceramic materials were considered as they can achieve higher maximum temperatures, but they are not suitable for the high moisture environment typical of an *in situ* application.

The Design B elements were limited by a maximum operating watt density (recommended by the manufacturer to be 23kW/m^2), as well by their general geometry for heat transfer. The Design C heater was developed in collaboration with Heatron Inc. of Leavenworth, Kansas and consisted of a 1.9 cm diameter stainless steel cartridge heater encased in a customized heat sink to promote injected air to more efficiently 'shed' the heat off the element's surface. Cartridge heaters are typically designed to operate at higher watt densities, thus a 9 kW heater was achievable within a 1.9 cm diameter element approximately 90 cm long. The cartridge heater had a recommended maximum skin temperature of 700^{o}C. Heat sinks were designed to clamp to the cartridge heating element and promote air flow between heat sink fins before being injected into the subsurface through the well screen (Figure 3.15).

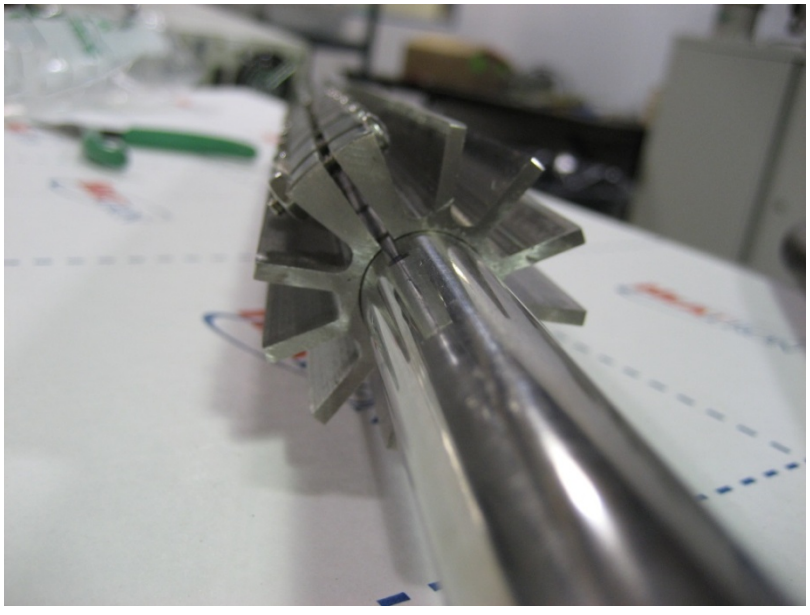

Figure 3.15: Photograph of Design C cartridge heater element with customized heat sink.

An above ground testing apparatus was developed to directly compare performance of the Design B and C heaters. The apparatus was designed to simulate the operation of the heater within a well (Figure 3.16), though in a horizontal configuration. The objective of the test was to quantify and compare skin temperatures, injected air ("well screen") temperatures and injected air volumes between the heater designs.

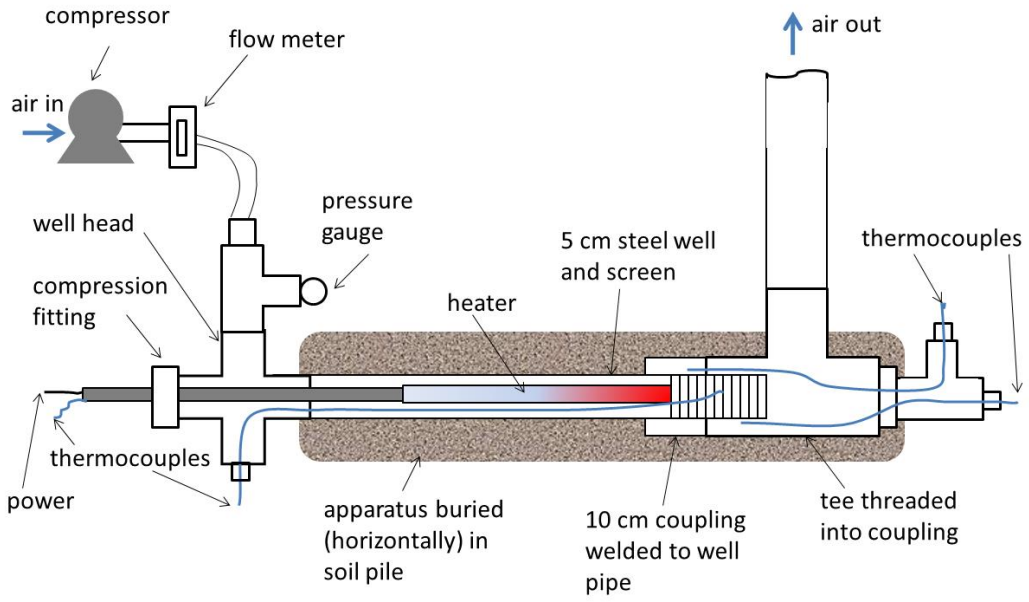

Figure 3.16: Schematic of above ground (horizontal) heater testing apparatus.

Figure 3.17 presents the results of the heater testing. The Design B heater, operating at a skin temperature of about 650^{o}C, was able to preheat approximately 12 standard cubic meters per hour (m^{3}/hr) of air to a maximum temperature of 350^{o}C at the well screen. The Design C heater, operating at a skin temperature of up to 700^{o}C, was able to preheat over 70 m^{3}/hr of air to a maximum temperature of 675^{o}C at the well screen. The significantly smaller difference in

temperature between skin and well screen air temperatures observed for the Design C heater is attributable directly to the heat sink design.

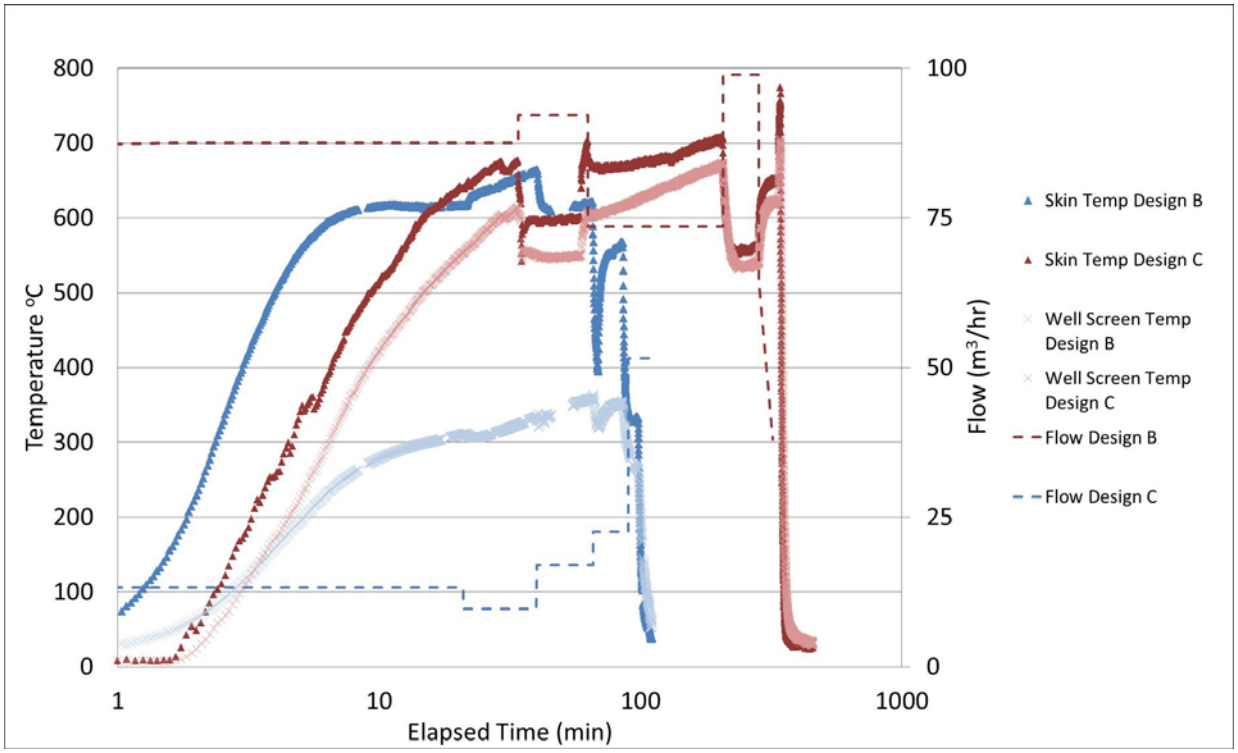

Figure 3.17: Skin and well screen temperature and air flow rate data from above ground heater testing program.

Field conditions will present significant variability (e.g., water saturation, back pressures, etc.,) which will affect the absolute values presented in Figure 3.17, but direct comparison between the original and newly designed heaters in the above ground testing program demonstrates a significant improvement in heater design. Table 3.3 summarizes the heater performance of the Design B and C heaters as well as the in- line heater used for laboratory convective ignitions (Experiments 5 to 8, Section 3.2), with a normalized power demand, defined for comparison purposes, as the wattage required to increase air 1 degree C flowing at a standard cubic meter per minute ($Wmin/m^{3o}C$). Table 3.3 reveals that Design C exhibits the lowest normalized power

demand, meaning it was the most efficient and/or effective heater. Based on the results of the above ground heater testing, heater Design C was selected for future *in situ* STAR field trials.

Table 3.3: Convective Heater Comparison Summary

Heater	Maximum Power Output (W)	Maximum Temperature Increase of Injected Air (^oC)[1]	Injected Air Flow Rate (m^3/min)	Normalized Power Demand (Wmin/$m^{3o}C$)
Laboratory inline heater	1150	620	0.08	23.2
Design B Heater	4100	320	0.28	45.8
Design C Heater	9000	645	1.12	12.5

notes:
[1] - temperature increase assumes an inlet air temperature of 30^oC

3.3.3 Field Application 2 – Deep Sand Test

Phase III of *in situ* testing of STAR at the New Jersey Site was completed in the summer and fall of 2012 utilizing the Design C heater. The well and well head design utilized in the Phase III testing was identical to the Phase II setup (Figure 3.3). Figure 3.18 presents thermocouple and combustion gas data for the ignition event in the deep test. Self-ignition was achieved as evidenced by spikes in combustion gas concentrations following only 90 minutes of heater operation during the first ignition attempt.

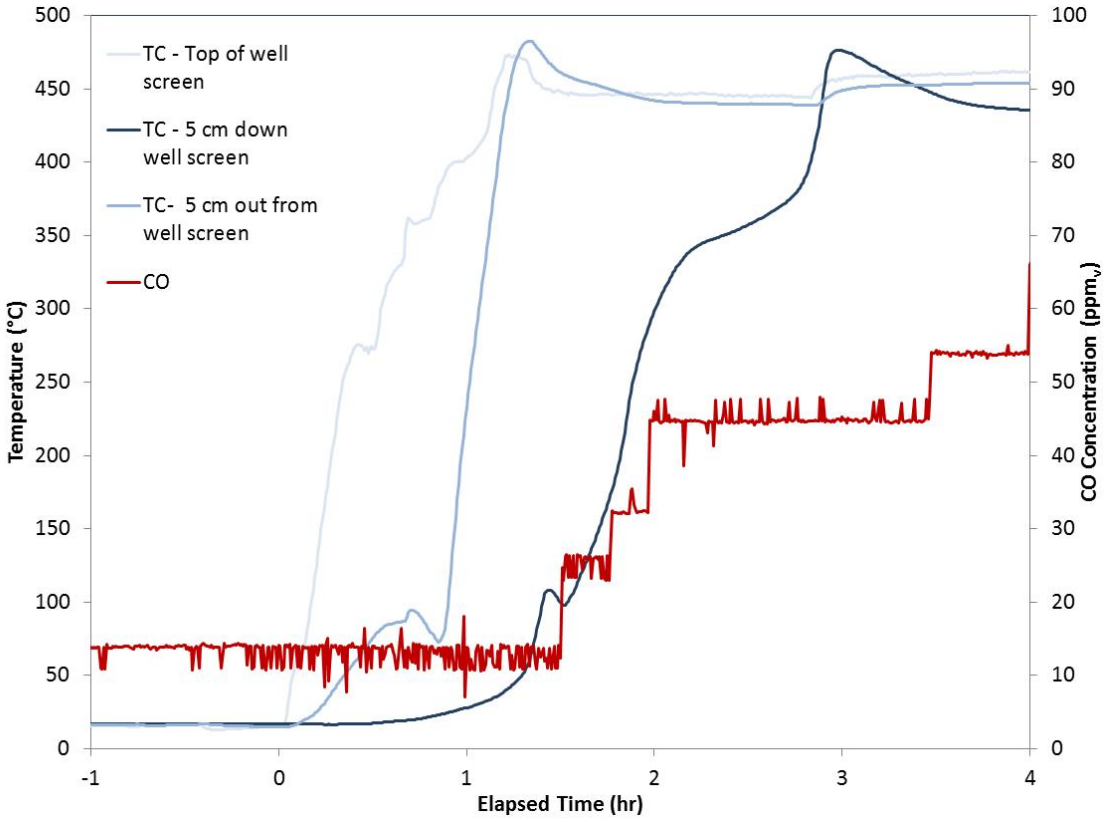

Figure 3.18: Ignition event during Phase III, deep test. Using heater Design C, 'self-ignition' was achieved following only 90 minutes of preheating. Temperature data from 3 thermocouples located at: the top of the well screen; 5 cm down the well screen; and 5 cm radially out from the well screen are shown to rapidly increase in temperature following between 0 and 90 minutes of preheating. A coincident spike in CO concentrations (as measured in vapours collected at ground surface) is observed following 90 minutes indicating the onset of combustion.

The single ignition event initiated a robust self-sustaining smouldering reaction which propagated to the outer limit of the 7.5 m diameter thermocouple monitoring network over the course of 10 days of operation. Chapter 4 describes the test and results in detail.

3.4 Conclusions

Laboratory proof of concept experiments demonstrated that ignition of a smouldering reaction of coal tar-contaminated sands is achievable using a convective heating process. The method was

demonstrated at the laboratory scale to ignite materials through a clean lens of sand and in a fully water-saturated condition encouraging use of the method under *in situ* field conditions.

The convective heating method was developed for the field scale to be applied through standard construction 5 cm diameter wells utilizing a removable and reusable down-well heater. Successful ignition was achieved under field conditions, and it was determined through multiple ignition attempts that 'self- ignition', by which the reaction initiates during the heating process without changes to the air flow rate, leads to the most robust and sustainable smouldering reactions.

Heater design improvements lead to higher volumes of higher temperature air being injected into the subsurface. Above ground testing of the revised design demonstrated a more than 3-fold reduction in normalized power demand from the original convective heater. The newly developed convective heaters were able to achieve self- ignition in the subsurface in 90 minutes in two separate field tests.

The convective ignition method will serve to reduce costs of STAR field implementation by:

1) Reducing drilling costs by enabling the use of smaller diameter boreholes;
2) Reducing heater costs by being reusable, and deployed such that the heater is not exposed to a corrosive environment; and
3) Reducing operational time by reducing time to ignition.

The convective ignition method was utilized exclusively in field pilot testing of the STAR technology at the New Jersey Site in both the shallow fill materials and deeper sand unit. The results of the field testing program are described in detail in Chapter 4.

4 Smouldering Remediation of Coal Tar Contaminated Soil: Pilot Field Tests of the STAR Technology

4.1 Introduction

Coal tar and creosote (composed of various coal tar fractions) are a class of non-aqueous phase liquids (NAPLs) that consist of a complex mixture of aliphatic and aromatic compounds produced as a by-product of historical manufactured gas plant operations and blast furnace coke production [9] [28]. Coal tar is classified as a human carcinogen [11] [29] and over 1,500 coal tar waste sites are listed by the USEPA [29] with many of them near or within heavily populated areas.

There are few remedial technologies capable of rehabilitating coal tar and creosote contaminated sites to applicable standards [3]. This is because they exhibit a combination of physical and chemical properties that make them unsuitable for most treatment processes. They exhibit low densities (1,010 to 1,100 kg/m3) and viscosities (20 to 100 cP) that allow continued migration over long periods and lateral distances after release [9] [2] and make them resistant to removal via pumping-based technologies. In addition, coal tar and creosote are composed of both large aromatic and long-chain hydrocarbons, which are resistant to biodegradation [12] and, due to high boiling points, unsuitable for volatility-driven technologies such as soil vapour extraction. Frequently, coal tar source areas are treated via excavation and disposal or encapsulation [3].

Thermal remedies such as *in situ* thermal desorption may be used on coal tar sites in two modes: low temperature (up to 100°C) which volatilizes lighter compounds but leaves heavier

components behind, or high temperature (greater than 100°C) [16] which can require significant energy input [13]. Surfactant-enhanced in situ chemical oxidation has recently been reported to show some promise for reducing coal tar concentrations in soil and groundwater [17] but this approach, like all amendment-based remediation approaches, relies on effective contact between the injected amendment and the NAPL, which is challenging in most subsurface environments. An effective, low-cost *in situ* remedial option for coal tar and creosote has been unavailable to date.

Recently, the concept of NAPL remediation via smoldering combustion was introduced [3] [5]. Smoldering combustion is an exothermic oxidation reaction that occurs on the surface of a condensed (i.e., solid or liquid phase) fuel, converting organic material into primarily heat, carbon dioxide, and water [6]. Glowing red charcoal in a barbeque is a typical example. Smoldering is an oxygen limited reaction that has been well documented for solid porous materials (e.g., fibrous materials, coal, and polyurethane foam) [22] [6] [21]. Pironi et al were the first to demonstrate that smoldering of an organic liquid (i.e., NAPL) embedded within an inert porous matrix was possible [18]. That work also demonstrated that the reaction would continue in a self-sustaining manner (i.e., continue in the absence of external energy input following a one-time, local ignition) and would completely destroy the NAPL as long as an oxidant (oxygen in air) and fuel (NAPL) were in sufficient quantity.

Switzer et al. (2009) demonstrated remediation via smoldering destruction in a series of laboratory column experiments for synthetic mixtures of coal tar and sand and for coal tar contaminated soils taken from field sites [3]. These experiments characterized the conductive

ignition method required to initiate the smoldering reaction, the ignition protocol for coal tar mixtures (i.e., rate of heat energy and air flux required to initiate smoldering), and the controllability of the smoldering process through manipulation of the air injection rate. A suite of column experiments by Pironi et al (2011) demonstrated that a minimum NAPL content was required to support self-sustaining smoldering [5]. It also demonstrated that (1) the velocity of the smoldering front, and thus the mass destruction rate, was linearly related to the air injection rate, and (2) water content of up to 75% of pore space reduced peak temperatures but did not impede self-sustainability of the reaction for both coal tar and crude oil NAPLs [5].

The commercial application of smoldering combustion to treat NAPLs (including coal tar and creosote) is referred to as the Self-sustaining Treatment for Active Remediation (STAR) technology. STAR treatability testing, performed in laboratory columns for 15 soils extracted from contaminated sites, demonstrated successful self-sustaining smoldering that generally resulted in 100% concentration reductions (see Table 2.1 Summary of Commercial Treatability Studies (SiREM)). Although this process has been extensively evaluated at the laboratory-scale, it has not been demonstrated to treat NAPLs *in situ* and under water-saturated conditions in the field.

This work presents the first field pilot-scale tests of STAR and an evaluation of its ability to effectively remediate coal tar NAPLs *in situ* and beneath the water table at a former industrial facility in Newark, New Jersey. The field tests were conducted in two lithological units at the site[1] and were designed to systematically demonstrate the ability to initiate and maintain a self-

[1] Materials used in Treatability Test #8 (Table 2.1) were collected from the Fill Unit in the vicinity of the 'shallow' field test

sustaining smoldering combustion reaction in the subsurface and below the water table while quantifying peak temperatures, smoldering velocities, treatment rates, treatment efficiencies, and emission rates.

4.2 Layout and Operation of Field Pilot Tests

Two pilot tests were conducted in the area of a backfilled lagoon at a former industrial facility located in Newark, New Jersey that was operated from the turn of the century until 1983. The lagoon was used to dispose of coal tar and its by-products and was closed in 1965 by backfilling with 2.5 to 3.5 m of materials that contained sand, gravel, rock, cinders, ash, brick, concrete, wood, slag, metal, glass and trash. Beneath this historical fill unit is 0.3 to 0.6 m thick confining clay 'Meadow Mat' layer composed of clay, silt and peat with an average hydraulic conductivity of 1.1×10^{-7} m/s. It is underlain by an alluvium unit, composed of medium to coarse sands up to 6 m thick. Depth to water at the site is approximately 1 m below ground surface (bgs, Figure 4.1a). Coal tar DNAPL exists as a mobile pool up to 1.3 m thick within the historic fill layer (hereafter referred to as the 'shallow fill unit'). Coal tar is also present in the upper 4 to 5 meters of the alluvium unit (herein referred to as the 'deep sand unit') in locations where the original lagoon excavation activities removed the Meadow Mat creating pathways for NAPL penetration. Average hydraulic conductivities in the shallow fill and deep sand units are 6.8×10^{-4} and 1.4×10^{-4} m/s respectively. Coal tar concentrations in the former lagoon footprint within the shallow fill range from 1,500 to 190,000 mg/kg of total petroleum hydrocarbons (TPH) (average =

37,900 mg/kg, 15 samples) and from 2,700 to 48,000 mg/kg of extractable petroleum hydrocarbons (EPH) within the deep sand unit[2] (average = 18,500 mg/kg, 8 samples).

The two pilot tests were conducted between October 2010 and November 2012. The first field test was conducted in the historic fill layer and is referred to as the "shallow test". The shallow test cell was applied in a 6.0 m by 18.3 m (plan view) area constrained by sheet piling keyed into the underlying Meadow Mat in order to prevent adjacent coal tar migrating into the cell following the test (Figure 4.1a). The "deep test" was conducted in the deep sand unit of the same lagoon, adjacent to the shallow test cell and did not use a sheet pile wall (Figure 4.1b). Each test area each had a centrally installed 5 cm diameter stainless steel well with a 30 cm long wire-wrapped (10 slot) screen that served as the ignition point and for delivering air. The shallow test used a hollow stem auger to install the well with the screen located at 2.4 to 2.7 m bgs (Figure 4.1: Schematic cross section of shallow (a) and deep (b) field test cells. The shallow field test consisted of ignition points installed to the base of the shallow fill unit in a test cell contained by a sheet pile barrier. The deep field test consisted of an ignition point installed in the deep sand unit with no sheet pile barrier. Both field tests were initiated under fully saturated conditions (i.e., below the water table). Hemispherical propagation of the smouldering front is shown outside the ignition well screens (t1 coincides with the pre-heated zone and onset of smouldering while the front location at t2 represents self-sustained smouldering with only air injection.). The deep ignition well was installed with sonic drilling with the screen placed at a depth of 7.9 m bgs (Figure 4.1b).

[2]TPH analyzed by EPA method 8015B was the accepted analytical method for petroleum hydrocarbon analysis for site remediation until September 1, 2010 after which the prescribed analytical method was switched to New Jersey Department of Environmental Protection (NJDEP) EPH Method Revision 3. The two methods are similar; however, each field test uses only one the analytical methods for consistency.

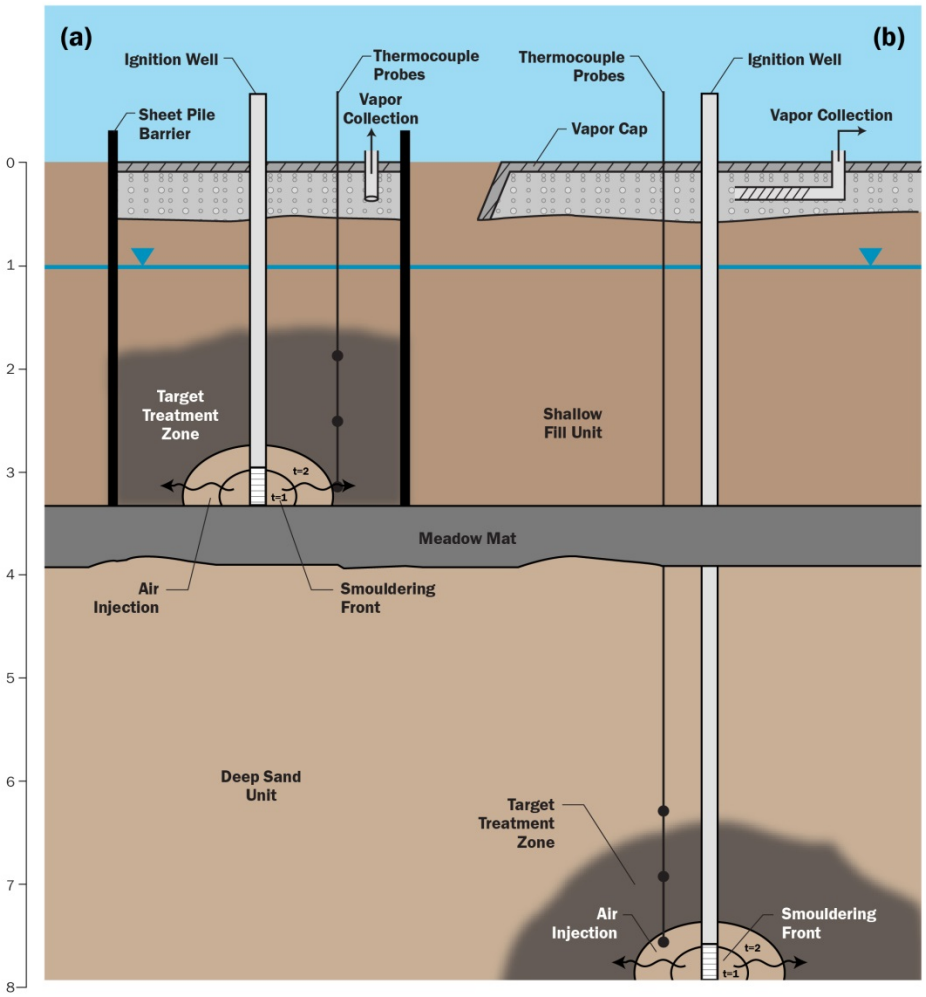

Figure 4.1: Schematic cross section of shallow (a) and deep (b) field test cells. The shallow field test consisted of ignition points installed to the base of the shallow fill unit in a test cell contained by a sheet pile barrier. The deep field test consisted of an ignition point installed in the deep sand unit with no sheet pile barrier. Both field tests were initiated under fully saturated conditions (i.e., below the water table). Hemispherical propagation of the smouldering front is shown outside the ignition well screens (t1 coincides with the pre-heated zone and onset of smouldering while the front location at t2 represents self-sustained smouldering with only air injection.

Custom-built, removable, down-well electrical heaters were used to convectively ignite NAPL adjacent to the ignition wells. The shallow and deep test used 4.1 kilowatt (kW) electrical resistance and 9 kW cartridge heating elements, respectively. The heaters were turned off following ignition (confirmed by the detection of combustion gases in collected vapours) and air

injection flow rates were manipulated manually at the ignition point to maintain and propagate the combustion front in a self-sustaining manner. Air was supplied by above ground electric rotatory screw compressors (shallow test: Kobelco KNWA1-G/H; deep test: Sullair TSR-20-200). Air injection flow rates were measured using rotameters (McMaster Carr panel-mount 2-20 SCFM) and venturi flow meters (Venturi 'V' series lo-Loss style, 1-1.5" throat; brass) and injection pressures using pressure gauges (Dwyer SGY-D10522N). Injected pressures and flow rates were controlled using inline pressure regulators and gate valves located adjacent to flow elements.

A vapour cap was installed to control and monitor combustion gases and vapours for both tests that consisted of an approximately 0.2 m thick layer of 2 cm diameter stone overlain with 15 cm of lean concrete. Within each vapour cap, vertical or horizontal extraction conduits were emplaced to collect vapours for the shallow and deep tests, respectively. The vapour cap for the shallow test extended to the sheet pile perimeter wall, whereas the deep test vapour cap was 15.3m by 15.3 m (plan view). Vapours were collected under vacuum applied to the gravel layer by extraction blowers and treated via a series of vapour phase granular activated carbon (GAC) vessels prior to discharge through a stack. Extracted vapours were collected during each test via an automated sampling probe with heated umbilical line (M&C SP2000) and analyzed using a continuous emissions monitoring (CEM) system for carbon monoxide (CO, Thermo Fisher -48C dual range), carbon dioxide (CO_2) and oxygen (O_2) (Servomax, 1440) that were recorded every 30 seconds by a data acquisition system (Agilent 3890A multi-switch unit). Extracted vapour samples were also collected periodically via Summa canisters from sampling ports located before and after the GAC vessels. These samples were analyzed by commercial analytical laboratories

for volatile organic compounds via United States Environmental Protection Agency (EPA) method TO-15. The velocity of the extracted vapours was measured a minimum of two times daily in the extraction piping using a digital handheld thermo-anemometer (TSI VelociCalc Plus).

Subsurface temperatures were measured using inconel-sheathed Type-K thermocouple probes installed via direct push drilling methods. The shallow test contained 166 measurement locations using a combination of multi- and single depth subsurface thermocouples placed throughout the cell at depths of 1.5, 1.8, 2.1, 2.4 and 2.6 m bgs with the greatest frequency of thermocouples placed near the ignition point (Figure D.1, Appendix D). The deep test thermocouple network consisted of 99 measurement locations using 16 multilevel (six junction) subsurface thermocouples installed at the four points of the compass at radial distances of 0.3, 0.6, 1.5 and 3.7 m, each with measurement points at 4.2, 5.1, 6.3, 6.9, 7.5, and 8.1 m bgs, (Figure D.2, Appendix D), as well as three thermocouple junctions installed in the ignition well boring. Temperature data was collected every 30 seconds throughout both test periods using a data acquisition system (Agilent 3890A multi-switch with internal temperature calibration cell) and transferred daily to a Microsoft Access database.

Direct push coring methods were used to collect pre- and post-test soil samples for analysis by commercial analytical laboratories. For the shallow test 15 pre- and 8 post-test samples were collected and analyzed for Total Petroleum Hydrocarbons (TPH) according to EPA Method 8015B. For the deep test, 8 pre- and 14 post-test samples were collected and analyzed for

Extractable Petroleum Hydrocarbons (EPH) via New Jersey Department of Environmental Protection Extractable Petroleum Hydrocarbons Method, Version 3.

4.3 Methods to Estimate Combustion Front Propagation and Mass Destroyed

Following ignition, temperature measurements were used to infer the location and propagation pattern of the combustion front. Two-dimensional temperature isosurface interpretations of the maximum achieved temperatures from each thermocouple location (at any depth) were generated using kriging algorithms (Surfer™, Golden Software©). The shallow data set was compiled into 24 plan view locations (i.e. data points) from the southern half of the test cell only, and the deep data set was compiled into 17 plan view locations for the interpretations. A point kriging method was used on the compiled temperature data sets with the test areas (approximated as an 8m long by 8m wide domain) represented by a 10,000 node square grid (0.08m spacing). Combustion zones were defined as kriged regions exhibiting temperatures above 400^{o}C. This procedure provided an estimate of the evolution of the treated region in plan view.

Smoldering front propagation velocities were estimated using a modified version of that developed for column experiments [5]. The arrival time of the smoldering front was determined for a thermocouple location using an average of the first arrival times of 250, 350, and 450^{o}C. Then a mean smoldering front propagation velocity was calculated by dividing the straight line distance between the thermocouple and the ignition origin by this arrival time.

The mass of coal tar destroyed was estimated via a carbon mass balance using the combustion gases CO_2 and CO extracted and by applying, as a surrogate for coal tar, the chemical composition of naphthalene, frequently the dominant remaining compound in present day coal tars [9]:

$$M_{CoalTar} \cong M_{Napthalene} = \frac{\left[M_{CO_2} \bullet \frac{MW_C}{MW_{CO_2}} + M_{CO} \bullet \frac{MW_C}{MW_{CO}} \right]}{R^C_{Nathpalene}} \qquad [4.1]$$

Where:

- $M_{CoalTar}$ is the equivalent mass of coal tar destroyed;
- $M_{Napthalene}$ is the mass of naphthalene destroyed;
- M_{CO_2} is the mass of carbon dioxide measured in the vapour stream (calculated as the product of the carbon dioxide concentration and the vapour phase flow rate);
- M_{CO} is the mass of carbon monoxide measured in the vapour stream (calculated as the product of the carbon monoxide concentration and the vapour phase flow rate);
- MW_C is the molecular weight of carbon;
- MW_{CO_2} is the molecular weight of carbon dioxide;
- MW_{CO} is the molecular weight of carbon monoxide; and
- $R^C_{Nathpalene}$ is the mass ratio of carbon to the molecular weight of naphthalene equal to 0.94.

The mass ratio of carbon to molecular weight was calculated for each of 29 compounds in the standard semi-volatile organic compound analytical suite and had an average value of 0.92 (standard deviation of 0.53, and a 95% confidence interval of 0.11); therefore, the substitution of naphthalene for coal tar is estimated to impart up to an 11.5% error on the R^c parameter and

subsequent mass destroyed estimate. Vapour flow rates were calculated by multiplying the measured vapour velocities by the extraction duct cross-sectional areas, and correcting to standard conditions using the ideal gas law.

The mass removal rate of coal tar from the system by non-destructive process (i.e., mass loss from volatilization) was estimated by multiplying the sum of the concentrations of all individual volatile species detected in the Summa canister grab samples (collected during periods of peak combustion) from the vapour extraction system by the volumetric flow rate of extracted vapour at the time the sample was collected. "Reaction efficiency" was defined as the ratio of mass of contaminant destroyed *in situ* (Equation 4.1) to the total mass removed through both volatilization and *in situ* destruction per unit time. "Remediation efficiency" was defined as the average percent concentration reduction (as TPH or EPH for the shallow and deep tests, respectively) in soil samples collected from combustion zones post-STAR treatment to those collected pre-STAR treatment.

4.4 Results and Discussion

4.4.1 Ignition and Smoldering Front Propagation

Ignition of a self-sustaining subsurface smoldering combustion reaction was observed following a period of preheating in both the shallow and deep tests. Smoldering combustion was confirmed when: (1) temperatures measured in the subsurface were higher than injected air temperatures and therefore indicated an exothermic reaction; and (2) there was an increase in the

concentration above baseline of combustion gasses (CO and CO_2) in the collected vapours. Initiation of smoldering combustion was observed within 24 hours and 1.5 hours of heater operation in the shallow and deep tests respectively. The shorter preheating period for the deep test is a direct result of improvements in heater design. Upon confirmation of smoldering, the heaters were turned off and only air injection was continued.

Figure 4.2 presents temperature isosurface interpretations of maximum achieved subsurface temperatures (for any depth) following one, three, and eight days of operation for the shallow and deep tests. In the shallow test, the combustion front was observed to initially propagate a distance of about 6.7 m from the ignition point (IP-5S) to the southern portion of the test cell (to TC-4, Figure 4.2 a) following a narrow path along the centerline of the cell at a depth of about 2.4 m bgs (level to top of ignition point screen interval) over a period of approximately 40 hours. The initial rapid propagation from IP-5S to the observed emergence of the combustion front at TC-4 is believed to have occurred through a thin (less than 0.3 m, based on thermocouple density) preferential pathway as a result of preferential pathway in the shallow fill materials; this pathway was confirmed to be a trough of bricks when the cell was excavated. Emergence of the combustion front at TC-4 is used as the combustion origin and time (i.e., t=0) in subsequent analysis of the smouldering front propagation (Figure 4.2 a to c) since more typical (non-preferential) radial smouldering through the fill started at this time. Figure 4.2 (b) shows that the combustion front had propagated to the southern and eastern boundaries of the test cell, three days after emergence at TC-4. After 8 days, the combustion front had extended further north, as well as reached the eastern extents of the test (Figure 4.2 c). Air injection was terminated after

decreases in temperature and corresponding decreases in combustion gas concentrations (down to ambient levels) were observed two days later, following approximately 10 days of operation.

In contrast to the shallow fill test, the deep test exhibited a more uniform combustion front propagation pattern immediately after ignition, as shown in Figure 4.2 (d to f). Thermocouple measurements showed steady and spatially uniform propagation of the combustion front in the relatively homogeneous alluvial sand over eight days of self-sustaining smoldering (Figure 4.2 d to f). The test was terminated after 10 days when the combustion front had propagated beyond the extent of the monitoring network, leaving a treated zone of up to 3.7 m radius (centralized around the ignition point) with a thickness of up to 1.9 m (at a measured depth of 6.2 to 8.1 m bgs).

It is important to note that the interpretations in Figure 4.2 show only the total extents of the smouldering front up to a given time, not the real time distribution of temperature; the smouldering front is relatively thin: as it propagates outward, cooling occurs between the front and the air injection origin. As an example, on Day 8 of the deep test (Figure 4.2f), combustion temperatures are observed in thermocouples 3.7 m from the ignition origin, while all temperatures inside this radius at this time (i.e., measured in the thermocouples 0.3, 0.6, and 1.5 m from the ignition origin) were below 60^{o}C. Confidence contour plots of the krigged values in presented in Figure 4.2 (day 8) are provided in Appendix D.

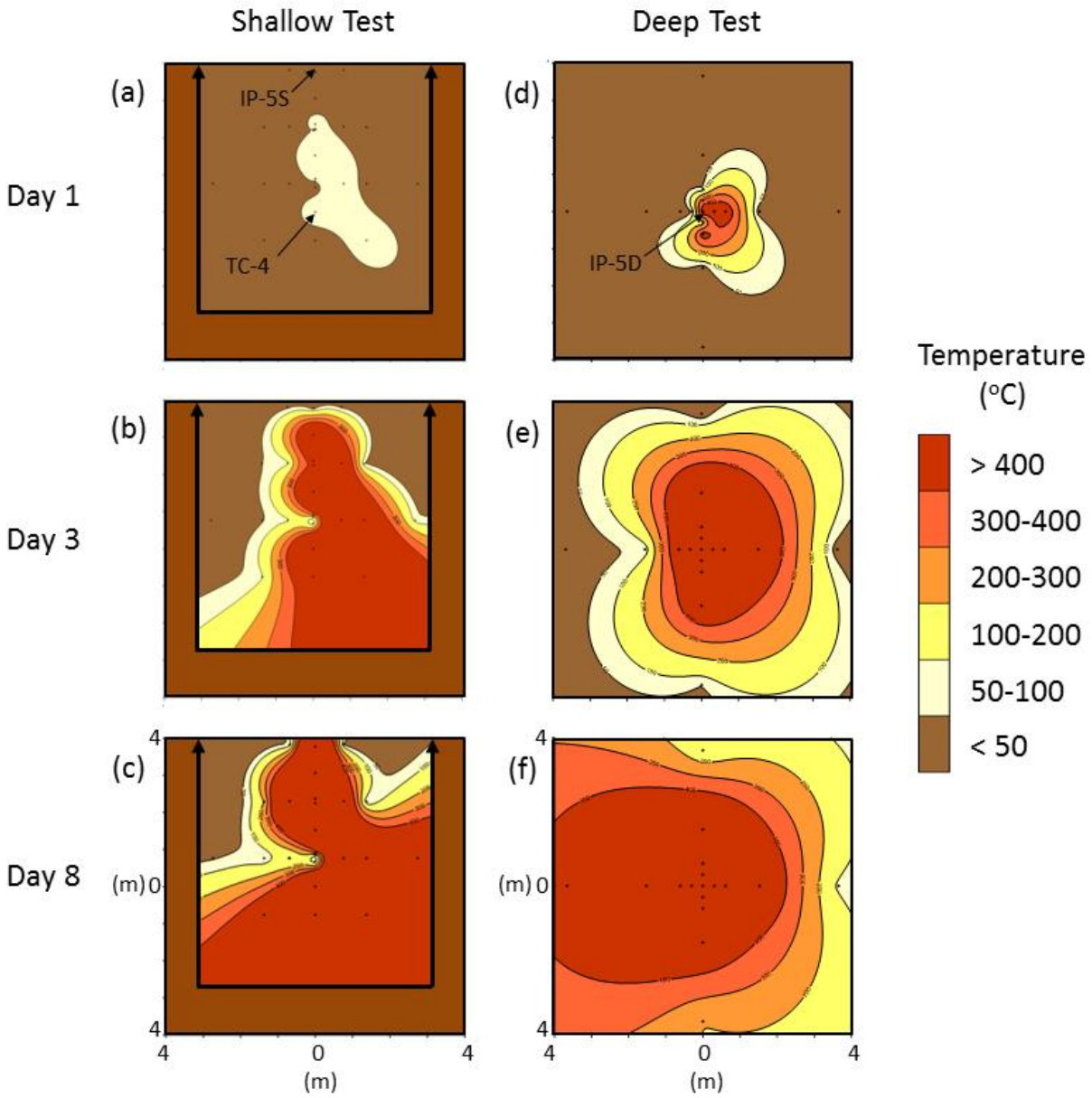

Figure 4.2: Maximum temperatures achieved at any depth following 1, 3 and 8 days of operation in the shallow (a to c) and deep (d to f) tests. Plot origins correspond to ignition origins. Thermocouple locations marked by + symbol. Arrowed outline around Shallow Test cell represents sheet pile wall (continues out of view). Note that maximum plotted temperature is above 400 °C to indicate combustion; peak temperatures in the shallow test reached over 1000°C, and in the deep test exceeded 600°C. Note that the figure does not show how temperatures rapidly cooled after the relatively thin combustion front passed through each thermocouple location.

The peak combustion zone temperatures observed in the shallow test ranged from 450 to 1200^{o}C while in the deep test were typically around 650^{o}C. The difference in observed peak temperatures between the shallow and deep tests cannot be attributed to a single factor. Pironi et al (2011) and Switzer et al (2009) demonstrated peak temperature sensitivity to moisture content, properties of the porous medium, air injection rate, smouldering velocity and degree of thermal equilibrium with the porous medium [5] [3] all of which could be contributing at the field scale to the observed differences.

For the shallow test, smouldering propagation velocities are calculated outwards from TC-4, ignoring for this analysis the initial rapid and preferential smoldering front propagation from the ignition point to TC-4. For the deep test, all thermocouples were used to calculate the front velocities. The calculated velocities were not normally distributed; therefore, the Wilcoxon Rank Sum (WRS) test (a non-parametric test) was used to compare the medians of the two populations [30]. The calculated median velocities in the shallow and deep tests were 1.04 and 0.67 meters per day (m/day), respectively (n=22 for each). The null hypothesis of the test states that there is no difference in medians while the alternative states that the shallow median velocity is greater than the deep. As such, a one-sided WRS test was conducted at the 5% level of significance. The test determined that the median velocity was greater in the shallow test than the deep (p-value=0.008). The higher calculated smouldering propagation velocity in the shallow test could be attributable to intrinsic permeability differences (it is on average more than four times higher in shallow fill than deep sand) and heterogeneity differences which could lead to higher air velocities in the shallow test (e.g., the non-uniform smouldering propagation pattern in the shallow test [Figure 4.2 a-c] could imply a preferential flow path which could have

led to increased air velocities). Higher air velocities are directly related to higher smouldering front propagation velocities [5].

4.4.2 Mass Removed, Remediation and Reaction Efficiencies

The mass of coal tar destroyed in the shallow and deep tests were estimated to be 3,728 kg and 864 kg respectively. Mass destruction rates ranged from 1 to 43 kg/hr in the shallow test and 1 to 7 kg/hr in the deep test. Combustion gas (CO and CO_2) concentrations in extracted vapours from the shallow and deep tests are provided in Figures D1 and D2, respectively. The mass destroyed calculation assumes complete capture of all generated combustion gases, and therefore is a conservative estimate of the mass destroyed (e.g., some CO_2 likely dissolved in the overlying groundwater and soil moisture). The calculation is particularly conservative for the deep test cell that had (i) no confining sheet pile, (ii) an overlying confining layer which could force some gas outside the vapour capture zone, and (iii) a substantial thickness of overlying groundwater for the gases to traverse.

TPH was reduced in the shallow test cell from a mean pre-test concentration of 37,900 mg/kg (n=15, stdev =50,800 mg/kg) to a mean post-test concentration of 258 mg/kg (n=8, stdev =185 mg/kg) equating to an average remediation efficiency of 99.3%. In the deep test, EPH was reduced from a mean pre-test concentration of 18,400 mg/kg (n=8, stdev =13,400 mg/kg) to a mean post-test concentration of 450 mg/kg (n=14, stdev =1,100 mg/kg) for an average remedial efficiency of 97.6%. Figure 4.3 presents the TPH/EPH concentrations of all pre- and post-field test soil samples collected from within the treatment areas for the shallow and deep field tests as a function of depth of sample.

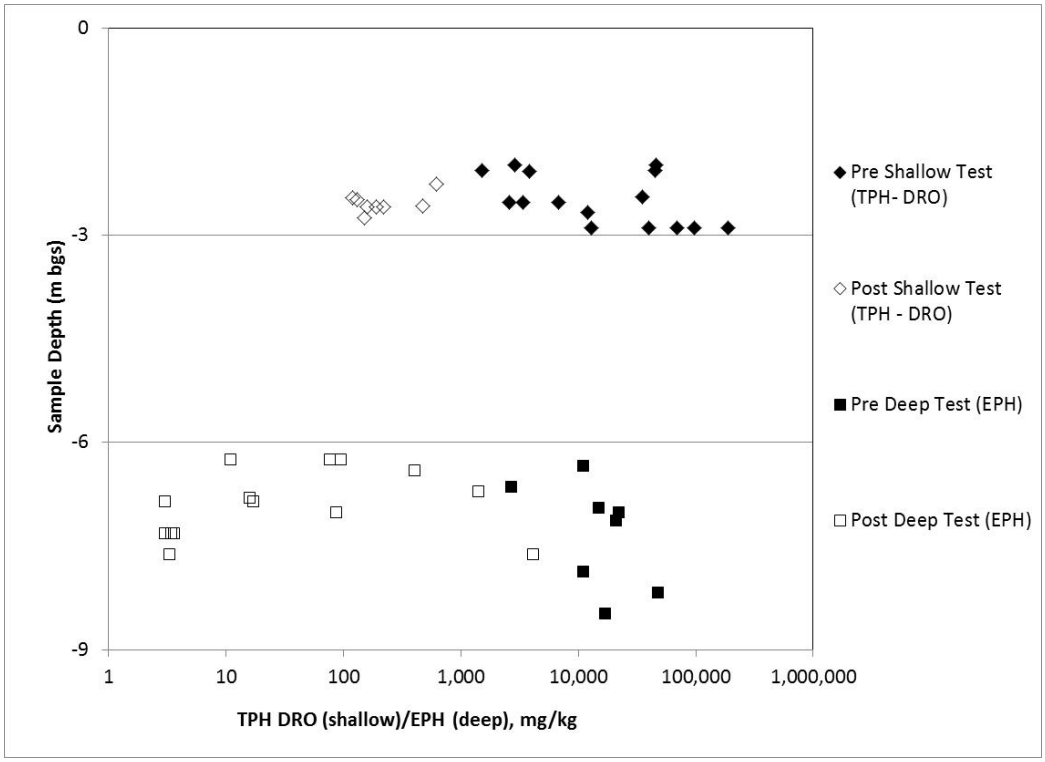

Figure 4.3: Pre- and post-TPH (shallow) and EPH (deep) soil concentrations by sample depth. All post test samples are collected from within inferred combustion zones. Note that the depth (vertical) axis is linear scale and the soil concentration (horizontal) axis is logarithmic.

Figure 4.4 presents before and after photos of representative soil cores collected from combustion zones in the shallow and deep field tests, as well as before and after photos of the shallow fill material from the laboratory treatability test. Post-test soil cores from both pilot tests (8 in shallow test and 9 in deep test) from within the combustion zones indicated no NAPL and visibly reduced moisture levels; this is consistent with results reported in the treatability test.

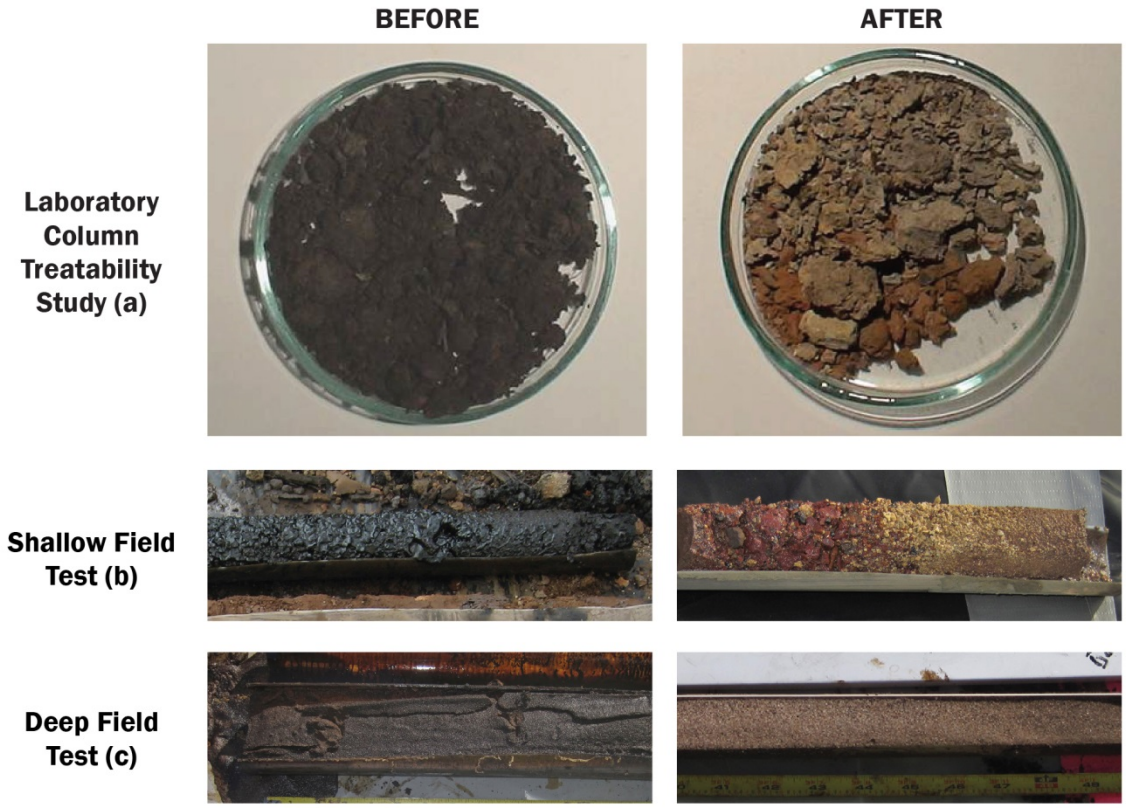

Figure 4.4: Photographs of soils from before and after STAR in: (a) laboratory column treatability test (performed on shallow fill materials); (b) shallow field test soil cores; and (c) deep field test soil cores. Before soils contain significant quantities of moisture and coal tar NAPL. Post STAR Soils from after laboratory and field testing appear visibly drier and remediated. Concentration reductions for shallow and deep tests were 99.4, and 97.8% respectively.

The mass removal rate by volatilization for the shallow test was calculated (one total vapour sample) to be 0.22 kg/hr corresponding to a coincident *in situ* mass destruction rate of 36 kg/hr yielding a reaction efficiency of 99.4%. The mass removal rate by volatilization was calculated (average of two vapour samples) in the deep test to be 0.12 kg/hr, which corresponded to an average of coincident *in situ* mass destruction rates of 5.55 kg/hr yielding a reaction efficiency of 97.8%.

The shallow and deep tests; the first STAR field tests, demonstrated the ability to ignite and propagate a smouldering reaction in coal tar contaminated soils *in situ* and below the water table. In Situ destruction of coal tar was observed at rates up to 43 kg/hour resulting from a single ignition point, and smouldering fronts were found to propagate greater than 4 m from an ignition point at rates up to 1 m per day. Mass removed through volatilization was determined to be on the order of one percent of the coal tar mass destroyed *in situ*. Petroleum hydrocarbon concentrations in treated soils (i.e. from combustion zones) were reduced on average by 98.5 percent, with visual results of treated materials consistent with those from column scale STAR tests. The results of these field tests can be used in designing the full scale STAR implementation at the site.

5 Conclusions and Recommendations

5.1 Conclusions

This thesis focused on the first in situ field demonstration of the STAR technology. A new smouldering combustion ignition method, based on convective heat transfer, was developed. The method was validated at the column scale through a series of 8 laboratory column experiments, and convective ignition metrics were compared to the traditional conductive ignition method. The convective ignition method was then tested in the field in two *in situ* trials, with an improved heater design developed between the two field trials.

Following ignition, the two field trials, conducted in two different geological units at the site (shallow fill and deep alluvium) were each able to sustain smouldering reactions for 10 days *in situ* and below the water table. During the field trials, qualitative and quantitative comparisons between the deep and shallow tests were made on smouldering propagation patterns and velocities, peak reaction temperatures, mass removed, visual effects on soils, remediation efficiency, and reaction efficiency.

Results of the laboratory testing program suggest that:

- Ignition of a smouldering reaction of coal tar contaminated sands is possible at the column scale through convective heat transfer via hot air injection.
- Early experiments (1 and 2) may have had a significant quantity of heat transfer via radiation. This contribution was eliminated through insertion of a clean sand gap (Experiment 4) and use of an external air heater (Experiments 5 through 8).

- The convective ignition process was able to achieve ignition of a smouldering reaction in a fully water saturated condition at the column scale (Experiment 3).
- The convective ignition experiments had a higher ignition temperature (around 450^{o}C) than conductive ignition under similar conditions at the column scale (around 400^{o}C).
- The convective ignition process was highly repeatable at the column scale (Experiments 5 through 8) in terms of duration of preheating and energy supplied for ignition
- The average energy supplied for convective ignition (4131kJ) at the column scale was on the order of 5 times greater than that of a similar conductive ignition experiment (813 kJ), though neither process was optimized or accounts for external heat losses.
- The preheating profiles between a convective and conductive ignition at the column scale were similar, with initial heating rates increasing rapidly in the first ten minutes of heating to between 6 and 10 ^{o}C/min where they plateau until ignition
- The convective ignition process demonstrated a more gradual, 'automatic' transition to smouldering than conductive ignition under similar conditions at the column scale.
- Significantly higher temperatures throughout the column were observed prior to convective ignition than conductive ignition. This may account for the differences in energy supplied for ignition; though a larger preheating zone may be beneficial to field application.
- The convective ignition method was sufficiently validated at the column scale for use in field trials.

The results of *in situ* convective ignition testing during STAR field trials suggest:

- A convective ignition system was developed for *in situ* application of STAR such that:

  - Heated air can be delivered to the subsurface at temperatures in excess of 400°C;
  - The heater can be deployed into a standard 5cm steel well; and
  - The heater can be removed and reused for multiple ignition events.

- ‘self-ignition’, whereby smouldering initiates without alteration to the air flow rate during preheating results in a more reliable and robust smouldering reaction than ‘timed ignition’.
- Ability to achieve ‘self-ignition’ is dependent on supplying air to the subsurface sufficiently hot to preheat soils outside the well screen to ignition temperatures and sufficient in volume to supply adequate oxygen for combustion.
- A more efficient heater (Design C) was developed to increase the temperature and volume of injected air into the subsurface between the Phase II and III field trials.
- Above ground testing of heater Designs B and C demonstrated that the Design C heater had a nearly 4 fold improvement, expressed as a reduced normalized power demand over Design B.
- The Design C heater was able to achieve in situ ignition of smouldering following only 90 minutes of preheating in the Phase III trial (versus preheating duration on the order of tens of hours in the Phase II trials).
- The development of the convective ignition method will serve to reduce costs of STAR field implementation by:
  - Reducing drilling costs by enabling the use of smaller diameter boreholes;
  - Reducing heater costs by being reusable, and deployed such that the heater is not exposed to a corrosive environment; and
  - Reducing operational time by reducing time to ignition.

In Situ STAR field trial results further suggest:

- Initiation and propagation of a smouldering combustion reaction is achievable in situ and below the water table in varying geologies, and under natural groundwater flow conditions.
- The shallow and deep tests were estimated to have destroyed 3,728 kg and 864 kg of coal tar respectively during 10 days of self-sustained smouldering.
- Field results of in situ STAR application are consistent with reported column studies in terms of visual effects on soils and remediation efficiency. Specifically:
    - Soils cores collected from combustion zones following STAR treatment in both the shallow and deep tests appear visibility drier and free of NAPL compared to pre-STAR soil cores which show high levels of water and NAPL saturation
    - Remediation efficiency (comparison of pre- to post-STAR soil concentrations) was found to be 99.3 and 97.6% in combustion zones for the shallow and deep tests respectively.
- Smouldering propagation was controlled to some extent in the shallow test by heterogeneity in the fill materials creating a non-uniform smouldering pattern.
- Smouldering propagation in the relatively uniform alluvium in the deep test was highly uniform and extended radially outward from the ignition point to the extent of the thermocouple monitoring network (a distance of 3.6 m from the ignition point).
- Smouldering propagation velocity was higher in the shallow test than the deep test, possibly as a result of higher permeability in the shallow fill materials, and/or increased

air injection velocities (due to potential channelling through preferential pathways resulting from heterogeneity in the shallow fill).

- Peak temperatures in the shallow test were generally higher in the shallow test than the deep test.
- Finally, volatile emissions relative to mass destroyed *in situ* during field trials were very low. Reaction efficiencies were 99.4% and 97.8% in the shallow and deep tests respectively.

5.2 Recommendations

Through this work, STAR has been demonstrated to be scalable from the laboratory to the *in situ* field scale, for the highly effective remediation of coal tar contaminated soils. The convective ignition method proved effective and robust. Several recommendations for further research and development of STAR are provided below:

- Convective ignition has been demonstrated at the column scale on 'base case' (25% saturation of pore space) coal tar in coarse sands only. A detailed evaluation on the sensitivity to parameters for convective ignition (similar to Pironi et al, 2011, [5]) and detailed comparison to the conductive data set would be beneficial.
- Optimization of the convective ignition protocol at the column scale should be explored.
- *In situ* STAR has been demonstrated only on coal tar contaminated soils. Additional *in situ* testing on a range of contaminant types (evidenced to support self-sustaining combustion at the column scale) is recommended.
- The *in situ* field trials produced an abundance of temperature data, which could likely be mined in greater detail to learn more about the smouldering front propagation dynamics

observed. The data could possibly be used for validation of a potential 3D smouldering propagation model.

- While the *ex situ* application of STAR was not discussed in this thesis, the convective ignition process should be explored at increasing scales for *ex situ* STAR as removing the need for direct contact heating elements presents significant logistical advantages.
- Heat transfer via radiation appeared to contribute significantly to the reduced ignition timing of Experiments 1 and 2. Impractical for *in situ* STAR, ignition via radiation should be explored for *ex situ* STAR.

6 Works Cited

[1] B. Kueper, G. Wealthall, J. Smith, S. Leharne and D. Lerner, "An illustrated handbook of DNAPL transport and fate in the subsurface," Environment Agency Rio House, Bristol, UK, 2003.

[2] J. Gerhard, T. Pang and B. Keuper, "Time Scales of DNAPL Migration in Sandy Aquifers Examined via Numerical Simulation," *Groundwater,* vol. 45, no. 3, pp. 147-157, March-April 2007.

[3] C. Switzer, P. Pironi, J. Gerhard, G. Rein and J. Torero, "Self-Sustaining Smoldering Combustion: A Novel Remedation Process for Non-Aqueous-Phase Liquids in Porous Media," *Environmental Science and Technology,* vol. 43, pp. 5871-5877, 11 February 2009.

[4] G. Rein, "Smouldering Combustion Phenomena in Science and Technology," *International Review of Chemical Engineering,* vol. 1, pp. 3-18, JAn 2009.

[5] P. Pironi, C. Switzer, J. Gerhard, G. Rein and Torero.J, "Self-Sustaining Smoldering Combustion for NAPL Remediation: Laboratory Evaluation of Process Sensitivity to Key Parameters," *Environmental Science and Technology,* vol. 45, no. 7, pp. 2980-2986, 25 February 2011.

[6] T. Ohlemiller, "Smoldering Combustion," in *SFPE Handbook of Fire Protection Engineering (3rd Edition)*, 2002, pp. 200-210.

[7] M. Anderson, T. Sleight and J. Torero, "Downward smolder of polyurethane foam: ignition signatures," *Fire Safety Journal,* vol. 35, pp. 131-147, 2000.

[8] J. Pankow and J. Cherry, Dense Chlorinated Solvents and other DNAPLs in Groundwater, Portland, OR: Waterloo Press, 1996.

[9] B. Kueper and K. Davies, "Assessment and Delineation of DNAPL Source Zones at Hazardous Waste Sites," United States Environmental Protection Agencyy, Cincinnati, OH, 2009.

[10] NY State Department of Environmental Conservation, "New York State's Approach to the Remediation of Former Manufactured Gas Plant Sites," NY State Department of Environmental Conservation, NA.

[11] D. Gaylor, S. Culp, L. Goldstein and F. Beland, "Cancer Risk Estimation for Mixtures of Coal Tars and Benzo(a)pyrene," *Risk Analysis,* vol. 20, no. 1, pp. 81-85, 2000.

[12] C. Cerniglia, "Aromatic hydrocarbons:metabolism by bacteria, fungi and algae," *Toxicology,* vol. 3, pp. 321-361, 1981.

[13] McGowan, "Thermal Treatment and Non-Thermal Technologies for Remediation of Manufactured Gas Plant Site," *Waste Management,* pp. Vol.1, No.8 pp.691-698, 1996.

[14] G. Heron, K. Parker, J. Galligan and T. Holmes, "Thermal Treatment of Eight CVOC Source Zones to Near Nondetect Concentrations," *Ground Water Monitoring and Remediation,* vol. 29, no. 3, pp. 56-65, 2009.

[15] G. Heron, S. Carroll and S. Nielsen, "Full-Scale Removal of DNAPL Constituents Using Steam-Enhanced Extraction and Electrical Resistance Heating," *Ground Water Monitoring and Remediation,* vol. 25, no. 4, pp. 92-107, 2005.

[16] R. Baker, J. Bierschenk, J. LaChance, G. Heron and D. C. J. Phelan, "In-Situ Thermal Treatmnet of MGP Waste and Creosote," [Online]. Available: http://www.terratherm.com/pdf/white%20papers. [Accessed 15 February 2013].

[17] J. Collins, "Coal Tar Contamination Remediation," *Pollution Engineering,* pp. 26-29, 2012.

[18] P. Pironi, C. Switzer, G. Reid, J. Gerhard and J. Torero, "Small-Scale Forward Smouldering Experiments for Remediation of Coal Tar in Inert Media," *Proceedings of the Combustion Institute,* vol. 32, no. 2, pp. 1957-1964, 2009.

[19] D. Drysdale, An Introduction to Fire Dynamics, 2nd Edition, New York: John Wiley and Sons Ltd., 1998.

[20] J. Howell, M. Hall and J. Ellzey, "Combustion of Hydrocarbon Fuels Within Porous Inert Media," *Progress in Energy and Combustion Science,* vol. 22, pp. 121-145, 1996.

[21] J. Torero and A. Fernandex-Pello, "Forward Smoldering of Polyurethane Foam in a Forced Air Flow," *Combustion and Flame,* vol. 106, no. 1-2, pp. 89-109, 1996.

[22] K. Palmer, "Smoldering Combustion in Dusts and Fibrous Materials," *Combustion and Flame,* p. 129, 1957.

[23] D. Shultz, B. Matkowsky and V. Volpert, "Forced Forward Smolder Combustion," *Combustion and Flame,* vol. 104, pp. 1-26, 1996.

[24] I. Akkutlu and Y. C. Yortsos, "The dynamics of in-situ combustion fronts in porous media," *Combustion and Flame,* vol. 134, pp. 229-247, 02 April 2003.

[25] C. Switzer, P. Pironi, G. Rein, J. Torero and J. Gerhard, "Experimental Studies of Self-Sustainign Thermal Aquifer Remediation (STAR) For Non-Aqueous-Phase Liquid (NAPL) Sources," in *Proceedings from ConSoil 2008,* Milano, Italy, 2008.

[26] S. MacPhee, J. Gerhard and G. Rein, "A novel method for simulation smoldering propagation and its application to STAR (Self-sustaining Treatment for Active Remediation)," vol. 31, pp. 84-98, 9 September 2012.

[27] F. Incropera, D. DeWitt, T. Bergman and A. Lavine, Fundamentals of Heat and Mass Transfer, Hoboken, New Jersey: John Wiley & Sons, 2007.

[28] EPRI, "DNAPL Site Characterization for Waste Management at Manufactured Gas Plant (MGP) Sites," EPRI, PaloAlto, CA, 2004.

[29] U.S Environmental Protection Agency, "Health Effects Assessment for Coal Tars," Washington, DC, 1984.

[30] H. Mann and D. Whitney, "On a Test of Whether One of Two Random Variables is Stochastically Larger than the Other," *Annals of Mathematical Statistics,* vol. 18, no. 1, pp. 50-60, 1947.

[31] D. Brown, L. Gupta, H. Moo-Young and A. Coleman, "Raoult's Law-Based Method for Determination of Coal Tar Average Molecular Weight," *Environmental Toxicology and Chemistry,* vol. 24, no. 8, pp. 1886-1892, 2005.

[32] EPRI, "Development of a Characterization and Assessment Framework for Coal Tar at MGP Sites," EPRI, Palo Alto, CA, 2006.

Appendix A: Column Experiment Notes and Data

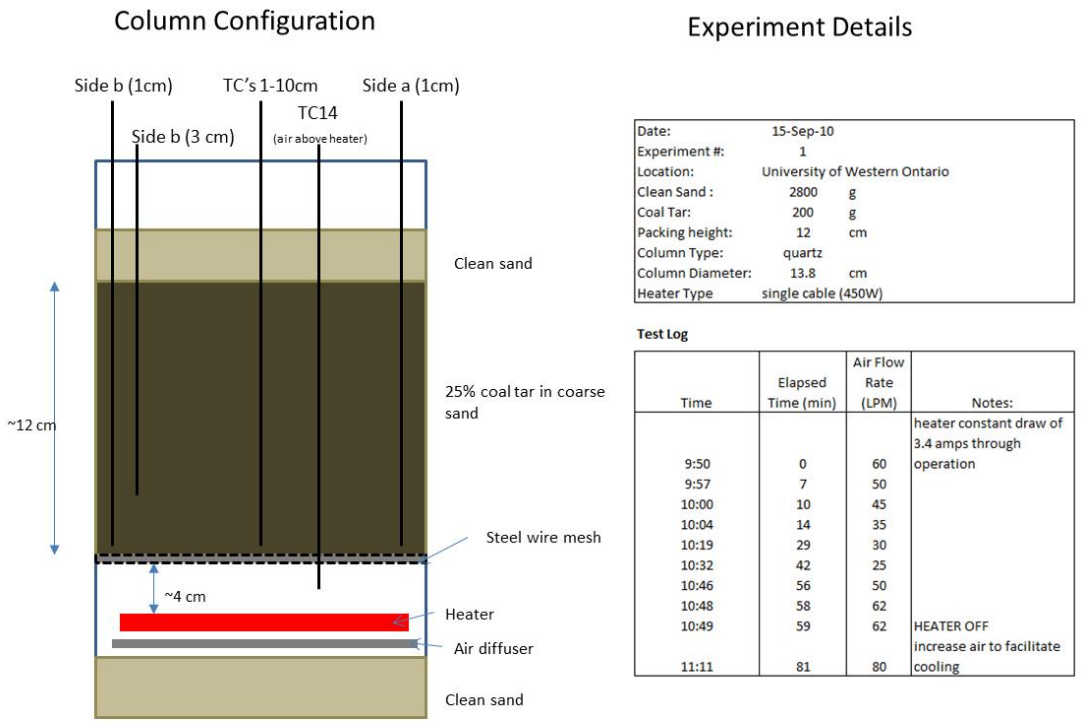

Figure A.1: Experiment #1 Column configuration and experimental notes.

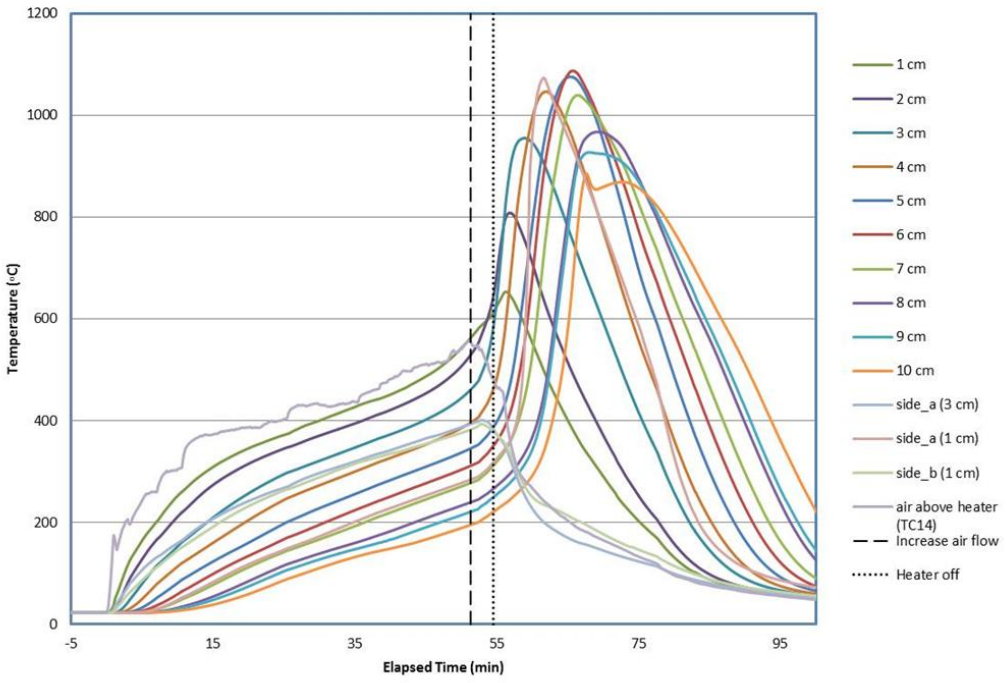

Figure A.2: Experiment # 1 thermocouple temperature profiles.

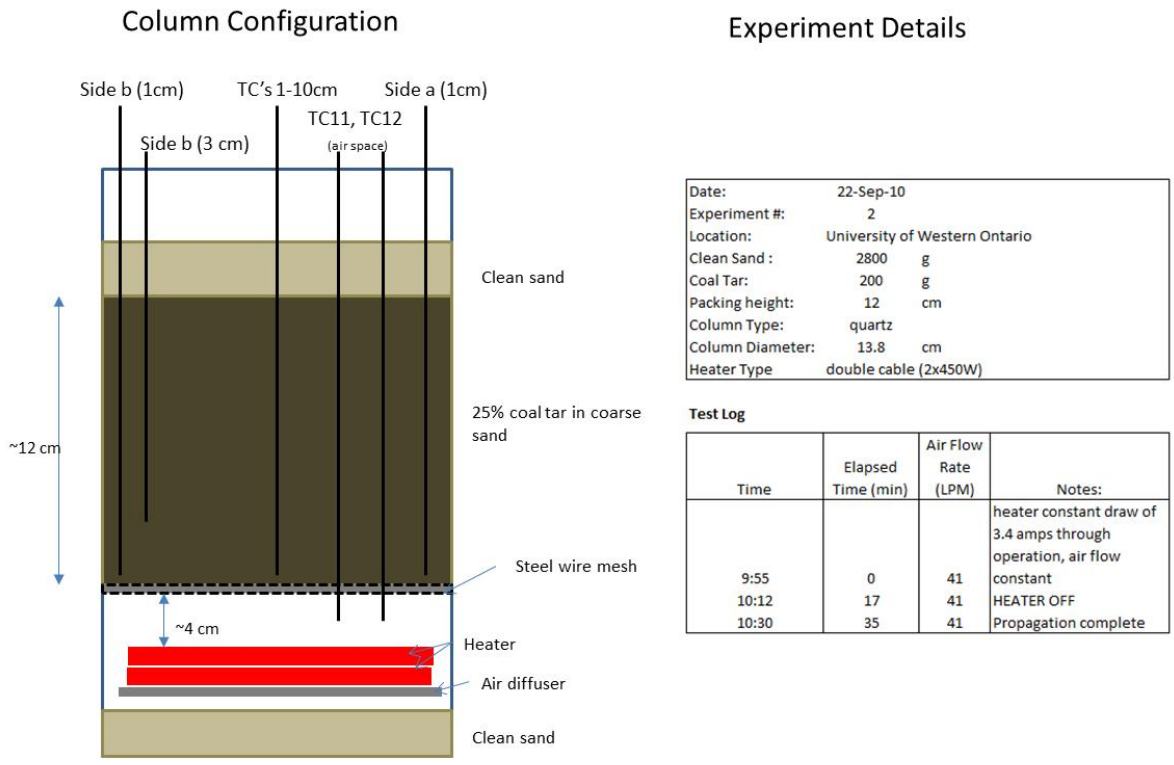

Figure A.3: Experiment #2 column configuration and experimental notes.

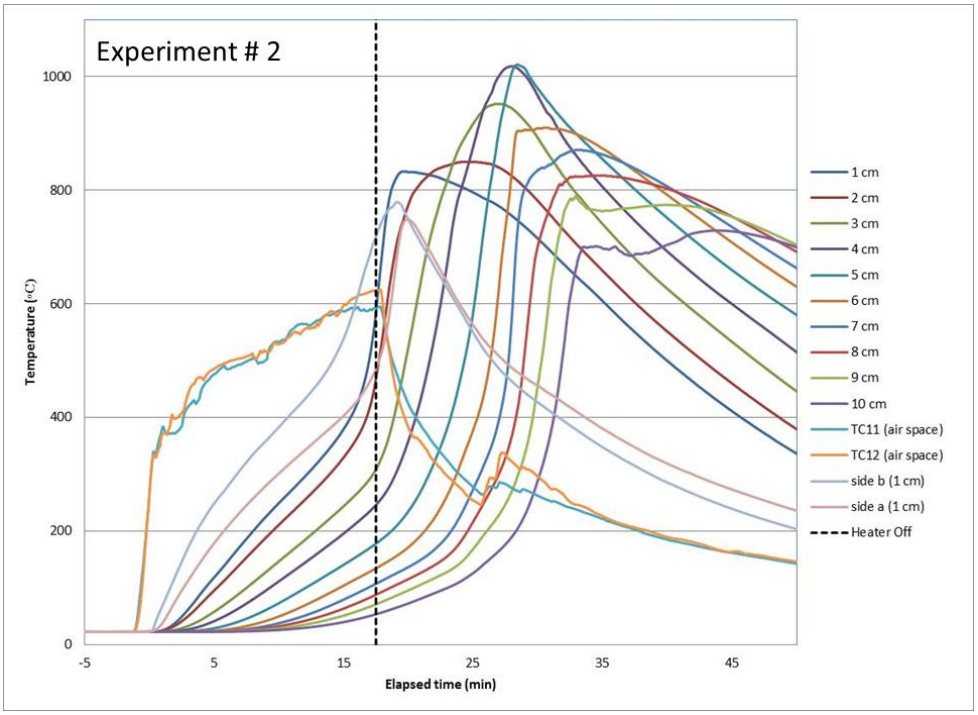

Figure A.4: Experiment # 2 thermocouple temperature profiles.

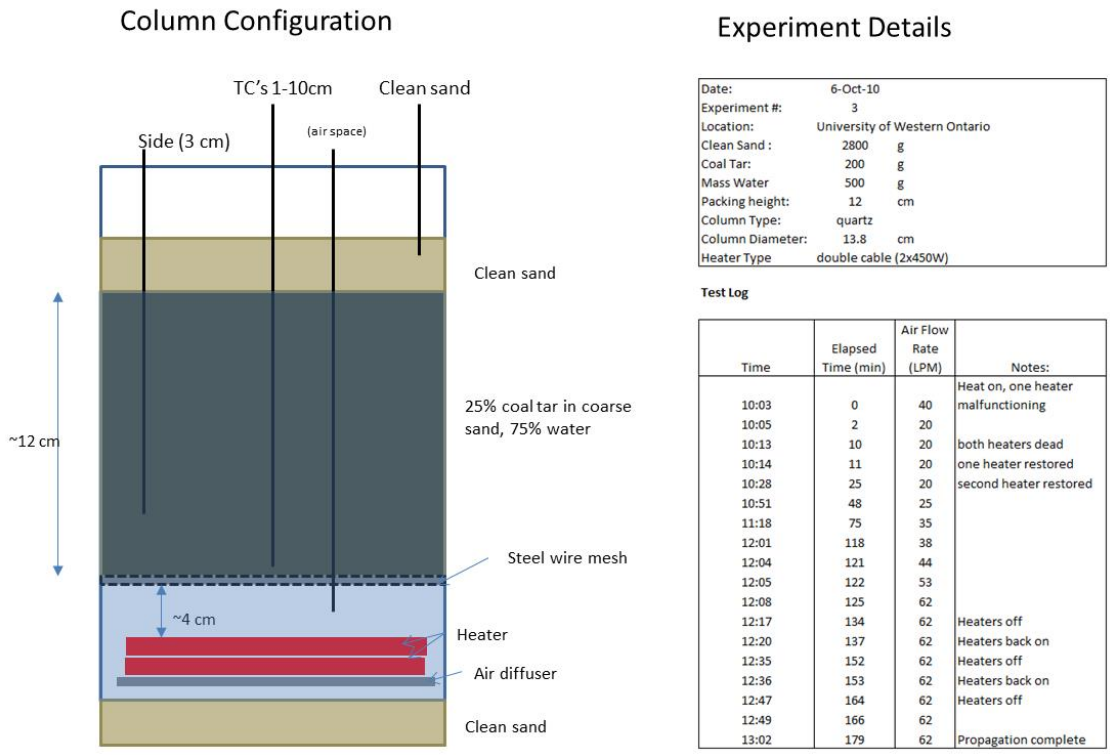

Figure A.5: Experiment #3 column configuration and experimental notes.

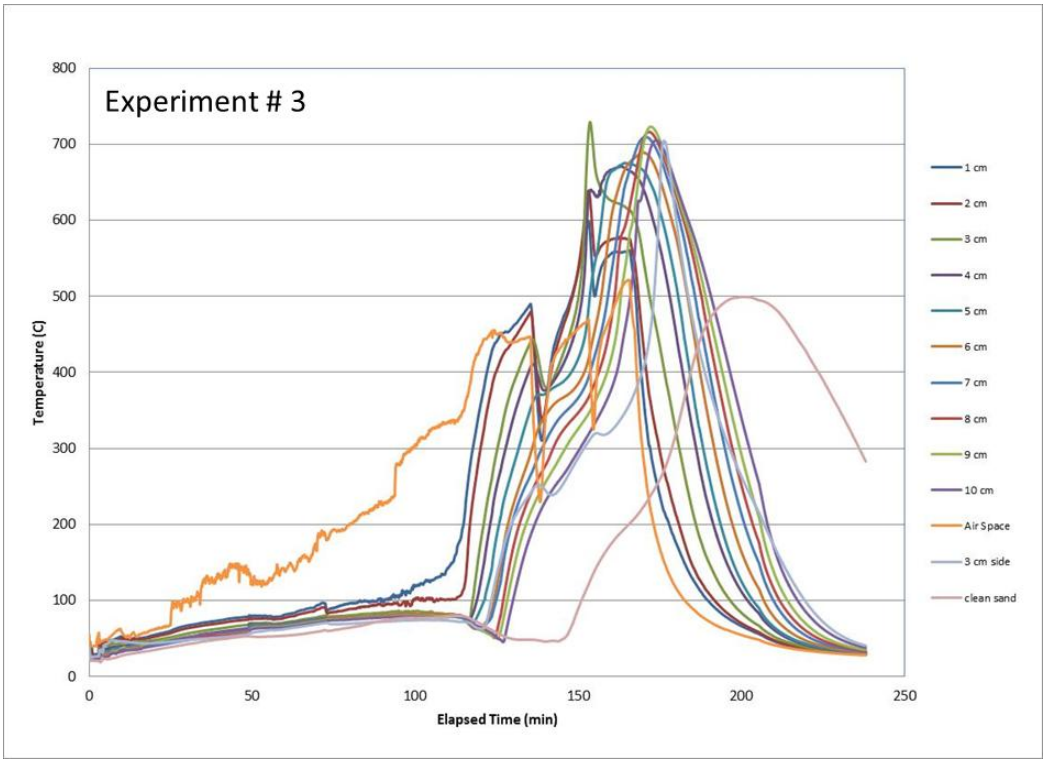

Figure A.6: Experiment # 3 thermocouple temperature profiles.

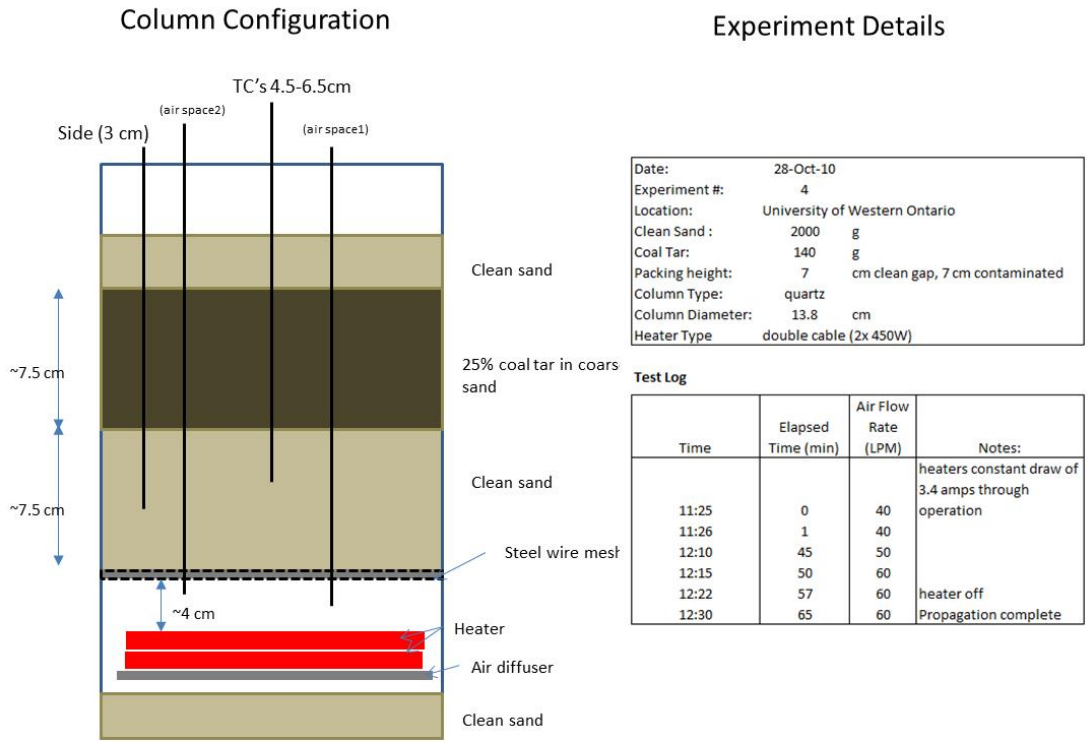

Figure A.7: Experiment #4 column configuration and experimental notes.

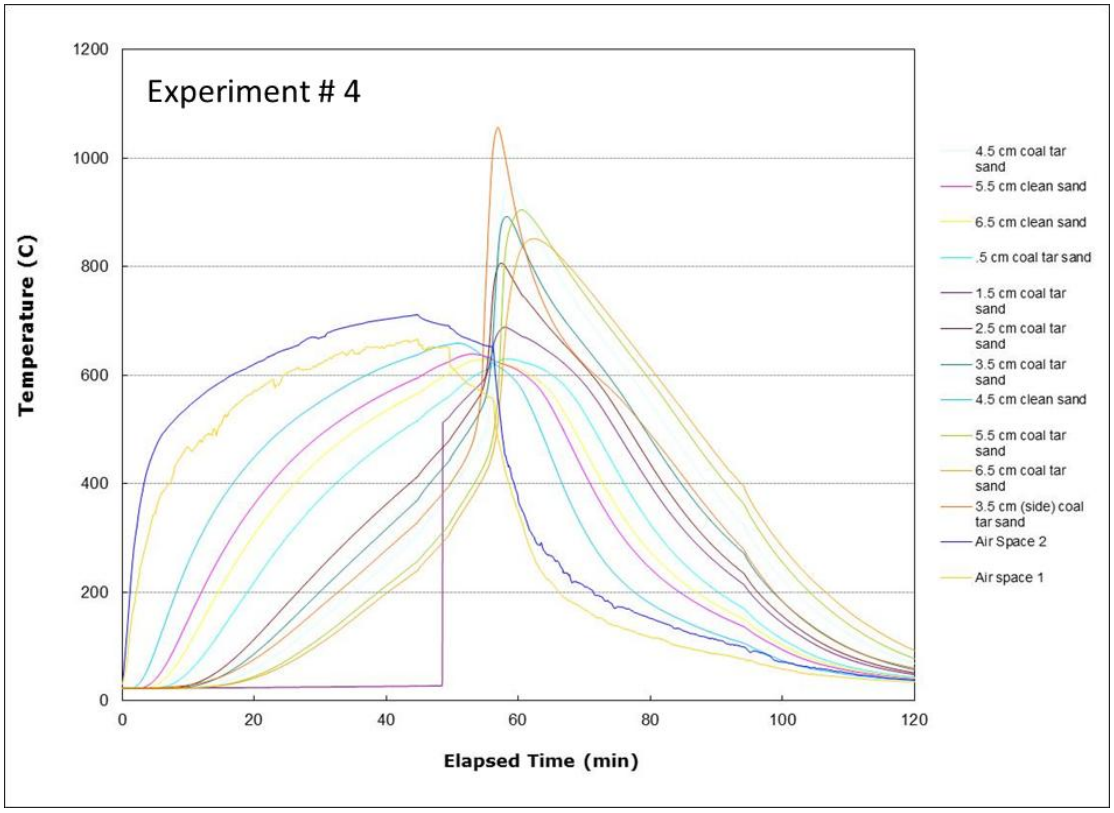

Figure A.8: Experiment # 4 thermocouple temperature profiles.

Column Configuration

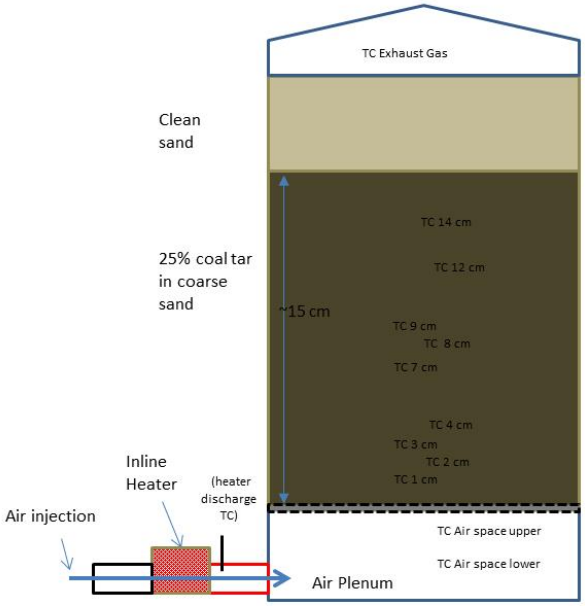

Experiment Details

Date:	1-Dec-10	
Experiment #:	5	
Location:	University of Western Ontario	
Clean Sand :	4800	g
Coal Tar:	335	g
Packing height:	15	cm clean gap, 7 cm contaminated
Column Type:	Stainless Steel	
Column Diameter:	16	cm
Heater Type	External Inline (1.8 kW)	

Test Log

Time	Elapsed Time (min)	Air Flow Rate (LPM)	Notes:
13:56	0	80	start air flow
13:59	3	80	Heater on. 40% variac
14:01	5	80	Variac @ 60%
14:05	9	80	Variac @ 80%
14:35	39	80	Variac @ 75%
14:37	41	80	Variac @ 78%
15:02	66	80	HEATER OFF
15:14	78	70	
15:30	94	80	Propagation complete

Figure A.9: Experiment #5 column configuration and experimental notes.

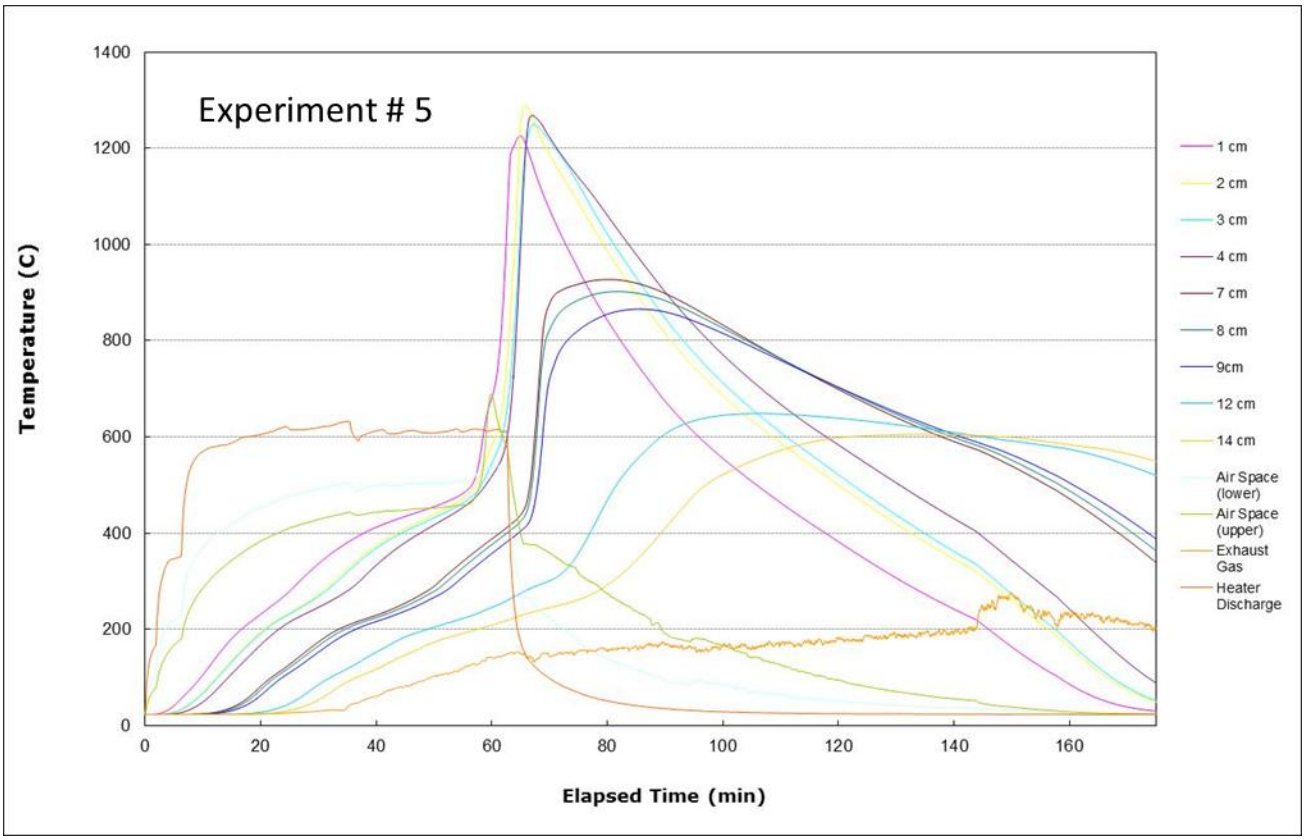

Figure A.10: Experiment # 5 thermocouple temperature profiles.

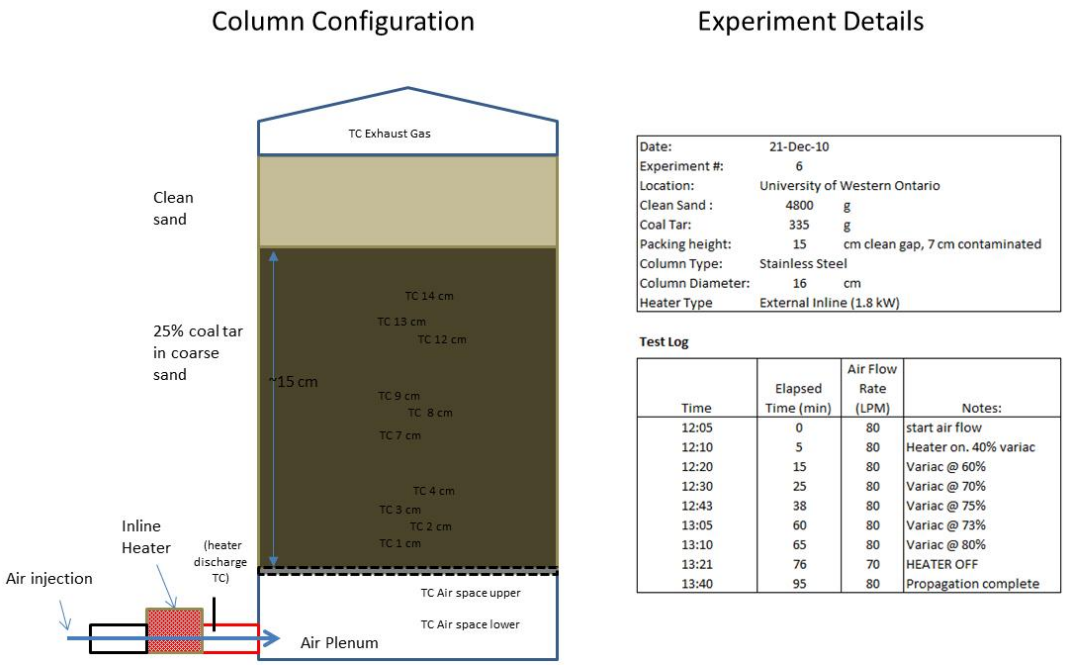

Figure A.11: Experiment #6 column configuration and experimental notes.

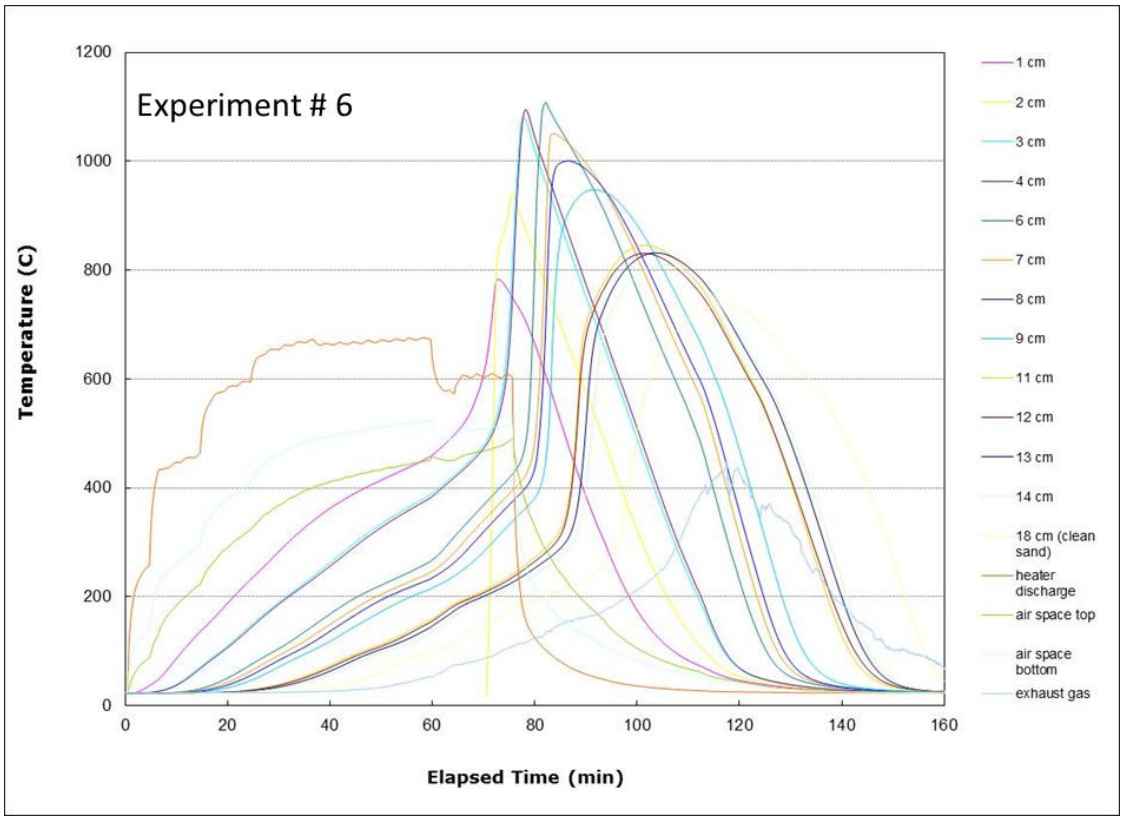

Figure A.12: Experiment # 6 thermocouple temperature profiles.

Column Configuration

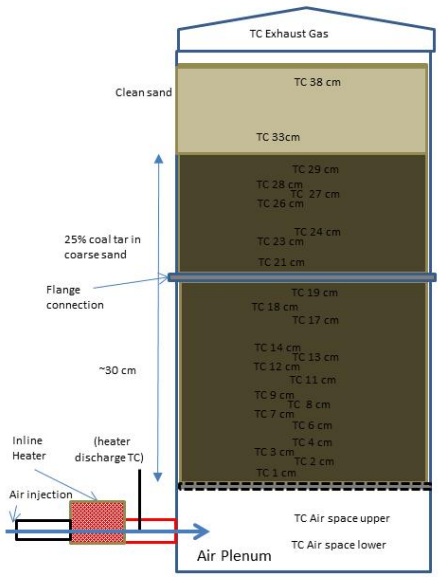

Experiment Details

Date:	1-Feb-11	
Experiment #:	7	
Location:	University of Western Ontario	
Clean Sand :	9600	g
Coal Tar:	670	g
Packing height:	30	cm clean gap, 7 cm contaminated
Column Type:	Stainless Steel	
Column Diameter:	16	cm
Heater Type	External Inline (1.8 kW)	

Test Log

Time	Elapsed Time (min)	Air Flow Rate (LPM)	Notes:
9:26	0	60	Heater on. 40% variac
9:31	5	60	Variac @ 60%
9:37	11	60	Variac @ 70%
9:51	25	60	Variac @ 80%
10:18	52	80	Variac @ 80%
10:37	71	80	HEATER OFF
11:40	134	90	Propagation complete

Figure A.13: Experiment #7 column configuration and experimental notes.

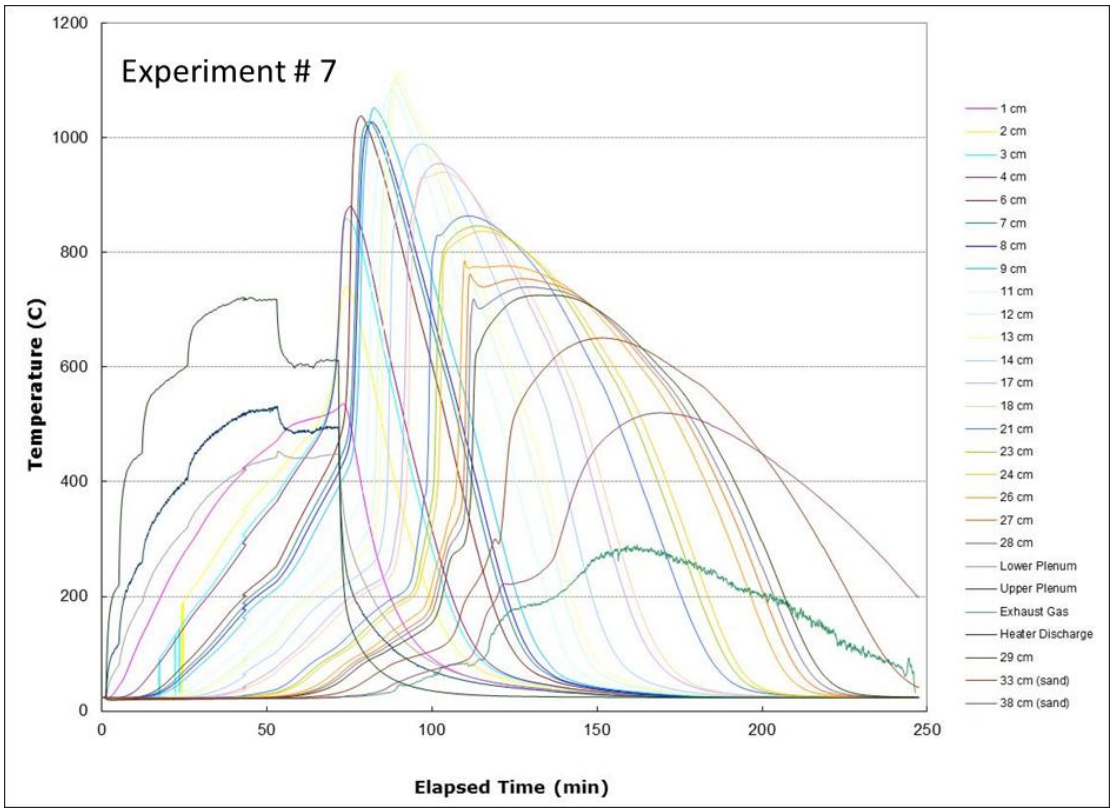

Figure A.14: Experiment # 7 thermocouple temperature profiles.

Column Configuration

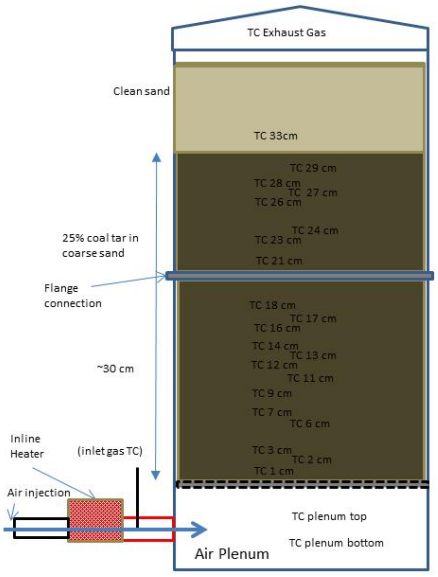

Experiment Details

Date:	16-Feb-11	
Experiment #:	8	
Location:	University of Western Ontario	
Clean Sand :	~9600	g
Coal Tar:	~670	g
Packing height:	30	cm
Column Type:	Stainless Steel	
Column Diameter:	16	cm
Heater Type	External Inline (1.8 kW)	

Test Log

Time	Elapsed Time (min)	Air Flow Rate (LPM)	Notes:
10:25	0	60	Heater on.
11:25	60	80	HEATER OFF
12:15	110	80	Propagation complete

Figure A.15: Experiment #8 column configuration and experimental notes.

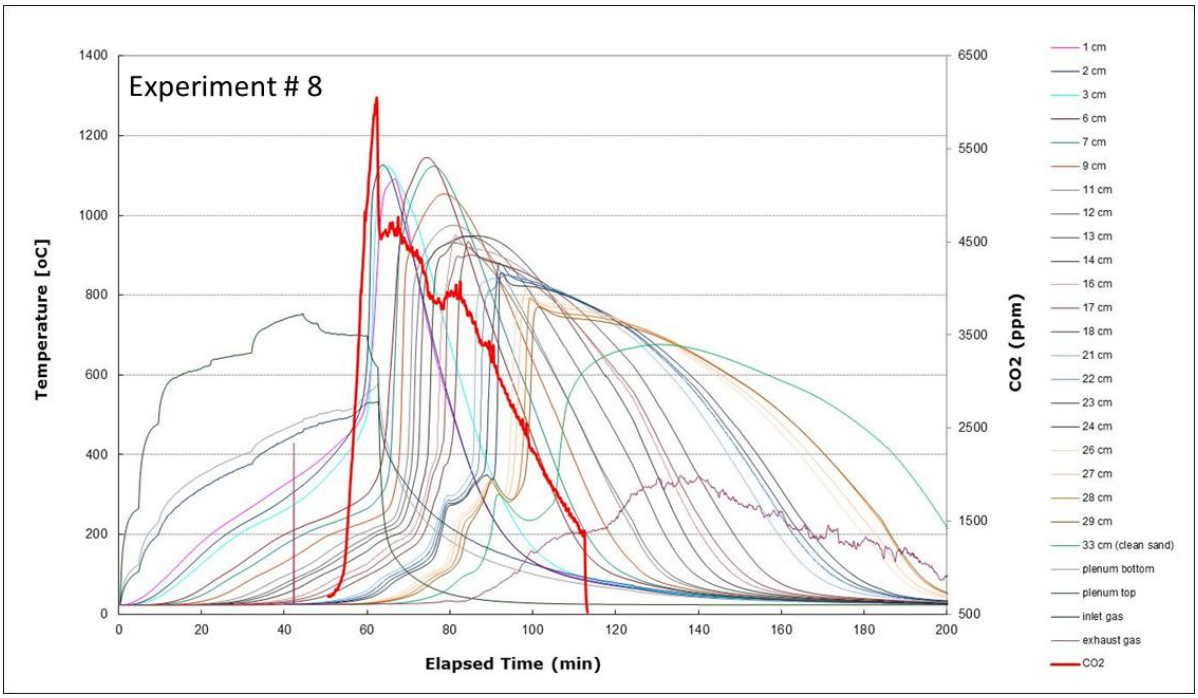

Figure A.16: Experiment # 8 thermocouple temperature and CO2 profiles.

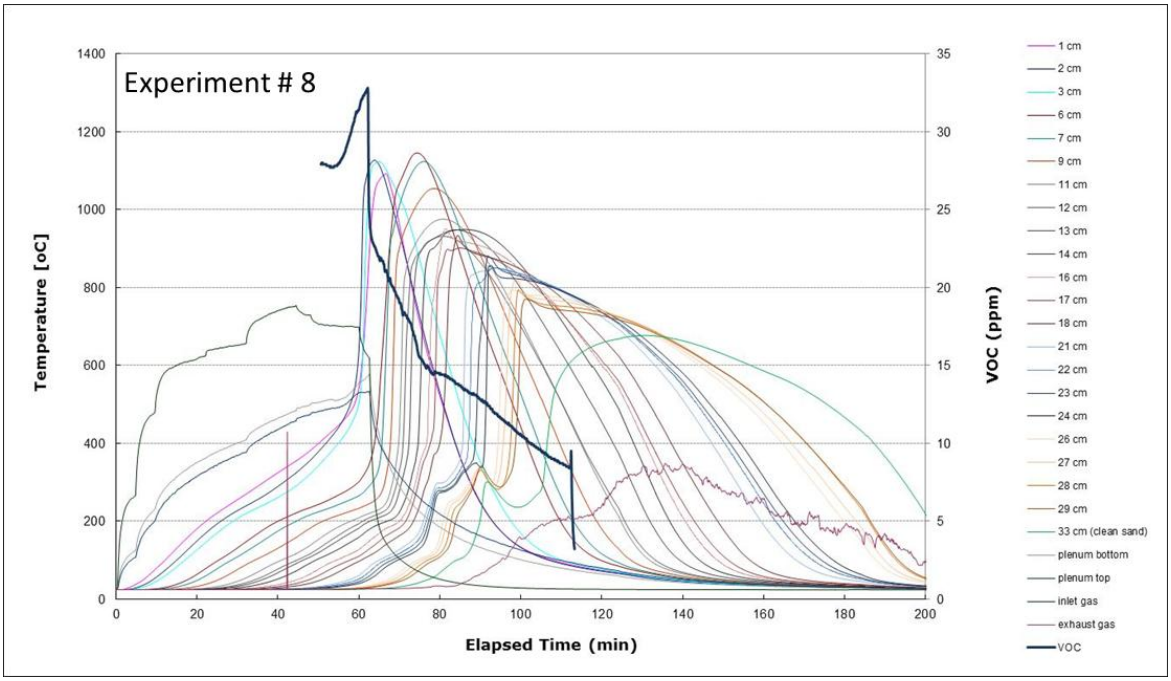

Figure A.17: Experiment #8 thermocouple temperature and VOC profiles.

Column Configuration

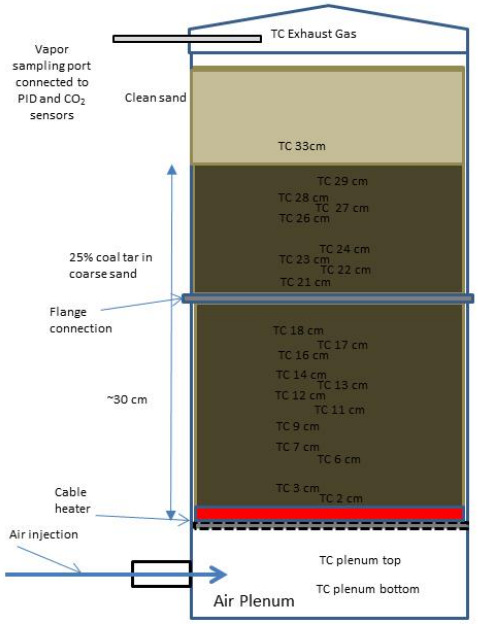

Experiment Details

Date:	NA	
Experiment #:	CONDUCTIVE	
Location:	University of Western Ontario	
Clean Sand :	NA	g
Coal Tar:	NA	g
Packing height:	30	cm
Column Type:	Stainless Steel	
Column Diameter:	16	cm
Heater Type	400W Cable Heater	

Test Log

Time	Elapsed Time (min)	Air Flow Rate (LPM)	Notes:
Test notes unavailable. Test performed by Paolo Pironi and Tanzeer Hasan on 25% coal tar saturation materials.			

Figure A.18: Conductive experiment and notes (test performed by Paolo Pironi and Tanzeer Hasan).

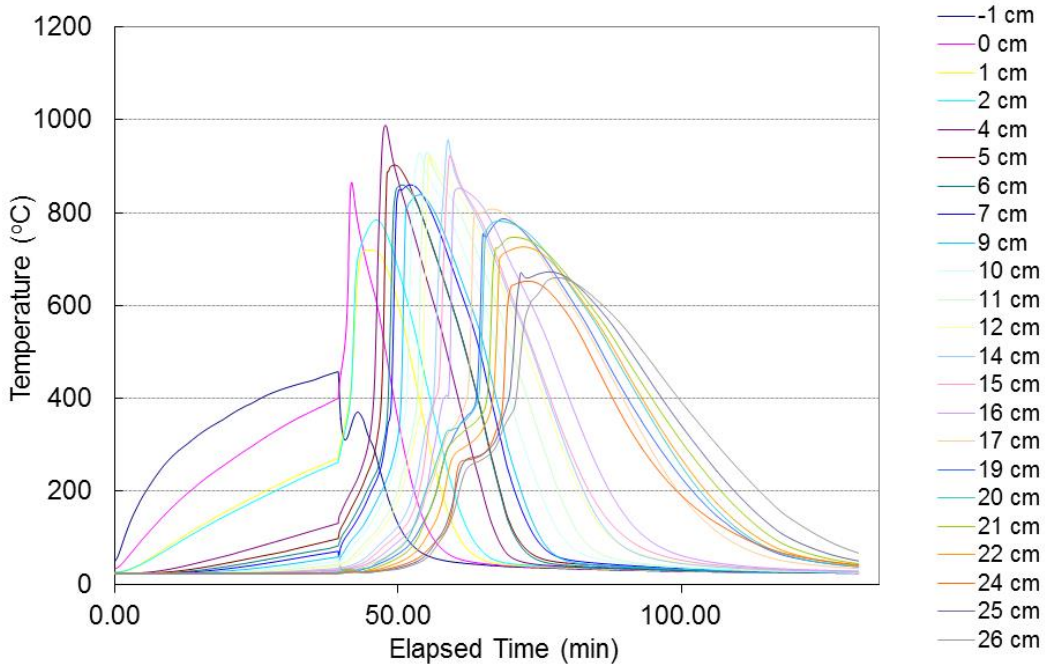

Figure A.19: Conductive experiment temperature profiles (test performed by Paolo Pironi and Tanzeer Hasan).

Appendix B: Ignition Power Calculations

Table B.1: Energy Supplied for Ignition Calculations for Conductive and Convective Column Tests

Experiment	Interval Start	Interval End	Δ time (min)	Δtime (hr)	Variac Setting (%)	Voltage[1] (V)	Current[2] (A)	Power[3] (W)	Energy[4] (kJ)
5	13:59	14:01	2	0.03	40%	48	6	288	35
	14:01	14:05	4	0.07	60%	72	9	648	156
	14:05	14:35	30	0.50	80%	96	12	1152	2074
	14:35	14:37	2	0.03	75%	90	11	1013	122
	14:37	15:02	25	0.42	78%	94	12	1095	1643
	TOTAL ENERGY SUPPLIED FOR IGNITION[5] (kJ)								**4028**
6	12:05	12:10	5	0.08	40%	48	6	288	86
	12:10	12:20	10	0.17	60%	72	9	648	389
	12:20	12:30	10	0.17	70%	84	11	882	529
	12:30	12:43	13	0.22	75%	90	11	1013	790
	12:43	13:05	22	0.37	73%	88	11	959	1266
	13:05	13:10	5	0.08	75%	90	11	1013	304
	13:10	13:21	11	0.18	80%	96	12	1152	760
	TOTAL ENERGY SUPPLIED FOR IGNITION[5] (kJ)								**4124**
7	9:26	9:31	5	0.08	40%	48	6	288	86
	9:31	9:37	6	0.10	60%	72	9	648	233
	9:37	9:51	14	0.23	70%	84	11	882	741
	9:51	10:18	27	0.45	80%	96	12	1152	1866
	10:18	10:37	19	0.32	80%	96	12	1152	1313
	TOTAL ENERGY SUPPLIED FOR IGNITION[5] (kJ)								**4240**
AVERAGE ENERGY FOR SUPPLIED FOR CONVECTIVE IGNITION (kJ)									**4131**
Conductive	--	--	10	0.17	60%	72	2.3	162	97
	--	--	10	0.17	80%	96	3.0	288	173
	--	--	10	0.17	90%	108	3.4	365	219
	--	--	12	0.20	100%	120	3.8	450	324
	TOTAL ENERGY SUPPLIED FOR IGNITION[5] (kJ)								**813**

Notes:

[1] Voltage (V) calculated as product of plug voltage (120V) and variac setting.

[2] Current (A) calculated by dividing voltage by heater resistance (8 Ω for covective tests and 32Ω for conductive test).

[3] Power (W) calculated as product of voltage (V) and current. (A)

[4] Energy (kJ) calculated by Power (W) x Δtime (hr) x 3.6 (conversion factor to kJ).

[5] Total energy for ignition is calculated as the sum of the interval energy inputs for an experiment.

Appendix C: Photographs from Field Trials

Figure C.1: Field trial study site prior to construction of test cells. Former industrial facility, New Jersey.

y

Figure C.2: Test pit adjacent to test cells. Water table, saturated with highly mobile coal tar NAPL approximately 1 m bgs.

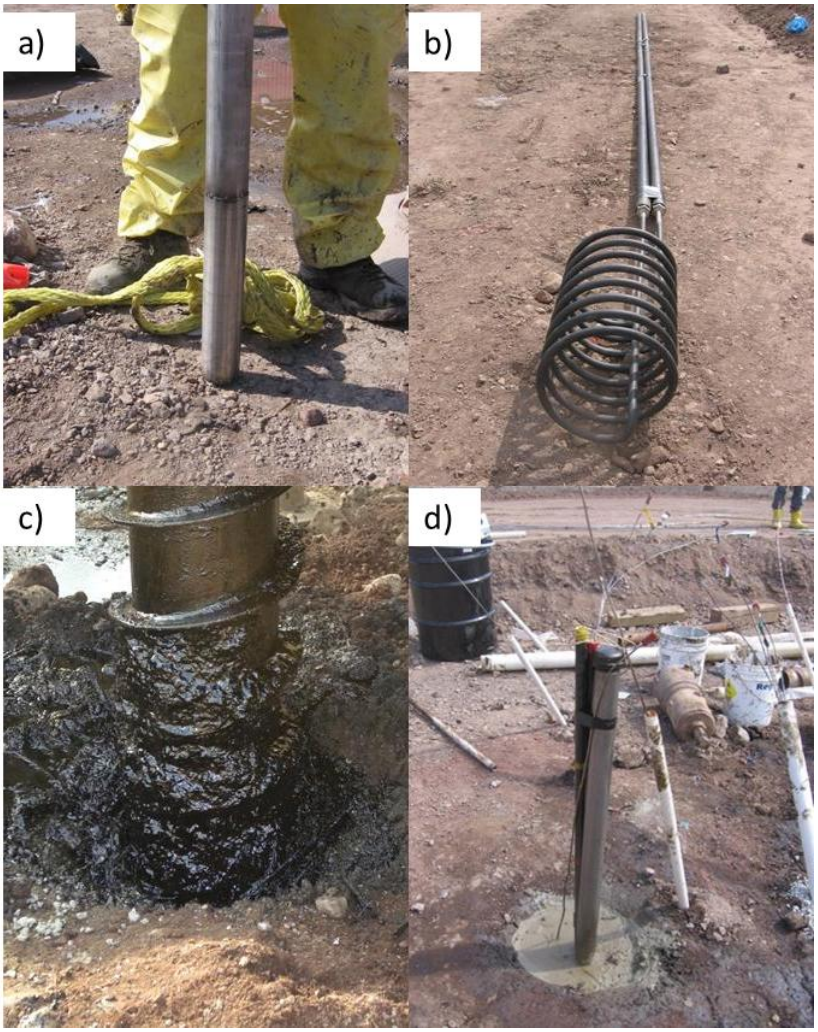

Figure C.3: Phase I, Design A conductive heater installation. a) ignition well screen; b) electrical resistive heating coil; c) drill auger flight installing borehole into coal tar contaminated fill; d) completed ignition well.

Figure C.4: Phase I and II test cell mid construction. Ignition points visible running down center line, thermocouple probes installed with PVC sleeves protecting sheaths and rubber gloves covering plugs.

Figure C.5: Phase I and II test cell; installation of vapour collection layer.

Figure C.6: Phase I and II test cell; vapour cap installation.

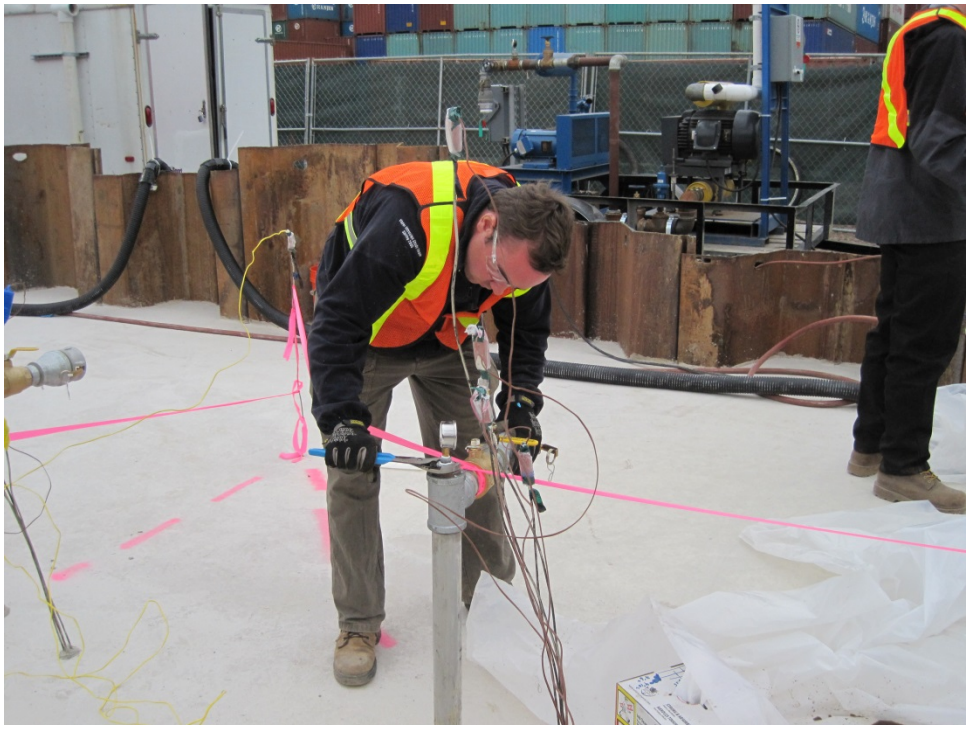

Figure C.7: Phase I and II test cell; installation of ignition well heads (by the author).

Figure C.8: Assembly of thermocouple wiring harnesses prior to field deployment. Phase II field trial collected subsurface temperature data from 166 thermocouple locations at 30 second intervals throughout the duration of the test.

Figure C.9: Phase I and II test cell; field connection of thermocouples.

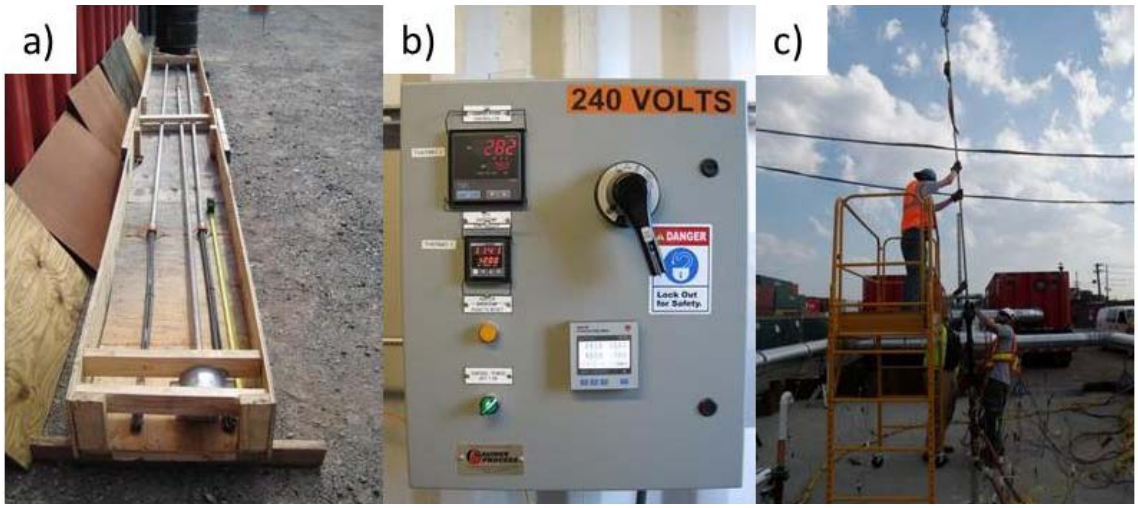

Figure C.10: Phase II, Design B convective heater installation. a) heaters pre-installation; b) heater control panel; c) field deployment into ignition well.

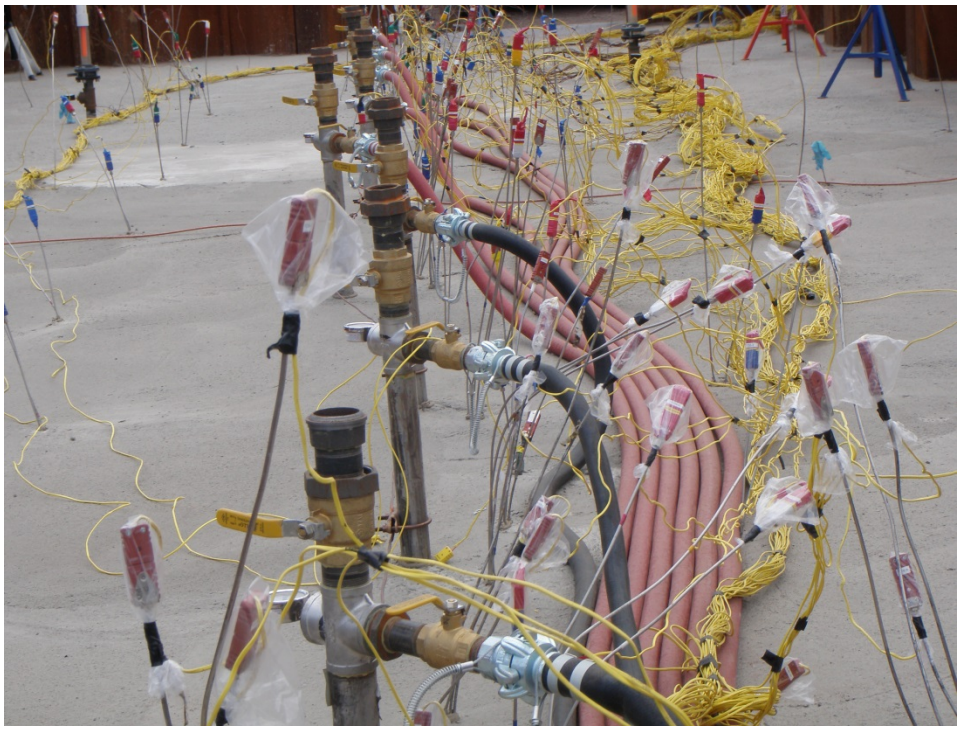

Figure C.11: Phase II field trial; close up of ignition wells, air injection lines (orange hose) and thermocouple wires (yellow).

Figure C.12: Phase II field trial; aerial view of test cell and process equipment.

Figure C.13: Phase II field trial; completed cell, modified to contain leakage at sheet pile walls.

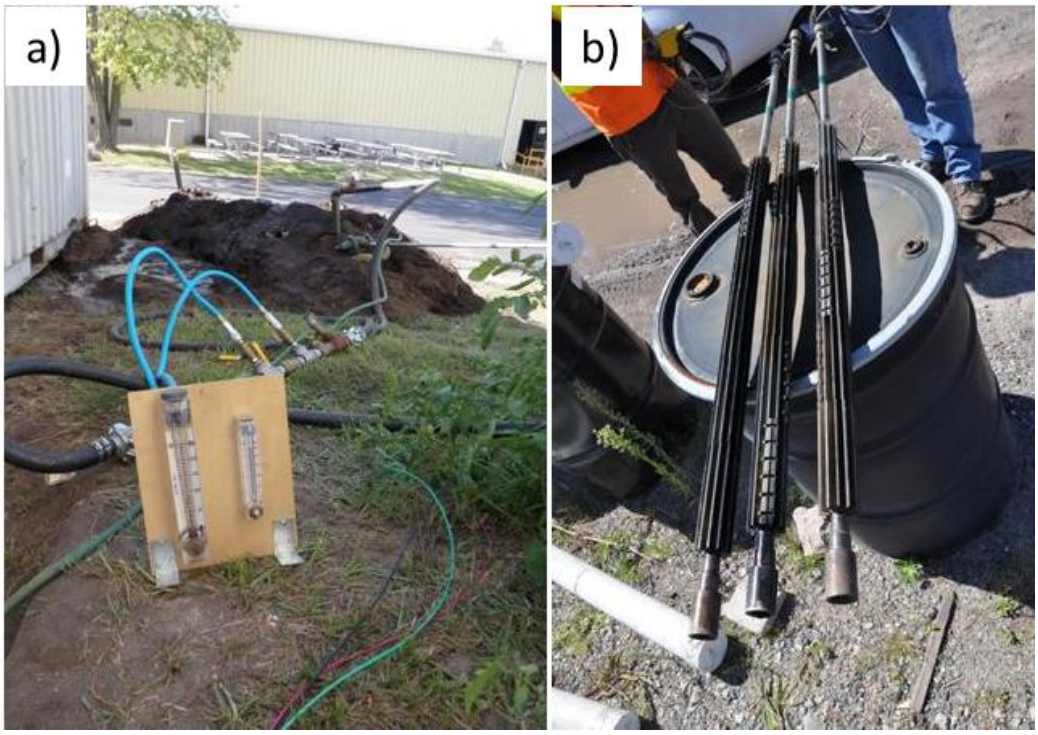

Figure C.14: Phase III, Design C convective heater. a) above-ground testing apparatus, b) three heaters above ground prior to deployment.

Figure C.15: Phase III test cell; installation of thermocouples using direct push drill rig.

Figure C.16: Phase III test cell; installation of vapour collection layer.

Figure C.17: Phase III test cell; vapour collection manifold.

Figure C.18: Phase III field trial; completed cell and process equipment.

Appendix D: Chapter 4 Supplemental Figures

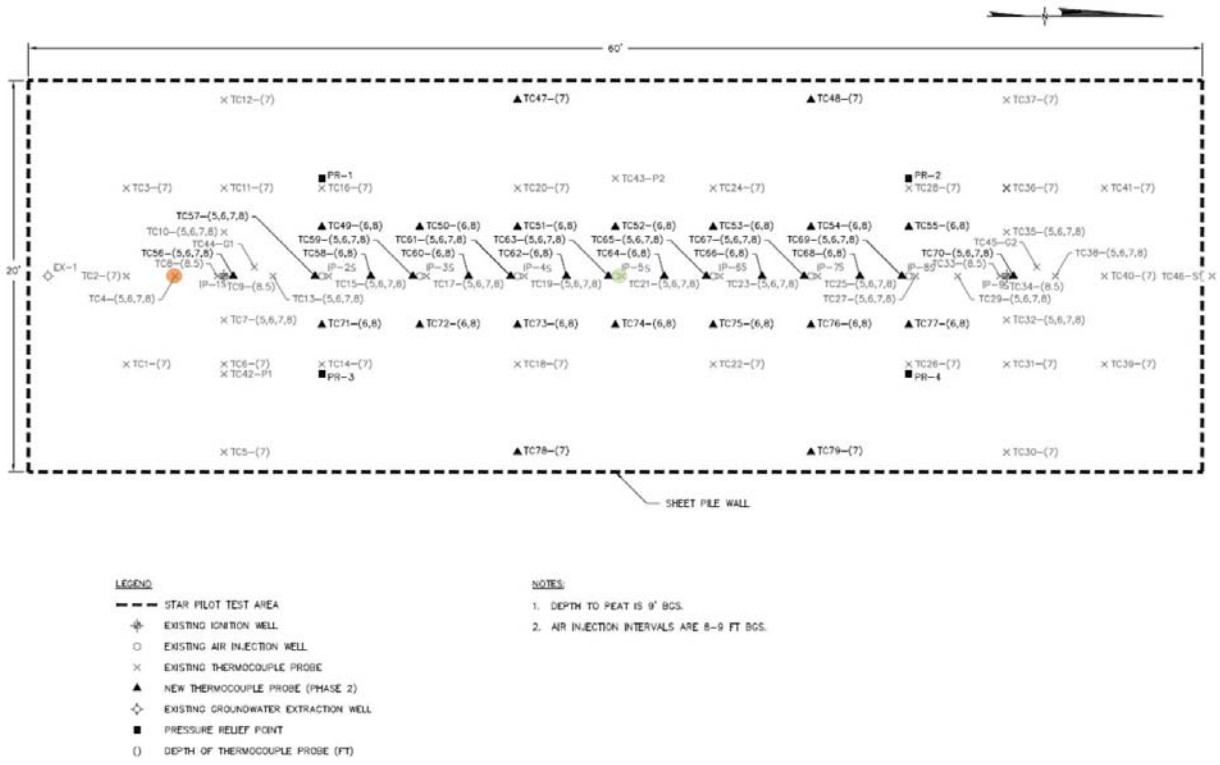

Figure D.1: Plan view of Phase II pilot test cell. Central ignition point IP-5S and smouldering front emergence point TC-4 highlighted green and orange respectively. Note all measurements in imperial units (From Geosyntec).

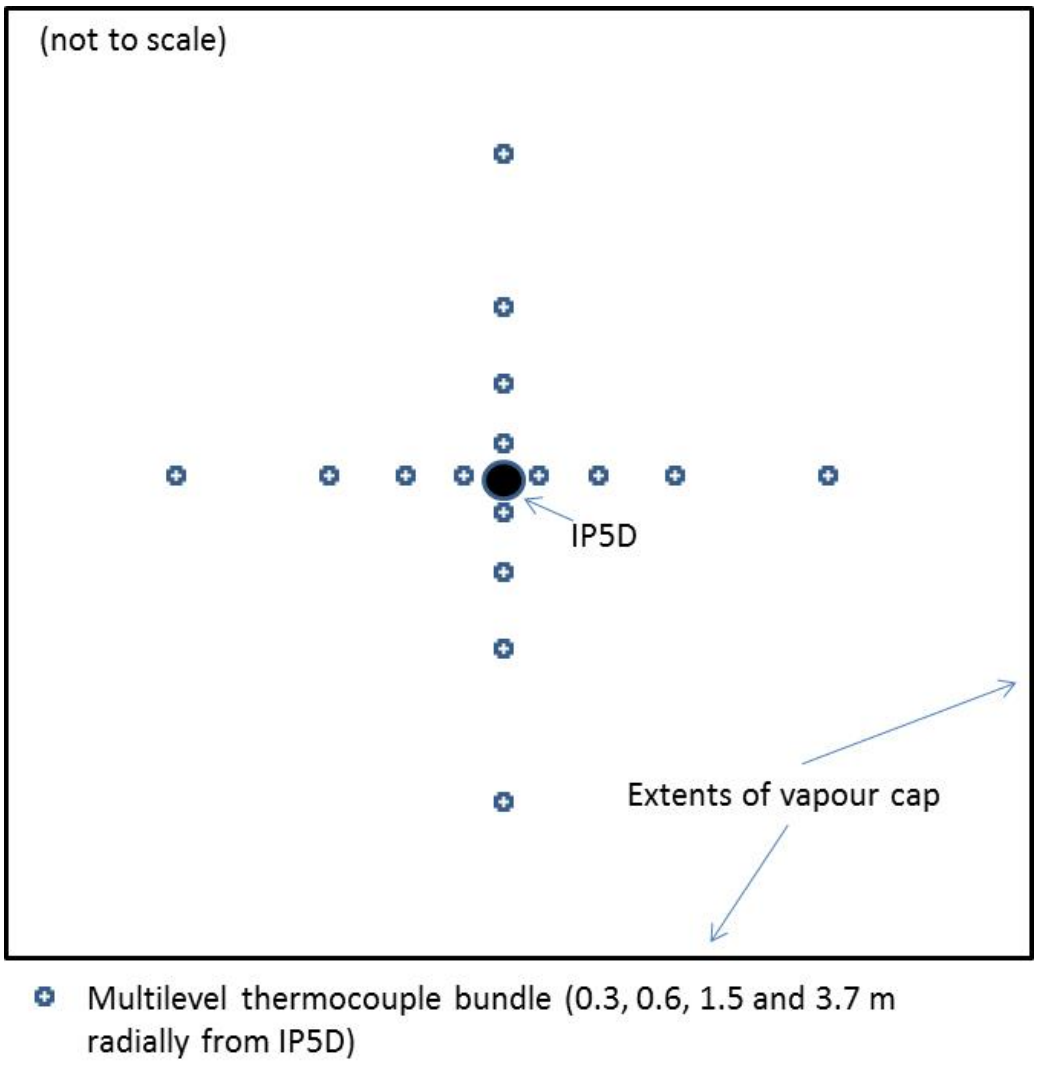

Figure D.2: Plan view schematic of Phase III pilot test cell.

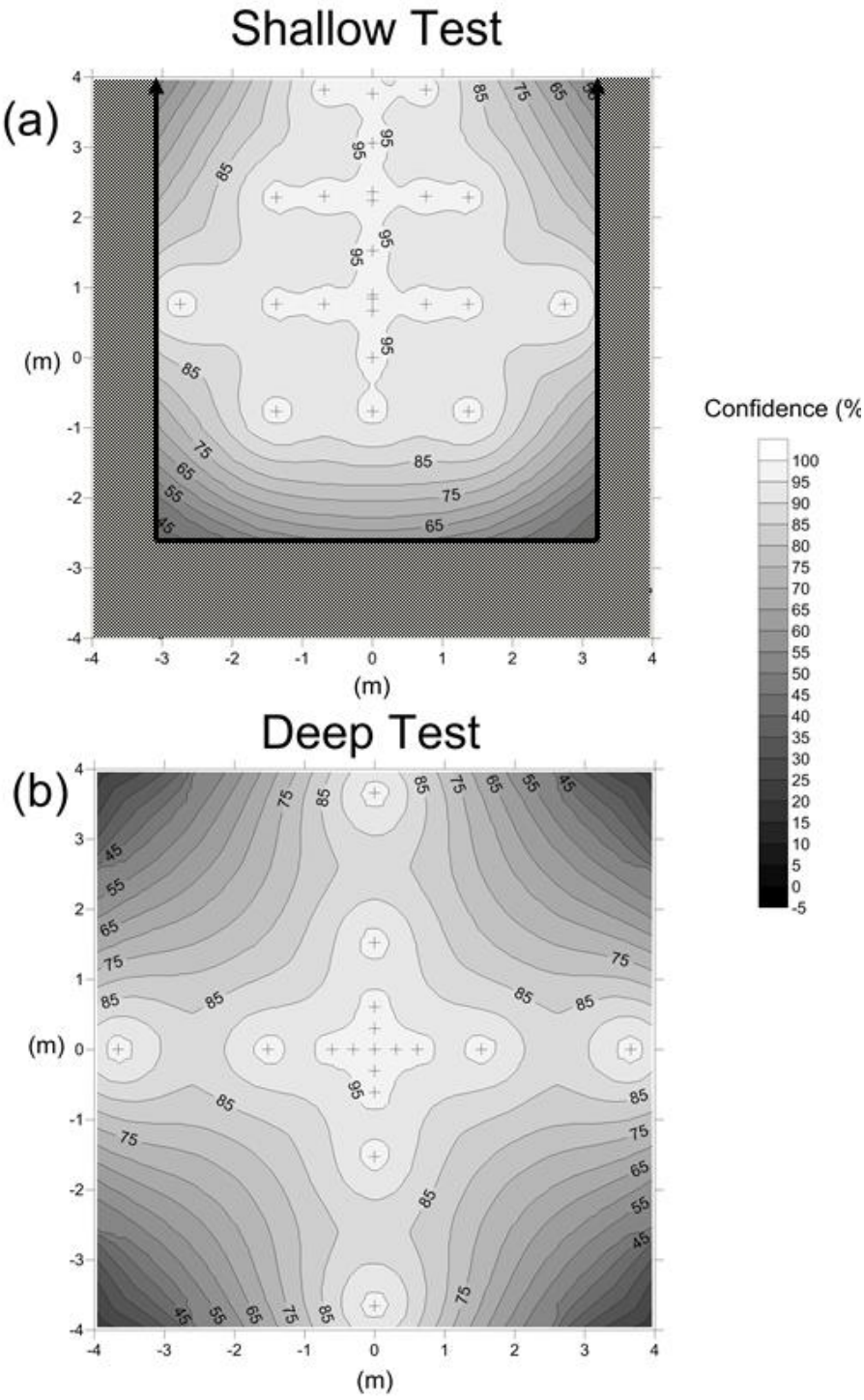

Figure D.3: Confidence contours of krigged temperature values (Day 8) from the Shallow (a) and Deep (b) Tests. Confidence values were calculated at each grid location as the standard error at a given location (a function of krigged values and distance from known locations) divided by the krigged value at that location. Calculations were performed using "R" statistical software and contour plots were generated in Surfer.

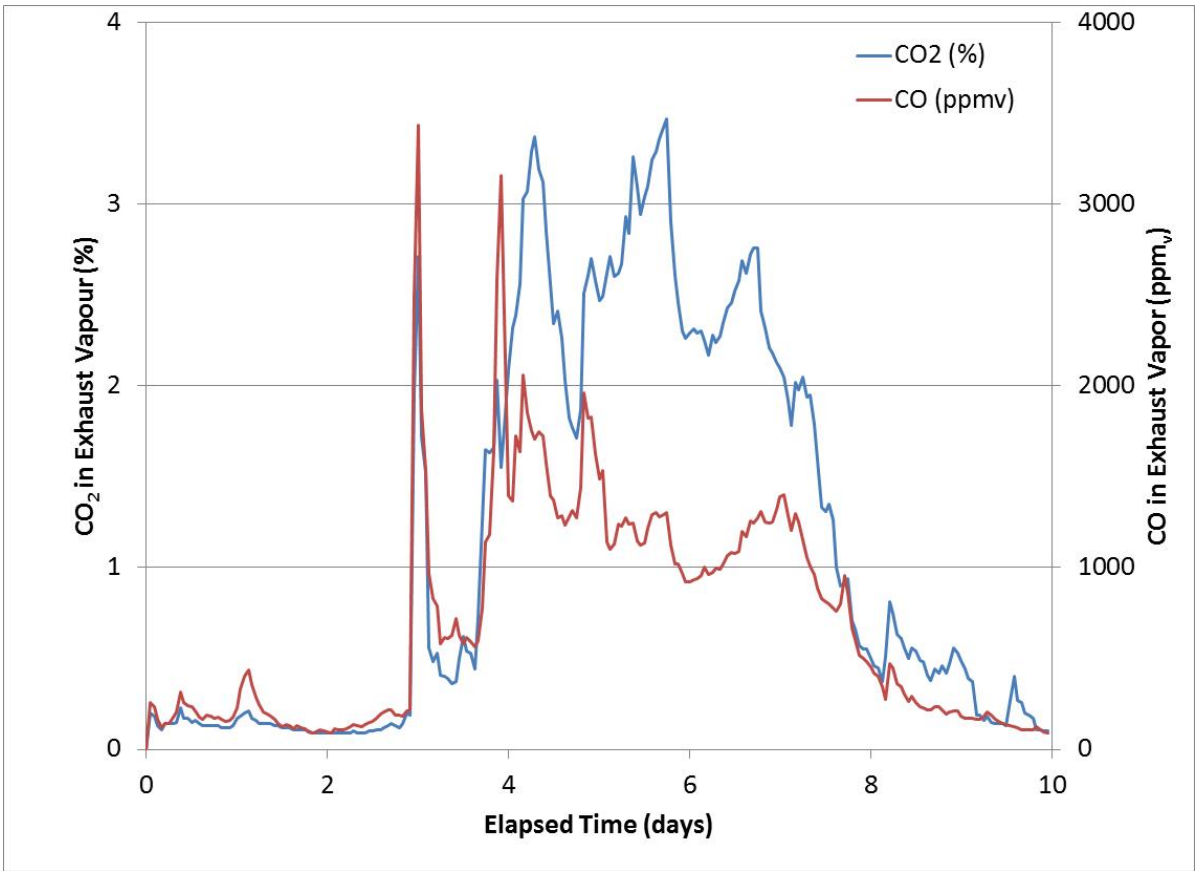

Figure D.4: Phase II, Shallow Test Combustion gas (CO2 and CO) concentrations in collected exhaust vapours. Combustion gases are used for mass destroyed calculations.

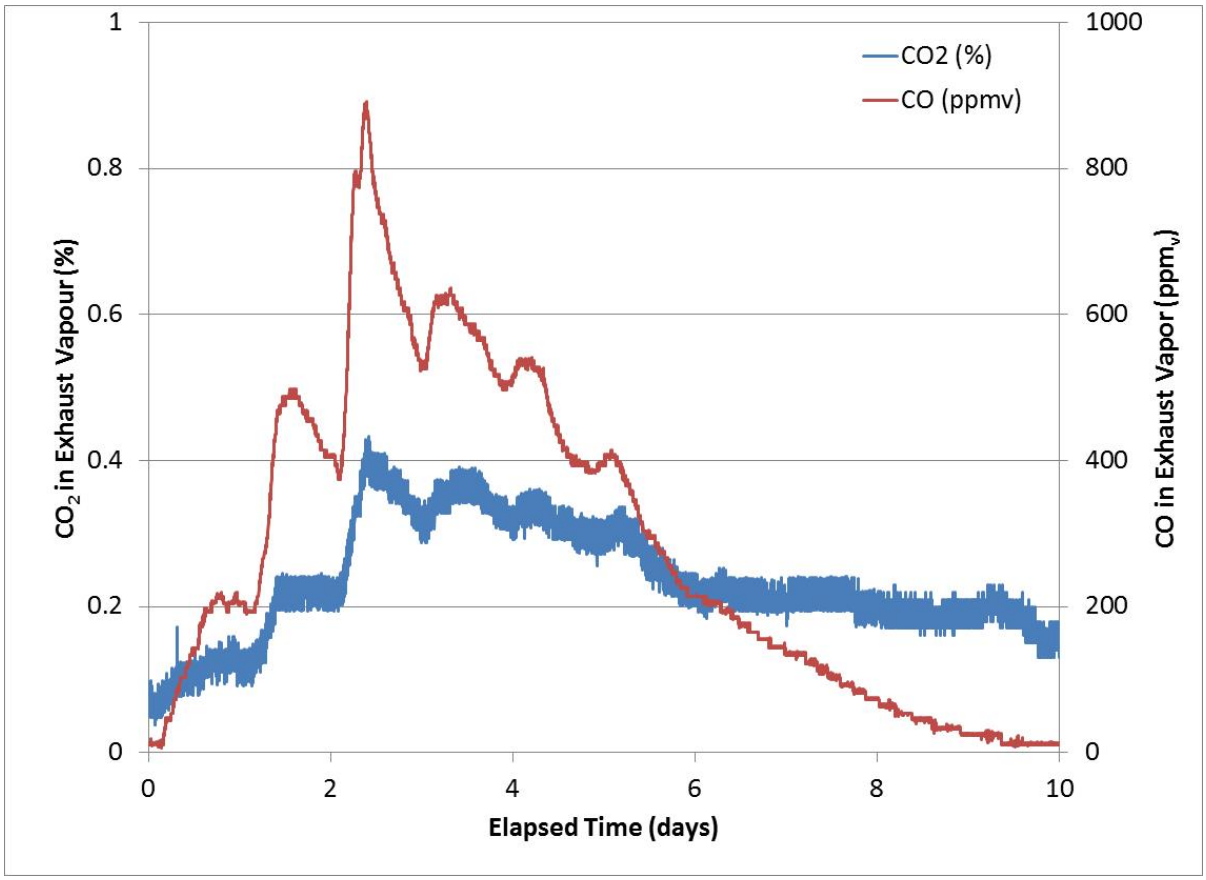

Figure D.5: Phase III, Deep Test Combustion gas (CO2 and CO) concentrations in collected exhaust vapours. Combustion gases are used for mass destroyed calculations.

Table D.1: Shallow Test - VOCs in Vapour and Reaction Efficiency

Test	Shallow
Sample Location	Undiluted Extracted Vapour
Volatile Organic Compound (µg/m3)1	
1,2,4-Trimethylbenzene	**1600**
1,3,5-Trimethylbenzene	**760**
1,3-Butadiene	**900**
2-Butanone (MEK)	**1100**
Benzene	**25000**
Carbon disulfide	**1000**
Chloromethane	**810**
Dichloromethane (Methylene chloride)	**800**
Ethyl benzene	**2300**
Heptane	**1400**
Hexane	**1500**
m&p-Xylenes	**5300**
Naphthalene	**31000**
Octane	**1100**
o-Xylene	**2300**
Pentane	**2100**
Styrene	**1700**
Toluene	**7400**
TVOC	**88070**

Extraction Flow (m3/hr)	2549
Mass Loss by Volatilization (kg/hr)	0.2244
Coincident Coal Tar Destruction Rate (kg/Hr)[2]	36.0
Reaction Efficiency	99.38%

Notes:

[1] - Detected compounds only

[2] - Calculated as average of 4 hour period around sample interval

Table D.2: Deep Test - VOCs in Vapour and Reaction Efficiency

Test	Deep	Deep	
Sample Location	Undiluted Extracted Vapour	Undiluted Extracted Vapour	
Volatile Organic Compound (µg/m3)			
1,2,4-Trimethylbenzene	**1,500**	**2,100**	
1,3,5-Trimethylbenzene	**770**	**1,100**	
1,3-Butadiene	**25**	--	
4-Ethyltoluene	**470**	**680**	
Acetone	**1,700**	**840**	
Benzene	**8,700**	**10,000**	
Chloromethane	**64**	**67**	
Cyclohexane	**180**	**160**	
Ethyl benzene	**2,200**	**3,300**	
Heptane	**200**	**250**	
m&p-Xylenes	**7,400**	**11,000**	
n-Hexane	**200**	**210**	
o-Xylene	**2,300**	**3,500**	
Styrene	**94**	3 U	
Toluene	**17,000**	**19,000**	
TVOC	42,803	52,207	
			AVERAGE
Extraction Flow (m3/hr)	2549	2549	
Mass Loss by Volatilization (kg/hr)	0.11	0.13	0.12
Coincident Coal Tar Destruction Rate (kg/Hr)[1]	5.87	5.24	5.56
Reaction Efficiency	98.2%	97.5%	97.8%

Notes:

[1] - Detected compounds only

[2] - Calculated as average of 4 hour period around sample interval

Curriculum Vitae

Name:	Grant Scholes
Post-secondary Education and Degrees:	University of Waterloo Waterloo, Ontario, Canada 1998-2003, B.A.Sc. Environmental Engineering (Chemical Specialization)
Licensure	P.Eng (Professional Engineers Ontario)
Related Work Experience	Project Engineer Geosyntec Consultants 2002-present